Cyprus University of Technology

Faculty of Engineering and Technology

.

**Doctoral Dissertation**

# A passivity based, system reference frame approach for decentralized stability analysis and control design in future power grids

**Chrysovalantis Spanias**

**Limassol, December 2020**

CYPRUS UNIVERSITY OF TECHNOLOGY
FACULTY OF ENGINEERING AND TECHNOLOGY
DEPARTMENT OF ELECTRICAL ENGINEERING, COMPUTER ENGINEERING AND INFORMATICS

Doctoral Dissertation

# A passivity based, system reference frame approach for decentralized stability analysis and control design in future power grids

Chrysovalantis Spanias

Limassol, December 2020

# Approval Form

Doctoral Dissertation

## A passivity based, system reference frame approach for decentralized stability analysis and control design in future power grids

Presented by
Chrysovalantis Spanias

Supervisor: Michalis P. Michaelides, Assistant Professor
[Cyprus University of Technology, Faculty of Engineering and Technology, Department of Electrical Engineering, Computer Engineering and Informatics]

Signature: .....

Member of Committee: Charalambos A. Charalambous, Associate Professor
[University of Cyprus, Faculty of Engineering, Department of Electrical and Computer Engineering]

Signature: .....

Member of Committee: Petros Aristidou, Lecturer
[Cyprus University of Technology, Faculty of Engineering and Technology, Department of Electrical Engineering, Computer Engineering and Informatics]

Signature: .....

Cyprus University of Technology
Limassol, December 2020

# Copyrights

I would like to dedicate this thesis to my beloved Giouli.

# Declaration

I hereby declare that the PhD thesis titled 'A passivity-based, system reference frame approach for decentralized stability analysis and control design in future power grids', has been carried out by me in the Department of Electrical Engineering, Computer Engineering and Informatics at the Cyprus University of Technology. The contents of this dissertation are original and have not been submitted in whole or partially for consideration for any other degree or qualification in this, or any other University. This dissertation is the result of my own work and includes nothing which is the outcome of work done in collaboration, except where specifically indicated in the text.

Chrysovalantis Spanias
Limassol, December 2020

# Acknowledgements

First of all, I would like to express my deep gratitude to my PhD supervisor Michalis Michaelides for his guidance throughout the last three years. Despite all the difficulties, he was always there for me, willing to discuss and propose solutions for various issues that I had faced carrying out my research. His support and persistence gave me the strength and the motivation to complete my PhD after seven years of hard work.

I might likewise wish to thank my former supervisor, Ioannis Lestas, for giving me the opportunity to pursue this PhD degree and stimulating my interest in the area of power system stability and control. His guidance and support through the first four years of my studies have been of great value to me in both academic and personal level.

My sincerest gratitude goes to Petros Aristidou, whose advice shaped my thinking and helped me improve the quality of my work. His willingness to discuss complex issues and various power system topics has been inspirational to my research. Spending much of his precious time providing me with feedback and proofreading my papers is much appreciated and hence, never be forgotten.

I would also like to give special thanks to the members of my examination Committee for proofreading my thesis and suggesting ways to improve it. Their valuable feedback is appreciated.

During all these years at the Cyprus University of Technology (CUT), I was privileged enough to meet and work with several people. However, through this point, I feel the urge to thanking those who after seven years, I can now call friends. That are Harris, Panayiotis and Maria. I would like to thank you for giving me the opportunity to collaborate and spend some joyful time with you. I would also like to express my gratitude to Dr Salomi Papadima-Sophocleous and Dr Kyriakos Kalli. Your kind support has been an important motive for me, especially during the difficult times that I had been through.

I also want to thank my former colleagues Kyriakos K., Marios, Kyriakos S. Despina, George, Michalis and Nicolas who offered me a pleasant work environment and helped me cope with the fact that I needed to work full time while pursuing my PhD degree. I feel very lucky to have met you. Spending four fruitful years with you will be one of the greatest memories of my life.

In 2018, I had the great opportunity to join Distribution System Operator at the Electricity Authority of Cyprus (EAC), a job position that I was always wishing. This change gave me the chance to collaborate with one of the greatest persons and the most inspiring manager I have ever met, Mr Stavros Stavrinos. I would like to thank him for his passion, persistence and enthusiasm that have been the cornerstone of my professional and personal development.

I would also like to thank my closest friends George G., George N., Constantinos, Erato, Marina, Andreas and Vaiva for their kind support and encouragement. I am really grateful for all the great memories we had together and for showing such understanding when I was not able to see you for a long time due to my exhausting schedule all these years. Moreover, I want to thank my brother, Minos, who although being far away, has always been there for me. I look forward to meeting you in Germany or anywhere else soon. Finally, I would like to thank my friends Thanasis and Eleni for all the joyful moments we had during our meetings in Cyprus and Greece.

At this point, I would like to express my wholehearted gratitude to my parents, Antonis and Elli, and my three sisters, Theklia, Zoe and Marina that have always been by my side. Your unconditional love and continuous support, not only during my PhD time but throughout my entire life, made me a better person. I could not of course forget these three people that even if I am not able to see often, I now feel like a second family. I would like to thank Pavlos, Fotini and Vaso for their continuous support and encouragement.

Last but certainly not least, I left the person who changed my life, my beloved partner Giouli. It is very hard to express in words how grateful I am to you. Your love, devotion, continuous support and encouragement were my driving force to achieve things I had not thought I could in my life. I can say with absolute confidence that I would never be able to repay your incredibly large patience during these seven difficult years. I can only promise that from now on, you will be my priority. As a thank you for all the things you have done for me, I would like to dedicate this thesis to you.

# Abstract

Over the last decades, power systems have been through critical changes as a result of the worldwide efforts to decelerate climate change and global warming. Such changes were the introduction of new generation and storage technologies, and the rapid increase of the share of Renewable Energy Sources (RES) in power generation. Although these advances contributed to technological and economic development, they have introduced numerous issues that were not previously encountered in traditional power grids. Specifically, the gradual replacement of the large fossil-fueled plants with a large number of small sparsely-located RES resulted in the significant decrease of system rotational inertia and the emergence of serious stability-related problems.

Despite the latest decisive steps in the area of stability analysis and control design, existing power systems are still in danger due to the continuously increasing challenges they encounter. An effective way to overcome these problems is the adoption of more accurate dynamical models for both the network and the power system components within stability studies. Such accurate modeling will not only assist in the design of more effective control mechanisms, but it will provide useful insights regarding the stability and the reliability of the system.

The current thesis aims to address the above problems by introducing a novel approach for decentralized stability analysis and control design in existing and future power grids wherein more detailed dynamical models are employed. The proposed approach relies upon the transformation of both the network and the bus dynamics into the system reference frame instead of each bus local $dq$ coordinates. In particular, this transformation allows the formulation of the network equations as an input-output system which we show it is passive even if the network's lossy and dynamic nature is taken into account. The passivity property of the adopted network model along with the local passivity conditions imposed on a broad class of bus dynamics guarantee the asymptotic stability of the whole power network in a completely decentralized manner. The use of such a general representation also facilitates the incorporation of more accurate dynamical models for the power system components and their control mechanisms, even though their inclusion in such a decentralized analysis has been difficult. A further detailed discussion regarding the advantages of the presented

approach for the reliable and robust operation of the future low-inertia power grids as well as the design of more effective distributed control mechanisms is provided. The proposed stability analysis framework is finally verified through realistic applications and simulations on several testbed systems such as the Two Area Kundur, the IEEE 68 Bus test systems and the IEEE 37 Node test feeder.

**Keywords:** power system stability, passivity, system reference frame, decentralized control, multi-variable dynamical systems.

# TABLE OF CONTENTS

**LIST OF TABLES** **xv**

**LIST OF FIGURES** **xvii**

**LIST OF ABBREVIATIONS** **xxii**

**1 Introduction** **1**

1.1 Motivation . . . . . 1

1.2 Contributions and structure of the thesis . . . . . 3

**2 Theoretical background to nonlinear systems analysis** **9**

2.1 Notation . . . . . 9

2.2 Dynamical System Classification . . . . . 11

2.3 Nonlinear Models and Nonlinear Phenomena . . . . . 12

2.4 Fundamental Properties . . . . . 14

2.4.1 Existence and Uniqueness . . . . . 14

2.4.2 Dependence on initial conditions . . . . . 15

2.5 Lyapunov Stability . . . . . 16

2.5.1 Invariant Sets . . . . . 17

2.5.2 Stability Definitions . . . . . 17

2.5.3 Linearization and Lyapunov's Indirect Method . . . . . 18

2.5.4 Lyapunov Functions and the Direct Method . . . . . 19

2.6 Passivity . . . . . 22

2.6.1 Memoryless Functions . . . . . 22

2.6.2 State Models . . . . . 23

2.6.3 Positive Real Transfer Functions . . . . . 24

2.6.4 Passivity Theorems for Feedback Systems . . . . . 26

**3 Related Literature** **31**
3.1 Introduction to power system stability . . . . . 31
3.1.1 The notion of power system stability . . . . . 31
3.1.2 Time scales of power system dynamic phenomena . . . . . 32
3.1.3 Classification of power system stability . . . . . 33
3.2 Overview of power system stability analysis approaches . . . . . 37
3.2.1 Centralized approaches . . . . . 38
3.2.2 Decentralized approaches . . . . . 41
3.3 Power system modeling in stability analysis studies . . . . . 43
3.3.1 Alternating Current (AC) three phase sources . . . . . 43
3.3.2 Phasor representation . . . . . 44
3.3.3 (0,d,q) or Clarke-Park transformation . . . . . 45
3.3.4 Power Network Structure . . . . . 46
3.3.5 Network Equations . . . . . 47

**4 Multi-variable network formulation** **51**
4.1 Static network representation . . . . . 51
4.1.1 Multi-input/multi-output formulation . . . . . 51
4.1.2 Passivity of the static network model . . . . . 52
4.2 Dynamic network representation . . . . . 54
4.2.1 Multi-input/multi-output formulation . . . . . 54
4.2.2 Passivity of the dynamic network model . . . . . 57
4.3 Discussion . . . . . 59
4.4 Assessment of the proposed network formulations . . . . . 60
4.4.1 Numerical applications . . . . . 60
4.4.2 Simulations . . . . . 62

**5 Incorporation of power system components and system-wide stability results** **67**
5.1 General multi-input/multi-output formulation of bus dynamics . . . . . 67
5.1.1 Static network representation . . . . . 67
5.1.2 Dynamic network representation . . . . . 68
5.2 Necessary passivity conditions on bus dynamics . . . . . 70
5.2.1 Static network representation . . . . . 70
5.2.2 Dynamic network representation . . . . . 72
5.3 Main stability results . . . . . 73
5.3.1 Static network representation . . . . . 73
5.3.2 Dynamic network representation . . . . . 75

5.4 Discussion . . . . . 76

**6 Applications** **79**

6.1 Passivity-based employment of SVCs for power system stability enhancement 80

6.1.1 Introduction . . . . . 80

6.1.2 Dynamic Models . . . . . 81

6.1.3 Passivity Indices in Power Grids . . . . . 83

6.1.4 SVC Employment Framework Formulation . . . . . 84

6.1.5 Discussion . . . . . 90

6.1.6 Framework Verification . . . . . 91

6.1.7 Conclusions . . . . . 99

6.2 Verification of local passivity conditions on synchronous generators . . . . 100

6.2.1 Introduction . . . . . 100

6.2.2 Generator dynamics . . . . . 100

6.2.3 Framework verification . . . . . 103

6.2.4 Modification of generator's excitation system . . . . . 105

6.2.5 Conslusions . . . . . 107

6.3 Passivity-based design of a load-side voltage control mechanism . . . . . 109

6.3.1 Introduction . . . . . 109

6.3.2 Controller design . . . . . 110

6.3.3 Passivity of load dynamics . . . . . 112

6.3.4 Simulations . . . . . 113

6.3.5 Conclusions . . . . . 115

6.4 Verification of local passivity conditions on grid-forming inverters . . . . . 116

**7 Conclusions** **119**

7.1 Conclusive summary . . . . . 119

7.2 Future work . . . . . 122

**REFERENCES** **125**

# LIST OF TABLES

6.1 The minimum damping ratio variation of the system compared to the population of the installed SVCs using the proposed passivity-based approach. . . 92
6.2 The average percentage steady state voltage deviation of IEEE 68 bus test system under normal and heavy loading conditions. . . . . 96
6.3 The selected values of maximum capacitive and the maximum inductive reactive power for profiles 1 and 2. . . . . 99
6.4 Description of the main variables and parameters appearing in the synchronous generator models . . . . . 101

# LIST OF FIGURES


1.1 Schematic representation of the connections among Chapters 4-6 based on the main application topics and analysis tools . . . . . 6

2.1 A closed-loop system represented as a feedback interconnection of two subsystems . . . . . 27

3.1 Time scales of power system dynamic phenomena. . . . . 33
3.2 Power system time scales. . . . . 34
3.3 Classification of power system stability. . . . . 37
3.4 Lumped circuit model ($\pi$-equivalent) representation of a network line from bus $i$ to bus $j$. . . . . 47
3.5 Relative position of the machine reference frame with respect to the system reference frame. . . . . 50

4.1 The network equations represented as a $(2 \times |\mathcal{N}|)$-input/$(2 \times |\mathcal{N}|)$-output system. . . . . 52
4.2 The power network represented as an interconnection of input/output systems associated with the bus and network dynamics, respectively. . . . . 54
4.3 Single line diagram of the Four Machine Two-Areas Kundur test system. . . 61
4.4 Single line diagram of a simple four area test system. . . . . 63
4.5 Voltage deviation at area 2 after a sudden load increase of 100MW (low RES penetration conditions). . . . . 64
4.6 Voltage deviation at area 2 after a sudden load increase of 100MW (medium RES penetration conditions). . . . . 64
4.7 Voltage deviation at area 2 after a sudden load increase of 100MW (high RES penetration conditions). . . . . 65
4.8 Frequency deviation at area 2 after a sudden load increase of 100MW (low RES penetration conditions). . . . . 65

4.9 Frequency deviation at area 2 after a sudden load increase of 100MW (medium RES penetration conditions). . . . . 66
4.10 Frequency deviation at area 2 after a sudden load increase of 100MW (high RES penetration conditions). . . . . 66

5.1 The power network represented as an interconnection of input/output systems associated with the bus dynamics and transmission lines, respectively. . . . 68
5.2 An overview of the proposed power system configuration. . . . . 69

6.1 Example of SVC structure . . . . . 81
6.2 The flowchart representation of the proposed approach for SVC employment. 85
6.3 Graphical representation of the Geshgorin disks corresponding to the $i^{th}$ column/row (bus $i$) of the matrices $G^N$ and $G^{AGG}$. . . . . 86
6.4 The aggregate network model $H^{AGG'}$ as a parallel interconnection of the network, the SVC and the load dynamics. . . . . 88
6.5 Single line diagram of the IEEE 68-bus test system (New York / New England). 92
6.6 Eigenanalysis of the IEEE 68-bus test system when no PSSs are applied to the generators. . . . . 93
6.7 Eigenanalysis of the IEEE 68-bus test system when PSSs are applied to the generators. . . . . 94
6.8 Voltage deviation at bus 24 when the (a) 0, (b) 4, (c) 7 and (d) 10 most vulnerable buses of the network are equipped with appropriately tuned SVCs (no PSSs are applied to generators). . . . . 94
6.9 Voltage deviation at bus 24 when the (a) 0, (b) 4, (c) 7 and (d) 10 most vulnerable buses of the network are equipped with appropriately tuned SVCs (PSSs are applied to generators). . . . . 95
6.10 Frequency deviation at bus 24 when the (a) 0, (b) 4, (c) 7 and (d) 10 most vulnerable buses of the network are equipped with appropriately tuned SVCs (no PSSs are applied to generators). . . . . 95
6.11 Frequency deviation at bus 24 when the (a) 0, (b) 4, (c) 7 and (d) 10 most vulnerable buses of the network are equipped with appropriately tuned SVCs (PSSs are applied to generators). . . . . 96
6.12 The probability density functions of two different reactive power profiles (samples). . . . . 97
6.13 The cumulative density functions of two different inductive reactive power profiles (samples). . . . . 98

6.14 The cumulative density functions of two different capacitive reactive power profiles (samples). . . . . 98
6.15 The cost of the SVC installation versus the robustness of its selected reactive power range for the two different reactive power profiles (samples). . . . . 99
6.16 A graphical representation of a generator model expressed in system reference frame. . . . . 102
6.17 Frequency deviation at bus 27 after a sudden change of 1pu at the load buses 1, 9 and 18. . . . . 105
6.18 Voltage deviation at bus 27 after a sudden change of 1pu at the load buses 1, 9 and 18. . . . . 106
6.19 Eigenvalues of $G(j\omega)+G^{\mathrm{T}}(-j\omega)$, where $G(s)$ is the transfer function of the linearized dynamics (5.1) at generator bus 53. The figure shows the eigenvalues in the problematic range where the passivity property is violated. 107
6.20 Frequency deviation at bus 27 after a sudden change of 3pu at the load buses 1, 9, 18, 20, 37 and 42. . . . . 108
6.21 Voltage deviation at bus 27 after a sudden change of 3pu at the load buses 1, 9, 18, 20, 37 and 42. . . . . 108
6.22 Eigenvalues of the linearized network dynamics of the IEEE 68 bus test system. 109
6.23 The load-side voltage controller connected in a negative feedback arrangement to bus/load dynamics. . . . . 111
6.24 Single line diagram of IEEE 37 Node Test Feeder. . . . . 114
6.25 Voltage deviation at bus 32 after a sudden load change at buses 1, 7, 21, 28 and 46. . . . . 114
6.26 Frequency deviation at bus 32 after a sudden load change at buses 1, 7, 21, 28 and 46. . . . . 115
6.27 Voltage deviation at the node 775 after a sudden load change of 500kW at the nodes 724, 728, 735 and 740. . . . . 116
6.28 Frequency deviation at the node 775 after a sudden load change of 500kW at the nodes 724, 728, 735 and 740. . . . . 116

# LIST OF ABBREVIATIONS

| | |
|---|---|
| RES: | Renewable Energy Sources |
| AVR: | Automatic Voltage Regulator |
| FACTS: | Flexible Alternating Current Transmission System |
| SVC: | Static Var Compensator |
| ODE: | Ordinary Differential Equation |
| DG: | Distributed Generation |
| DSM: | Demand Side Management |
| EU: | European Union |
| SG: | Smart Grid |
| HVDC: | High Voltage Direct Current |
| AC: | Alternating Current |
| DC: | Direct Current |
| EV: | Electric Vehicle |
| DR: | Demand Response |
| DA: | Distribution Automation |
| VPP: | Virtual Power Plant |
| AMI: | Advance Metering Infrastructure |
| PV: | Photovoltaic |
| ENTSO-E: | European Network of Transmission System Operators for Electricity |
| TEF: | Transient Energy Function |
| LTI: | Linear Time Invariant |
| KYP: | Kalman Yakubovich Popov |
| LMI: | Linear Matrix Inequality |
| DER: | Distributed Energy Resources |
| KDE: | Kernel Density Estimation |
| IFP: | Input Feed-forward Passive |
| PSS: | Power System Stabilizer |
| TCSC: | Thyristor-Controlled Series Compensation |
| UPFC: | Unified Power Flow Controller |
| STATCOM: | Static Synchronous Compensator |
| PST: | Power System Toolbox |
| LTC: | Load Tap Changer |

# Chapter 1

# Introduction

The current chapter contains an introduction on the future challenges related to power system stability analysis and control along with an extensive discussion on how these challenges motivate the research on the topic. The contributions and the structure of this thesis are then provided to enhance its readability.

## 1.1 Motivation

During the last decades, there is an ongoing worldwide effort to decarbonize the energy sectors of the countries and thus to reduce the greenhouse gas emissions as well as decelerate climate change and global warming. This effort began in the early 90s and became more intense in December 2015 during the Conference Of Parties (COP) in Paris. There, 195 countries-participants took several important decisions regarding the future evolution of the existing power grids [1]. The Paris Agreement which went into effect in November 2016, gave incentives for the gradual shift of the energy production from fossil-fueled power plants towards Renewable Energy Sources (RES), the deregulation of the existing electricity markets, the modernization of the existing power systems and the wide use of electric vehicles [1–8].

Although the latest technological advancements in power engineering have been identified as a promising tool for electric utilities to meet the above targets, changes of such scale imposed new, significant challenges that were not previously encountered in traditional power grids [9]. Existing electric utilities have enabled the energy generation and consumption with great success for many decades, yet they are still unable to cope with the ongoing radical operational and structural challenges. Such challenges included the significant reduction of the system's rotational inertia, the intermittent nature of power generation and the high load variability [8]. Their impact on power system stability, reliability and robustness is already

visible and is expected to increase rapidly shortly. Specifically, current power systems shall confront much steeper frequency and voltage deviations during disturbances as well as more severe instability phenomena. The employed frequency and voltage control mechanisms are not effective enough, as they have now become too slow with respect to the disturbance dynamics and thus, unable to prevent or even effectively damp the occurring frequency and voltage deviations. Existing power systems have also been facing serious congestion problems which in turn result in reduced operational efficiencies, significant electrical losses as well as serious power quality issues [10–14]. In some cases, congestion problems also led to disastrous events like the California blackouts in 2000 and 2001 [15–17].

This lack of stability, reliability and robustness coerced power engineers to seek more flexible frameworks to improve the accuracy of the stability analysis studies and the identification of various stability-related issues. The introduction of such frameworks could also facilitate the design of new, more accurate, fast-acting control mechanisms which could further assist in mitigating the majority of the previous problems. Even though recent centralized stability analysis approaches can provide useful results concerning the stability of a system and the effectiveness of a controller, they can be computationally intractable or even infeasible. Due to the size and the complexity of the existing interconnected systems, eigenanalysis - especially when this is performed with full space methods - is computationally and memory intensive [18]. On the contrary, when a network-wide stability analysis is carried out using local conditions, the complexity of the problem increases significantly while various simplifications are often necessary. These simplifications include, for example, the assumption of a lossless network, the independent study of voltage and frequency dynamics, or the adoption of less accurate dynamics to represent the power system components and their control policies. Nevertheless, such simplifications could be crucial for the accuracy of the derived stability results and consequently, the effectiveness of the proposed control mechanisms.

As both centralized and decentralized techniques are incapable of accurately capturing the stability of the rapidly changing power grids, a useful tool that could significantly improve the stability analysis and control design is the structural property of passivity. Passivity has been one of the cornerstones of nonlinear control theory since it can facilitate the stability analysis of large-scale interconnected systems and the design of effective and robust control mechanisms [19]. Its main advantage lies in the fact that every passive system is Lyapunov stable while passivity-based conditions can be used to determine the stability of large systems and decentralized subsystems according to the way they interconnect [19–21].

Based on the above, this thesis aims to introduce an alternative passivity-based framework for decentralized stability analysis and control design in future power grids. In contrast to

the related literature, where stability analysis is carried out on the local $dq$ coordinates, the proposed framework relies upon the transformation of both the network and the bus dynamics into the system reference frame. This change of reference frame does not eliminate natural passivity properties of the network or requires additional assumptions to maintain them. It also facilitates the derivation of completely decentralized stability results and provides useful insights for the design of more effective distributed control mechanisms. One of its main advantages is the fact that it allows the adoption of more detailed network models which can ensure the accuracy of the stability analysis and the utilization of a variety of bus dynamics, such as synchronous generators, smart loads, inverter-based RES and Flexible Alternating Current Transmission System (FACTS) devices. It additionally assists in the design of more accurate, decentralized control mechanisms that can provide fast-responding ancillary services to the grid and assist in overcoming the newly emerging challenges [4, 22–26].

The main aim and the contributions of this thesis are outlined in the following section along with a brief description of each chapter's content.

## 1.2 Contributions and structure of the thesis

The structure of this thesis along with its main contributions in the literature are provided in the forthcoming paragraphs.

Chapter 2 contains several key concepts of stability and passivity that are later addressed in this thesis. More specifically, the notation used throughout this manuscript is first presented along with the necessary mathematical background to improve readability. Then, some basic information is given regarding the nature of dynamical systems and their solutions. This information is presented through applicable theorems that guarantee properties such as the existence, the uniqueness and the continuity with initial conditions. Finally, Chapter 2 discusses the notions of Lyapunov stability and passivity while presenting the most important characteristics of systems derived through the feedback interconnection of two sub-systems and several stability and passivity theorems related to this context.

The current situation and the recent developments in the area of power system stability analysis are reviewed in Chapter 3. Firstly, some useful information is provided to help the reader understand the notion of power system stability and how this is classified into various categories based on the physical nature of the occurring disturbances and the resulting instability. The different stability analysis approaches are then briefly described while providing insights on their feasibility and the technical constraints of their application. Finally, Chapter 3 provides some basic preliminaries regarding the modeling used within

the majority of the power system stability analysis studies and apparently the rest of this manuscript.

The main technical content of this PhD thesis is extensively described in Chapter 4. In particular, the network equations are appropriately formulated to form a multi-input/multi-output system expressed into the system reference frame instead of each bus local reference frame. It then appears that under such formulation, any power network with arbitrary topology constitutes a passive system even when its lossy and dynamic nature is taken into account. This result is used in the sequel for the derivation of the proposed decentralized approach for power system stability analysis and control design. The opportunities and the advantages provided by the adoption of this network formulation are extensively discussed while numerical applications and dynamic simulations are finally employed to verify its accuracy and effectiveness.

Chapter 5 describes the proposed approach for stability analysis and control design in power grids. This approach allows power system components to be incorporated into the analysis using a broad class of bus dynamics that are viewed as multi-variable input/output systems and fit to the adopted network formulation. This representation facilitates the incorporation of a variety of bus dynamics such as synchronous generators, loads, FACTS devices and inverter-based RES while considering their frequency and voltage control policies. Subsequently, certain local passivity conditions are introduced for bus dynamics. As shown, imposing these conditions on every grid-connected device guarantees the asymptotic stability of the interconnected system in a completely decentralized manner.

Several applications of the proposed passivity-based approach for power system stability analysis and control design are presented in Chapter 6. The first application comprises of a framework for Static Var Compensator (SVC) employment. This framework describes in detail a complete methodology for SVC placement, tuning and sizing that aims to enhance power system stability and robustness while minimizing the cost of SVC installation. The second section of Chapter 6 examines the applicability and the feasibility of the presented local passivity conditions on synchronous generators. These conditions are used in the sequel to improve synchronous generators' existing excitation system and effectively damp the occurring power system oscillations. An additional application of the proposed approach deals with the design of a novel, demand-side, voltage droop controller that can provide effective voltage and frequency support to the future power grids. Chapter 6 concludes with the application of the proposed passivity-based framework on RES using grid-forming inverters.

Finally, Chapter 7 provides an extensive summary of the contributions of this PhD thesis along with several intuitive comments that allow the accurate interpretation of the main

results. Various suggestions and ideas on how to possibly extend the presented work are also provided.

There are various ways in which the main contribution chapters, Chapters 4-6, connect based on their content, application and methodology. These are summarized below:

1. All contribution chapters deal with distributed approaches for stability analysis and control design in power grids and provide network independent results.

2. All stability results in Chapters 4, 5 and 6 are derived using techniques from passivity and Lyapunov analysis.

3. The analysis presented in Chapter 4 concerns power networks with arbitrary topology while Chapters 5 and 6 deal with the incorporation of various power system components into the proposed stability analysis and control design framework.

4. The analysis and the results of Chapters 5 and 6 rely on the multi-variable, reference frame network formulation presented in Chapter 4.

5. Bus dynamics in Chapters 5 and 6 are represented as multi-input/multi-output systems to fit the proposed multi-variable network formulations and cover both linear and non-linear dynamic models. Chapter 6 on the contrary, presents several applications of the proposed stability analysis and control approach using specific power system components such as synchronous generators, SVCs, loads and inverter-based RES.

The aforementioned connections among the chapters are schematically presented in Figure 1.1.

The work within Chapters 4 - 6 is based upon the following publications which have been produced during the Ph.D. course [27–36].

**Peer Reviewed Journals:**

1. C. Spanias, P. Aristidou and M. Michaelides, "A Passivity-Based Framework for Stability Analysis and Control Including Power Network Dynamics," IEEE Systems Journal, 2020.

2. C. Spanias and I. Lestas, “A system reference frame approach for stability analysis and control of power grids,” IEEE Transactions on Power Systems, vol. 34, no. 2, pp. 1105–1115, 2018.

3. A. Kasis, E. Devane, C. Spanias, and I. Lestas, “Primary frequency regulation with load-side participation Part I: stability and optimality,” IEEE Transactions on Power Systems, 2016.

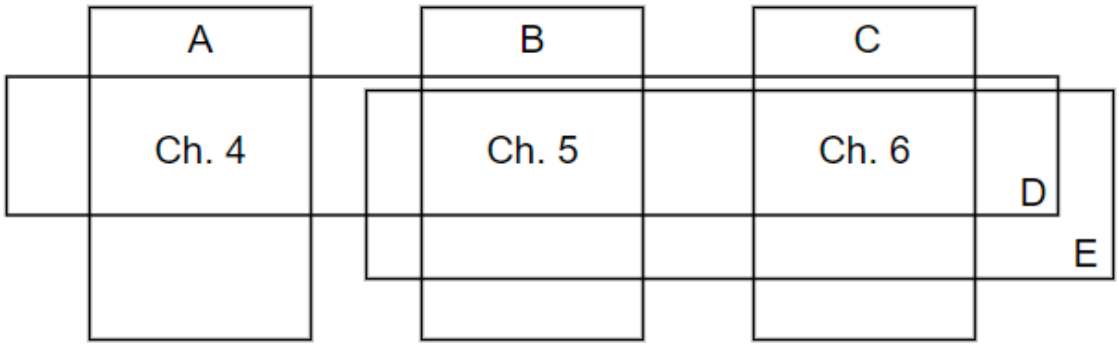


Fig. 1.1 Schematic representation of the connections among Chapters 4-6 based on the main application topics and analysis tools. The letters represent: A. Power network modeling, B. Bus dynamics/Power system components modeling, C. Applications, D. Passivity analysis techniques, E. Lyapunov analysis techniques.

**International Conference Proceedings:**

1. C. Spanias, P. Aristidou, and M. Michaelides, "A dynamical multi-input/multi-output network formulation for stability analysis in AC microgrids," in Innovative Smart Grid Technologies (ISGT) Europe, pp. 1–5, 2019.

2. C. Spanias, P. Aristidou, and M. Michaelides, "Demand-side Volt/Var/Watt regulation for effectivevoltage control in distribution grids," in Innovative Smart Grid Technologies (ISGT) Europe, pp. 1–5, 2019.

3. J. Watson, Y. Ojo, I. Lestas, and C. Spanias, "Stability of power networks with grid-forming converters," in 2019 IEEE Powertech Conference, pp. 1–6, IEEE, 2019.

4. M. Argyrou, C. Spanias, C. Marouchos, S. Kalogirou, and P. Christodoulides, "Energy management and modeling of a grid-connected BIPV system with battery energy storage," in 54th International Universities Power Engineering Conference (UPEC), pp. 1–6, IEEE, 2019.

5. C. Spanias, P. Aristidou, M. Michaelides, and I. Lestas, "Power system stability enhancement through the optimal, passivity-based, placement of SVCs," in 2018 Power Systems Computation Conference (PSCC), IEEE, 2018.

6. C. Spanias, P. Nikolaidis, and I. Lestas, "Techno-economic analysis of the potential conversion of the outdated moni power plant to a large scale research facility," in 5th International Conference on Renewable Energy Sources and Energy Efficiency, pp. 208–220, 2016.

**Book Chapters:**

1. E. Devane, A. Kasis, C. Spanias, M. Antoniou, and I. Lestas, "Distributed frequency control and demand-side management," in Smarter Energy: From Smart Metering to the Smart Grid (H. Sun, N. Hatziargyriou, L. Carpanini, H. V. Poor, and M. A. S. Fornié, eds.), ch. 9, pp. 157–192, IET, 2016.

# Chapter 2

# Theoretical background to nonlinear systems analysis

The current PhD thesis presents a detailed framework for stability analysis and control in power grids whereas the stability of various classes of dynamical systems is studied. Thus, the current chapter provides the mathematical background required to follow the presented analysis. Particularly, Section 2.1 contains the notation used throughout this manuscript while Section 2.2 provides useful information regarding dynamical systems. Several nonlinearities and nonlinear phenomena that can be met in various dynamical systems such as power grids are then provided in Section 2.3. Section 2.4 states some fundamental properties of the solutions of ordinary differential equations, i.e. existence and uniqueness, which in turn are essential for the representation of a physical system. The notion of stability of equilibrium points, namely the Lyapunov Stability, is extensively presented in Section 2.5. Finally, Section 2.6 deals with the structural property of passivity and how this can be utilized to deduce the stability of large scale systems. More detailed information on the presented analysis and the proofs of the presented theorems and lemmas can be found in [19, 21, 37, 38].

## 2.1 Notation

Within the rest of this manuscript, $\mathbb{R}$, $\mathbb{Z}$ and $\mathbb{C}$ are used to denote the set of real, natural and complex numbers, respectively. The superscript $n$ is used for the representation of the n-dimensional vectors of real/natural/complex numbers, that is $\mathbb{R}^n$, $\mathbb{Z}^n$ and $\mathbb{C}^n$. $\mathbb{R}^{n\times m}$, $\mathbb{Z}^{n\times m}$ and $\mathbb{C}^{n\times m}$ represent $n$-by-$m$ matrices of real/natural/complex numbers. Positive real and natural numbers are denoted by $\mathbb{R}^+$, $\mathbb{Z}^+$.

If $a$ and $b$ are real numbers with $a \leq b$, $[a,b]$ will denote the closed interval from $a$ to $b$ i.e. the set of all real numbers $x$ such that $a \leq x \leq b$. $[a,b)$ will denote the right-open interval from $a$ to $b$ (i.e. $a \leq x < b$) etc. No distinctions will be made between vectors and real numbers in the notation. Both vectors and real numbers will be denoted either by lower or upper case letters. Matrices will be represented only by upper case letters. Note here that $A_{ii}$ and $A_{ij}$ will be used to denote the diagonal entries and the entries corresponding to the i-th row and the j-th column of a matrix $A$, respectively.

The norm $||x||$ of a vector $x \in \mathbb{R}^n$ is a real valued function with the following properties:

1. $||x|| \geq 0$ for all $x \in \mathbb{R}^n$, with $||x|| = 0$ if and only if $x = 0$,
2. $||x+y|| \leq ||x|| + ||y||$, for all $x, y \in \mathbb{R}^n$ and
3. $||ax|| = |a|||x||$, for all $a \in \mathbb{R}$, $x \in \mathbb{R}^n$.

Consider an $n$-by-$m$ matrix $A$. The representation $A^T$ and $A^{-1}$ will be used to denote its transpose and its inverse matrix, respectively. If the matrix $A$ has the same number of rows and columns it is called square. When all entries of $A$ below the main diagonal are zero, $A$ is called an upper triangular matrix. Similarly, when all of its entries above the main diagonal are zero, $A$ is called a lower triangular matrix. $A$ is a diagonal matrix when all of its non-diagonal entries are zero. Moreover, the notation $I_n$ will be used to represent the identity matrix, i.e. the n-by-n matrix diagonal elements are equal to 1 and all other elements are equal to 0. A square matrix $B$ that is equal to its transpose, that is, $B = B^T$, is called a symmetric matrix. If instead, $B$ is equal to the negative of its transpose, that is, $B = -B^T$, then $B$ is called a skew-symmetric matrix. In complex analysis, symmetry is often replaced by the concept of Hermitian matrices, which satisfy $B^* = B$, where the star denotes the conjugate transpose of the matrix, that is, the transpose of the complex conjugate of $B$. Finally, let a symmetric matrix $D \in \mathbb{R}^{n \times n}$ and a non-zero vector $x \in \mathbb{R}^n$. This matrix is said to be:

- positive definite if and only if $x^T Dx > 0$ for all $x \in \mathbb{R}^n - \{0\}$
- positive semidefinite if and only if $x^T Dx \geq 0$ for all $x \in \mathbb{R}^n - \{0\}$
- negative definite if and only if $x^T Dx < 0$ for all $x \in \mathbb{R}^n - \{0\}$
- and negative semidefinite if and only if $x^T Dx \leq 0$ for all $x \in \mathbb{R}^n - \{0\}$.

The definiteness of the matrix D can be also deduced by its eigenvalues as follows:

- positive definite if and only if all of its eigenvalues are positive

- positive semidefinite if and only if all of its eigenvalues are non-negative
- negative definite if and only if all of its eigenvalues are negative
- and negative semidefinite if and only if all of its eigenvalues are non-positive.

The above definitions hold for complex matrices if $x^T$ is replaced by $x^*$.

For a function $f$, $\mathscr{D}(f)$ and $\mathscr{R}(f)$ are used to denote the domain and the range of $f$, respectively. The derivative of a function $f(x)$ is denoted by $\frac{df}{dx}$ or $f'$. Such function f is said to be of differentiability class $C_k$ if its k-th derivative $f^{(k)}$ exists and is continuous. The function f is invertible if there exists a function $f^{-1}$ defining the inverse function of $f$. Moreover, a function $f : \mathbb{R}^n \to \mathbb{R}$ is positive definite on a neighborhood $N$ around the origin if $f(0) = 0$ and $f(x) > 0$ for every non-zero $x \in N$. Finally, the derivative of a function $g(t)$ with respect to time is denoted either by $\frac{dg}{dt}$ or $\dot{g}$ and its Laplace transform by $\bar{g}(s) = \int_0^\infty e^{-st} g(t)dt$.

## 2.2 Dynamical System Classification

A dynamical system is a concept in mathematics where a fixed rule describes how a point in a geometrical space depends on time. Certain dynamical systems such as power systems, can also be influenced by external inputs which may represent either uncontrollable disturbances or control signals. Some dynamical systems may also have outputs representing either quantities that can be measured, or quantities that need to be regulated [21, 38].

Based on the type of their state, dynamical systems can be classified into the following categories:

1. **Continuous**, if the state takes values in Euclidean space $\mathbb{R}^n$ for some $n \geq 1$.
2. **Discrete**, if the state takes values in a finite set $\{q_1, q_2, \dots\}$ where variable $q$ denotes the state of a discrete system.
3. **Hybrid**, if part of the state takes values in $\mathbb{R}^n$ while another part takes values in a finite set.

Based on the set of times over which the state evolves, dynamical systems can be classified as:

1. **Continuous time**, if the set of times is a subset of real numbers. The term $t \in \mathbb{R}$ will be used to denote a continuous time system. The evolution of its state is described by an *ordinary differential equation (ODE)* of the following form:

$$\dot{x} = Ax$$

2. **Discrete time**, if the set of times is a subset of natural numbers. The term $k \in \mathbb{Z}$ will be used to denote a discrete time system. The evolution of its state is described by a *difference equation* of the following form:

$$x_{k+1} = Ax_k$$

3. **Hybrid time**, when the evolution is over continuous time but there are also discrete time "instants" where something "special" happens.

Continuous state systems can be further classified according to the form of the equations that describe the evolution of their state as follows:

1. **Linear**, if the evolution of the state is governed by a linear differential equation (continuous time) or difference equation (discrete time).

2. **Nonlinear**, if the evolution of the state is governed by a nonlinear differential equation (continuous time) or difference equation (discrete time).

This work deals with power system stability and control design and thus, the presented analysis will focus primarily on nonlinear, continuous state, continuous-time systems.

## 2.3 Nonlinear Models and Nonlinear Phenomena

Power systems are particularly large-scale, nonlinear dynamical systems that can be represented by a finite number of coupled first-order ODEs as follows:

$$\begin{aligned}
\dot{x}_1 &= f_1(t, x_1, \ldots, x_n, u_1, \ldots, u_p) \\
\dot{x}_2 &= f_2(t, x_1, \ldots, x_n, u_1, \ldots, u_p) \\
&\vdots \\
\dot{x}_n &= f_n(t, x_1, \ldots, x_n, u_1, \ldots, u_p)
\end{aligned}$$

where $x_i$ denotes the state of the dynamical system, The term $\dot{x}_i$ denotes the derivative of $x_i$ with respect to the time variable $t$ and $u_1, u_2, \ldots, u_p$ are specified input variables. Such a dynamical system can be represented in a more compact form using the following vector notation:

$$\dot{x} = f(t, x, u) \tag{2.1}$$

where $\dot{x} = [\dot{x}_1\ \dot{x}_2\ \ldots\ \dot{x}_n]^T$, $x = [x_1\ x_2\ \ldots\ x_n]^T$, $u = [u_1\ u_2\ \ldots u_n]^T$ and $f(t,x,u) = [f_1(t,x,u)$ $f_2(t,x,u)\ \ldots\ f_3(t,x,u)]^T$. Equation (2.1) is called the state equation and refer to $x$ and $u$ as

the state and the input of the dynamical system respectively. Sometimes, another equation i.e.

$$y = h(t,x,u) \tag{2.2}$$

is associated with (2.1). The variable $y$ is defined as the q-dimensional output vector that comprises variables of particular interest in the analysis of the dynamical system. Equation (2.2) is called the output equation and along with the equation (2.1) are denoted as the state-space model. Although dynamical systems are not always expressed in such a mathematical form, the above state model form can be derived by carefully choosing the state variables. This modelling approach will also be used throughout this thesis since the presented work focuses on the decentralized stability analysis and control of power grids. As will be shown in the following chapters, stability will be guaranteed using decentralized conditions that are directly related to certain variables of the system such as the bus voltages, the bus voltage angles, the network frequency, the line currents and the net-injected currents at each bus of the grid.

State equation can also take the form

$$\dot{x} = f(t,x) \tag{2.3}$$

which is called unforced state equation since there is no presence of an input $u$. Working with an unforced state equation does not necessarily mean that the input to the system is zero. It could be that the input has been specified as a given function of time, $u = \gamma(t)$, a given feedback function of the state, $u = \gamma(x)$, or both, $u = \gamma(t,x)$.

A special case of (2.3) arises when the function $f$ does not depend explicitly on $t$; that is,

$$\dot{x} = f(x). \tag{2.4}$$

In such case the system is said to be *autonomous* or *time invariant*. If the system is non *autonomous* (depends on t), then it is called *nonautonomous* or *time varying*.

An important concept in dealing with the state equation of a dynamical system is the concept of the equilibrium point. A point $x = \hat{x}$ is said to be an equilibrium point of (2.3) if it satisfies the condition that whenever the state of the system starts at $\hat{x}$, it will remain at $\hat{x}$ for all the future time. For the case of an autonomous system such as (2.4), the equilibrium points are the real roots of the equation

$$f(\hat{x}) = 0$$

For linear systems, the state model (2.1) - (2.2) takes the following simpler form:

$$\dot{x} = A(t)x + B(t)u \tag{2.5}$$

$$y = C(t)x + D(t)u \tag{2.6}$$

Since the analysis of nonlinear systems is complex, it is usually very helpful to use tools from linear systems analysis. The first step in analyzing a nonlinear system is usually to linearize it, if possible, about a nominal operating point and analyze the resulting linear model. Even though linearization is a powerful tool for analysis, there are two important limitations. Firstly, since linearization is an approximation in the neighborhood of an operating point, it can only predict the local behavior of the nonlinear system in the vicinity of that point. It cannot predict global behavior throughout the state space. Secondly, the dynamics of a nonlinear system are more complicated and thus, "essentially nonlinear phenomena" take place only in the presence of nonlinearity [21, 37].

It should be noted here that part of the elaborated work in this PhD thesis relies on the linearization of nonlinear dynamical models representing several power system components. In those cases, the stability results derived throughout these works refer to local stability.

## 2.4 Fundamental Properties

This section presents some fundamental properties of the solutions of ODEs, like the existence, the uniqueness and the continuous dependence on initial conditions and parameters [21]. These properties are essential for the mathematical representation of a deterministic physical system and consequently for the validity of the results that are presented in this manuscript.

### 2.4.1 Existence and Uniqueness

The necessary conditions for the existence and uniqueness of the solution of the initial value problem

$$\dot{x} = f(t,x), \quad x(t_0) = x_0 \tag{2.7}$$

are briefly presented in the forthcoming paragraphs. By a solution of (2.7) over an interval $[t_0,t_1]$, we mean a continuous function $x : [t_0,t_1] \to \mathbb{R}^n$ such that $\dot{x}(t)$ is defined and $\dot{x} = f(t,x(t))$ for all $t \in [t_0,t_1]$.

**Theorem 2.4.1** ***(Local Existence and Uniqueness)*** *Let $f(t,x)$ be piecewise continuous in $t$ and satisfy the Lipschitz condition*

$$\|f(t,x)-f(t,y)\| \leq L\|x-y\|$$

*$\forall x,y \in B = \{x \in \mathbb{R}^n \mid \|x-x_0\| \leq r\}$, $\forall t \in [t_0,t_1]$. Then, there exists some $\delta > 0$ such that the state equation $\dot{x} = f(t,x)$ with $x(t_0) = x_0$ has a unique solution over $[t_0,t_0+\delta]$.*

**Theorem 2.4.2** ***(Global Existence and Uniqueness)*** *Suppose that $f(t,x)$ is piecewise continuous in $t$ and satisfies*

$$\|f(t,x)-f(t,y)\| \leq L\|x-y\|$$

*$\forall x,y \in \mathbb{R}^n, \forall t \in [t_0,t_1]$. Then, the state equation $\dot{x} = f(t,x)$, with $x(t_0) = x_0$, has a unique solution over $[t_0,t_1]$.*

**Theorem 2.4.3** *Let $f(t,x)$ be piecewise continuous in $t$ and locally Lipschitz in $x$ for all $t \geq t_0$ and all $x$ in a domain $D \subset \mathbb{R}^n$. Let $W$ be a compact subset of $D$, $x_0 \in W$, and suppose it is known that every solution of* (2.7) *lies entirely in $W$. Then, there is a unique solution that is defined for all $t \geq t_0$.*

### 2.4.2 Dependence on initial conditions

A necessary condition for employing the state model (2.7) to represent any physical system is the continuous dependence of its solutions on initial conditions and parameters, i.e. the initial state $x_0$, the initial time $t_0$ and the function $f(t,x)$. Continuous dependence on the initial time $t_0$ can be easily deduced from the following integration

$$x(t) = x_0 + \int_{t_0}^{t} f(s,x(s))ds.$$

In order to examine the continuous dependence on the initial state $x_0$ and the function $f$ we let $y(t)$ be a solution of (2.7) that starts at $y(t_0) = y_0$ and is defined on the compact time interval $[t_0,t_1]$. The solution of (2.7) depends continuously on $y_0$, that is the initial state $x_0$ and the function $f(t,x)$, if solutions starting at nearby points are defined on the same time interval and remain close to each other in that interval. The previous statement can be examined through the following two theorems [21, 37].

**Theorem 2.4.4** *Let $f(t,x)$ be piecewise continuous in $t$ and locally Lipschitz in $x$ on $[t_0,t_1] \times W$ with a Lipschitz constant $L$, where $W \subset \mathbb{R}^n$ is an open connected set. Let $y(t)$ and $z(t)$ be*

*solutions of*

$$\dot{y} = f(t,y), \quad y(t_0) = y_0$$

*and*

$$\dot{z} = f(t,z) + g(t,z), \quad z(t_0) = z_0$$

*such that* $y(t),\ z(t) \in W$ *for all* $t \in [t_0,t_1]$. *Suppose that*

$$||g(t,x)|| \leq \mu, \quad \forall t \in [t_0,t_1] \ \times \ W$$

*for some* $\mu > 0$. *Then*

$$||y(t) - z(t)|| \leq ||y_0 - z_0|| e^{L(t-t_0)} + \frac{\mu}{L}\left(e^{L(t-t_0)} - 1\right)$$

$\forall t \in [t_0,t_1]$.

**Theorem 2.4.5** *Let* $f(t,x,\lambda)$[1] *be piecewise continuous in* $(t,x,\lambda)$ *and locally Lipschitz in* $x$ *on* $[t_0,t_1] \ \times \ D \ \times \ \{||\lambda - \lambda_0|| \leq c\}$, *where* $D \subset \mathbb{R}^n$ *is an open connected set. Let* $y(t,\lambda_0)$ *be a solution of* $\dot{x} = f(t,x,\lambda_0)$ *with* $y(t_0,\lambda_0) = y_0 \in D$. *Suppose that* $y(t_0,\lambda_0)$ *is defined and belongs to D for all* $t \in [t_0,t_1]$. *Then, given* $\varepsilon > 0$, *there is* $\delta > 0$ *such that if*

$$||z_0 - y_0|| < \delta \quad \textit{and} \quad ||\lambda - \lambda_0|| < \delta$$

*then there is a unique solution* $z(t,\lambda)$ *of* $\dot{x} = f(t,x,\lambda)$ *defined on* $[t_0,t_1 l$, *with* $z(t_0,\lambda) = z_0$, *and* $z(t,\lambda)$ *satisfies*

$$||z(t,\lambda) - y(t,\lambda_0)|| < \varepsilon \quad \forall t \in [t_0,t_1].$$

## 2.5 Lyapunov Stability

The current section deals with the stability analysis of the equilibria of dynamical systems, namely the Lyapunov Stability. Particularly, Lyapunov stability analysis is described in the following paragraphs through some of the most important stability definitions and theorems which can give sufficient conditions for the stability or the asymptotic stability of a system. It should be highlighted that Lyapunov stability theory is extensively used in power systems (i.e. for the design of various frequency and voltage regulation schemes) since it constitutes a powerful tool for alleging whether a system is stable / asymptotically stable or not [21, 37].

[1] In order to show whether the state equation (2.7) continuously depends on the initial state we adopt the mathematical representation $f(t,x,\lambda)$. The constant parameters $\lambda$ could represent physical parameters of the system, and the study of perturbation of these parameters accounts for modeling errors or changes in the parameter values due to aging.

### 2.5.1 Invariant Sets

Consider the autonomous dynamical system described by (2.4) with initial conditions $x(0) = x_0$ and state $x \in \mathbb{R}^n$. $f$ is assumed to be a Lipschitz continuous function while the unique trajectory of (2.4) is denoted by $x(.)$.

**Definition 2.5.1** ***(Invariant Set)*** *A set of states $S \subseteq \mathbb{R}^n$ of* (2.4) *is called an invariant set of* (2.4) *if for all $x_0 \in S$ and for all $t \geq 0$, $x(t) \in S$.*

An important class of invariant sets are the equilibrium points of a dynamical system. Thus, before proceeding with notions and results on stability, it is necessary to define here what an equilibrium is.

**Definition 2.5.2** *A state $\hat{x} \in \mathbb{R}^n$ is called an equilibrium of* (2.4) *if $f(\hat{x}) = 0$.*

For the sake of completeness, it should be noted that limit cycles constitute another important class of invariant sets that may be observed in systems of dimension 2 or higher. In higher dimensions, even more exotic types of invariant sets can be found, such as the invariant torus and the chaotic attractor.

### 2.5.2 Stability Definitions

Stability is the most commonly studied property of invariant sets. An invariant set is called stable if trajectories starting close to it remain close to it and unstable if they do not. An invariant set is called asymptotically stable if it is stable and in addition trajectories that they start close to it converge to it as $t \to \infty$. The main stability definitions of equilibria are stated in the following paragraphs. Similar definitions can be derived for more general types of invariant sets.

**Definition 2.5.3** ***(Stable equilibrium)*** *An equilibrium, $\hat{x}$, of* (2.4) *is called stable if for all $\varepsilon > 0$ there exists $\delta > 0$ such that $\|x_0 - \hat{x}\| < \delta$ implies that $\|x(t) - \hat{x}\| < \varepsilon$ for al $t \geq 0$. Otherwise the equilibrium is said to be unstable.*

**Definition 2.5.4** ***(Asymptotically stable equilibrium)*** *An equilibrium, $\hat{x}$, of* (2.4) *is called locally asymptotically stable if it is stable and there exists $M > 0$ such that $\|x_0 - \hat{x}\| < M$ implies that $\lim_{t\to\infty} x(t) = \hat{x}$. The equilibrium is called globally asymptotically stable if this holds for all $M > 0$.*

Another important term that is directly related to the stability analysis of equilibria is the **domain of attraction**. The domain of attraction of an asymptotically stable equilibrium is the set of all $x_0$ for which $x(t) \to \hat{x}$. By definition, the domain of attraction of a globally asymptotically stable equilibrium is the entire state space $\mathbb{R}^n$. For more information readers can refer to [39–41].

### 2.5.3 Linearization and Lyapunov's Indirect Method

Useful information regarding the stability of an equilibrium can be deduced through the linearization of the nonlinear system. This method is widely used in power systems as well to facilitate the analysis of power grids which are mainly complex, nonlinear systems. The following paragraphs provide the most important results of this method.

Consider the Taylor series expansion of the vector field $f : \mathbb{R}^n \to \mathbb{R}^n$ about $x = \hat{x}$.

$$\begin{aligned} f(x) =& f(\hat{x}) + A(x-\hat{x}) + \text{ higher order terms in } (x-\hat{x}) \\ =& A(x-\hat{x}) + \text{ higher order terms in } (x-\hat{x}) \end{aligned}$$

where

$$A = \begin{pmatrix} \frac{\partial f_1}{\partial x_1} & \cdots & \frac{\partial f_1}{\partial x_n} \\ \vdots & \vdots & \vdots \\ \frac{\partial f_n}{\partial x_1} & \cdots & \frac{\partial f_n}{\partial x_n} \end{pmatrix}$$

Setting $\delta x = x - \hat{x}$ and differentiating leads to

$$\dot{\delta x} = A\delta x + \text{ higher order terms in } \delta x$$

Since the analysis is carried out near the equilibrium, the higher order terms can be neglected. Thus, the behavior of the nonlinear system close to the equilibrium is similar to that of its linearization

$$\dot{\delta x} = A\delta x \tag{2.8}$$

and it can be deduced through the following theorem.

**Theorem 2.5.1** ***Lyapunov's indirect method*** *Let $\hat{x} = 0$ be the equilibrium of the linear system* (2.8)*. Then, the origin is*

1. *asymptotically stable if and only if all eigenvalues of A have negative real parts,*
2. *unstable if there exists an eigenvalue with positive real part.*

*If one or more eigenvalues the matrix A are zero, then the behavior of the nonlinear system* (2.4) *is indefinable.*

Although linearization constitutes a powerful tool for studying the stability of equilibria (and other similar interesting local properties of nonlinear dynamical systems), it has several significant disadvantages. The most important are stated below:

- It is inconclusive when the linearization is stable but not asymptotically stable.
- It provides no information about the domain of attraction.

### 2.5.4 Lyapunov Functions and the Direct Method

Apart from the Lyapunov's indirect method, the stability analysis of a nonlinear system's equilibria can be carried out using Lyapunov functions as well. This method, namely the Lyapunov's direct method, is crucial since it can provide important information regarding the region of attraction of an equilibrium point when employed along with La Salle's Invariance Principle. The presentation of several methods for deriving Lyapunov's functions is beyond the scope of this dissertation and, it is, therefore, omitted. For more information on Lyapunov Stability and the construction of candidate Lyapunov functions, the reader can consult [21, 37].

Let now the dynamical system

$$\dot{x} = f(x)$$

that has an equilibrium at $\hat{x}$. Without loss of generality we assume that $\hat{x} = 0$, to simplify notation and provide the following theorems regarding the stability of the system about this equilibrium.

**Theorem 2.5.2** ***(Lyapunov Stability)*** *Assume there exists a differentiable function $V : S \to \mathbb{R}$ defined on some open region $S \subset \mathbb{R}^n$ containing the origin, such that*

1. $V(0) = 0$
2. $V(x) > 0$ *for all* $x \in S$ *with* $x \neq 0$
3. $\dot{V}(x) \leq 0$ *for all* $x \in S$

*Then $\hat{x} = 0$ is a stable equilibrium of $\dot{x} = f(x)$.*

Here $\dot{V}$ denotes the derivative of $V$ along the trajectories of the dynamical system, i.e.

$$\dot{V}(x) = \sum_{i=1}^{n} \frac{\partial V}{\partial x_i}(x)\dot{x}_i = \sum_{i=1}^{n} \frac{\partial V}{\partial x_i}(x) f_i(x) = \nabla V(x) f(x). \tag{2.9}$$

The equation (2.9) is also called the *Lie Derivative* of the function $V$ along the vector field $f$. A function satisfying the conditions of the above theorem is called a *Lyapunov function*.

**Theorem 2.5.3** ***(Lyapunov Asymptotic Stability)*** *Assume there exists a differentiable function $V : S \to \mathbb{R}$ defined on some open region $S \subset \mathbb{R}^n$ containing the origin, such that*

1. $V(0) = 0$
2. $V(x) > 0$ *for all* $x \in S$ *with* $x \neq 0$
3. $\dot{V}(x) < 0$ *for all* $x \in S$ *with* $x \neq 0$

*Then $\hat{x} = 0$ is a locally asymptotically stable equilibrium of $\dot{x} = f(x)$.*

**Theorem 2.5.4** ***(LaSalle's Invariance Principle)*** *Let $S \subseteq \mathbb{R}^n$ be a compact (i.e. closed and bounded) invariant set. Assume there exists a differentiable function $V : S \to \mathbb{R}$ such that*

$$\dot{V}(x) \leq 0, \quad \forall x \in S$$

*Let $M$ be the largest invariant set contained in $[x \in S \mid \dot{V}(x) = 0]$ (the set of $x \in S$ for which $\dot{V}(x) = 0$). Then all trajectories starting in $S$ approach $M$ as $t \to \infty$.*

It is highlighted here that theorems 2.5.3 and 2.5.4 can be utilized to estimate the regions of attraction of the equilibria of a nonlinear system. Since the system can never leave sets of the form $\{x \in \mathbb{R}^n \mid \dot{V}(x) \leq c\}$ any such set contained in $S$ has to be a part of the domain of attraction of the equilibrium. Furthermore, the conditions of the theorems are sufficient but not necessary. If one can find a Lyapunov function that meets the conditions stated in the above theorems, we know that the equilibrium is stable or asymptotically stable. If such a function cannot be found, we can not draw an immediate conclusion. Note here that the region of attraction is a significant term in power systems and small-signal analysis. Since one has to determine whether a small disturbance occurring in the network can lead to instability or not, it is necessary to specify a boundary region where the reliable operation of the system under consideration is ensured.

At this point, some general instructions for finding an appropriate Lyapunov function is provided. However, it is necessary to mention that the construction of a Lyapunov function is

more of an art than an exact science. Particularly for physical systems, it is better trying to guess Lyapunov functions related to the energy of the system. Another popular choice is the quadratic functions. The simplest choice is

$$V(x) = \|x\|^2.$$

More generally, we can also try

$$V(x) = x^T P x \tag{2.10}$$

where $P$ is a symmetric, positive definite matrix. Quadratic Lyapunov functions always work for linear systems. For example, consider the following linear autonomous system

$$\dot{x} = Ax$$

and the candidate Lyapunov function (2.10) for some $P = P^T > 0$. Differentiating leads to

$$\begin{aligned}\dot{V}(x) =& \dot{x}^T P x + x^T P \dot{x} \\ =& (Ax)^T P x + x^T P (Ax) \\ =& x^T (A^T P + PA) x\end{aligned}$$

Therefore, a suitable Lyapunov function can be found if one can define a matrix $P = P^T > 0$ such that $x^T (A^T P + PA)x < 0$ for all $x$. This is possible if for some $Q = Q^T > 0$ the Lyapunov matrix equation

$$A^T P + PA = -Q \tag{2.11}$$

has a symmetric, positive definite solution $P = P^T > 0$.

**Theorem 2.5.5** ***(Linear Lyapunov Stability)*** *For any matrix A the following statements are equivalent*

1. *All eigenvalues of A have negative real parts.*
2. *We can find $P = P^T > 0$ that solves* (2.11) *for some $Q = Q^T > 0$.*

The method for the construction of an appropriate Lyapunov function for dynamical systems that contain memoryless nonlinearities is quite similar. More specifically, consider the memoryless nonlinearity $h(.)$ such that $h(0) = 0$ and $zh(z) > 0$ for $z \neq 0$. If the input to such nonlinearity is a state variable, that is $x_i$, then a positive function that could be used is

$$V(x) = \int_0^{x_i} h(z)dz.$$

In this case we get

$$\frac{\partial V}{\partial x_i}(x) = h(x_i).$$

If the quadratic candidate Lyapunov function does not work and the dynamical system under consideration has such memoryless nonlinearities, a possible guess would be

$$V(x) = x^T P x + \sum_{i=1}^{n} \int_0^{x_i} h_i(z) dz.$$

## 2.6 Passivity

One significant, structural property that can facilitate the stability analysis of large-scale, nonlinear systems is the notion of passivity. Passivity is an input/output property that can be easily applied to such systems and determine whether these are stable or not and design appropriate control mechanisms. It also relates nicely to Lyapunov and $\mathscr{L}_2$ stability. Passivity, whose use in Power Systems Analysis has been continuously expanding, is the key tool utilized for the presented analysis in the current PhD thesis and thus, a detailed presentation of its main aspects is provided. Specifically, this section defines first the passivity of memoryless nonlinearities and dynamical systems represented as state models. The terms of positive real and strictly positive-real systems are then introduced while explaining how one can deduce the passivity of a system in the frequency domain. The connection between passivity and stability is stated last by providing the main passivity theorems for Feedback Systems [19, 21, 37].

### 2.6.1 Memoryless Functions

This paragraph presents how passivity of the memoryless function $y = h(t,y)$ is defined, where $h : [0,\infty) \times \mathbb{R}^p \to \mathbb{R}^p$. Considering that this function constitutes a multi-input/multi-output system with input the vector $u \in \mathbb{R}^n$, the following definition is provided.

**Definition 2.6.1** *The system $y = h(t,u)$ is*

- *passive if $u^T y \geq 0$.*
- *lossless if $u^T y = 0$.*
- *input-feedforward passive if $u^T y \geq u^T \varphi(u)$ for some function $\varphi$.*
- *input strictly passive if $u^T y \geq u^T \varphi(u)$ and $u^T \varphi(u) > 0, \forall u \neq 0$.*

- *output-feedback passive if* $u^T y \geq y^T p(y)$ *for some function* $p$.
- *output strictly passive if* $u^T y \geq y^T p(y)$ *and* $y^T p(y) > 0, \forall y \neq 0$.

*In all cases, the inequality should hold for all* $(t,u)$.

As will be shown in Chapter 4, the above definition will be employed to proof the passivity of the network when the latter is formulated based on the presented approach.

### 2.6.2 State Models

This paragraph defines passivity for dynamical systems that are described by the state model

$$\dot{x} = f(x,u) \tag{2.12}$$

$$y = h(x,u) \tag{2.13}$$

where $f : \mathbb{R}^n \times \mathbb{R}^p \to \mathbb{R}^n$ is locally Lipschitz, $h : \mathbb{R}^n \times \mathbb{R}^p \to \mathbb{R}^p$ is continuous, $f(0,0) = 0$, and $h(0,0) = 0$. The above system has the same number of inputs and outputs and is passive if the energy absorbed over any period of time $[0,t]$ is greater than or equal to the increase in the energy stored in it over the same period; that is,

$$\int_0^t u(s)y(s)ds \geq V(x(t)) - V(x(0)) \tag{2.14}$$

where $V(x)$ is the energy stored in network. If (2.14) holds with strict inequality, then the difference between the absorbed energy and the increase in the stored energy must be the energy dissipated in the system. Since (2.14) must hold for every $t \geq 0$, the instantaneous power inequality

$$u(t)y(t) \geq \dot{V}(x(t),u(t)) \tag{2.15}$$

must hold for all $t$; that is, the power flow into the network must be greater than or equal to the rate of change of the energy stored in the system. We can investigate inequality (2.15) by calculating the derivative of $V$ along the trajectories of the system. The following definition states the terms of passivity as these derived using the function $V$ of such system.

**Definition 2.6.2** *The system* (2.12)-(2.13) *is said to be passive if there exists a continuously differentiable positive semidefinite function* $V(x)$ *(called the storage function) such that*

$$u^T y \geq \dot{V} = \frac{\partial V}{\partial x} f(x,u), \quad \forall (x,u) \in \mathbb{R}^n \times \mathbb{R}^p \tag{2.16}$$

*Moreover, it is said to be*

- *lossless if* $u^T y = \dot{V}$.
- *input-feedforward passive if* $u^T y \geq \dot{V} + u^T \varphi(u)$ *for some function* $\varphi$.
- *input strictly passive if* $u^T y \geq \dot{V} + u^T \varphi(u)$ *and* $u^T \varphi(u) > 0, \forall u \neq 0$.
- *output-feedback passive if* $u^T y \geq \dot{V} + y^T p(y)$ *for some function* $p$.
- *output strictly passive if* $u^T y \geq \dot{V} + y^T p(y)$ *and* $y^T p(y) > 0, \forall y \neq 0$.
- *strictly passive if* $u^T y \geq \dot{V} + \psi(x)$ *for some positive definite function* $\psi$.

*In all cases, the inequality should hold for all* $(x,u)$.

The above definition reads almost the same as definition for memoryless functions except for the presence of a storage function $V(x)$. If the convention that $V(x) = 0$ for a memoryless function is adopted, the above definition can be used for both state models and memoryless functions.

### 2.6.3 Positive Real Transfer Functions

As mentioned above, the passivity-based stability analysis of dynamical systems is carried out in the time domain and relies on the explicit construction of the storage function $V(x)$. Similarly to the case of Lyapunov functions, the task of finding an appropriate storage function for a nonlinear system is difficult. Although this procedure becomes significantly easier for linear or systems linearized around an equilibrium, the passivity of such systems can be easily deduced in the frequency domain via the positive realness of its corresponding transfer function matrix. More specifically, a linear system represented by a positive real transfer function is passive as well. Similarly, strict positive realness implies strict passivity. The previous statements are presented through the following definitions for proper rational transfer function matrices [19, 21].

**Definition 2.6.3** *A* $p \times p$ *proper rational transfer function matrix* $G(s)$ *is called positive real if*

- *poles of all elements of* $G(s)$ *are in* $\mathrm{Re}(s) \leq 0$.
- *for all real* $\omega$ *for which* $j\omega$ *is not a pole of any element of* $G(s)$*, the matrix* $G(j\omega) + G^T(-j\omega)$ *is positive semidefinite, and*
- *any pure imaginary pole* $j\omega$ *of any element of* $G(s)$ *is a simple pole and the residue matrix* $\lim_{s \to j\omega}(s - j\omega)G(s)$ *is positive semidefinite Hermitian*

*The transfer function $G(s)$ is called strictly positive real if $G(s-\varepsilon)$ is positive real for some $\varepsilon > 0$.*

When $p = 1$, the second condition of the above definition reduces to $\mathrm{Re}[G(j\omega)] \geq 0, \forall \omega \in \mathbb{R}$ which holds when the Nyquist plot of $G(j\omega)$ lies entirely in the closed right-half complex plane. This is a condition that can be satisfied only if the relative degree of the transfer function is zero or one.

The next lemma gives an equivalent characterization of strictly positive real transfer functions.

**Lemma 2.6.1** *Let $G(s)$ be a $p \times p$ proper rational transfer function matrix, and suppose $\det[G(s)+G^T(-s)]$ is not identically zero. Then $G(s)$ is strictly positive real if and only if*

- *$G(s)$ is Hurwitz; that is, poles of all elements of $G(s)$ have negative real parts,*
- *$G(j\omega)+G^T(j\omega)$ is positive definite for all $\omega \in \mathbb{R}$, and*
- *either $G(\infty)+G^T(\infty)$ is positive definite or it is positive semidefinite and $\lim_{\omega\to\infty} \omega^2 M^T[G(j\omega)+G^T(-j\omega)]M$ is positive definite for any $p \times (p-q)$ full-rank matrix $M$ such that $M^T[G(\infty)+G^T(\infty)]M = 0$ where $q = rank[G(\infty)+G^T(\infty)]$.*

For linear systems expressed in the form (2.5)-(2.6), the passivity property can be deduced from the positive realness of the transfer function matrix of the system as shown within the next two lemmas, which are known, respectively, as the *positive real lemma* and the *Kalman - Yakubovich - Popov lemma*. These lemmas provide an algebraic characterization of positive real and strictly positive real transfer functions.

**Lemma 2.6.2** ***(Positive Real)*** *Let $G(s) = C(sI-A)^{-1}B+D$ be a $p \times p$ transfer function matrix where $(A,B)$ is controllable and $(A,C)$ is observable. Then $G(s)$ is positive real if and only if there exist matrices $P = P^T > 0$, $L$, and $W$ such that*

$$\begin{aligned} PA + A^T P &= -L^T L \\ PB &= C^T - L^T W \\ W^T W &= D + D^T \end{aligned}$$

*For systems with $D = 0$ the above condition is reduced to*

$$\begin{aligned} PA + A^T P &< 0 \\ PB &= C^T \end{aligned}$$

**Lemma 2.6.3** ***(Kalman - Yakubovich - Popov)*** *Let $G(s) = C(sI - A)^{-1}B + D$ be a $p \times p$ transfer function matrix where $(A,B)$ is controllable and $(A,C)$ is observable. Then $G(s)$ is strictly positive real if and only if there exist matrices $P = P^T > 0$, $L$, and $W$, and a positive constant $\varepsilon$ such that*

$$\begin{aligned} PA + A^T P &= -L^T L - \varepsilon P \\ PB &= C^T - L^T W \\ W^T W &= D + D^T \end{aligned}$$

**Lemma 2.6.4** *The linear time-invariant minimal realization*

$$\begin{aligned} \dot{x} &= Ax + Bu \\ y &= Cx + Du \end{aligned}$$

*with $G(s) = C(sI - A)^{-1}B + D$ is*

- *passive if $G(s)$ is positive real;*
- *strictly passive if $G(s)$ is strictly positive real.*

### 2.6.4 Passivity Theorems for Feedback Systems

Considering that power systems consist of a large number of subsystems, they can be studied as a large interconnected system where all the power system components, i.e. the synchronous generators, the loads, the FACTS and the converter interfaced devices are connected to the power network in a feedback formation. Hence, it is useful to present here the most important passivity theorems related to feedback systems and provide useful information regarding the relationship between the structural property of passivity and the stability [19, 21].

Consider the feedback connection of the Figure 2.1 where each of the feedback components $H_1$ and $H_2$ is either a time-invariant dynamical system represented by the state model

$$\dot{x}_i = f_i(x_i, e_i) \tag{2.17}$$

$$y_i = h_i(x_i, e_i) \tag{2.18}$$

or a (possibly time-varying) memoryless function represented by

$$y_i = h_i(t, e_i) \tag{2.19}$$

Note here that $u_1, y_1, u_2$ and $y_2$ could be vectors of the same dimension.

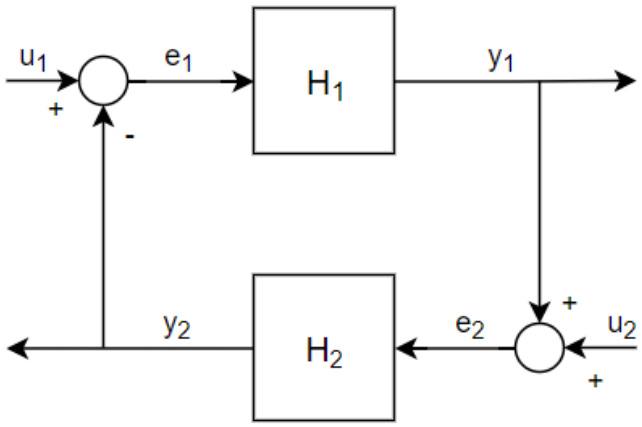


Fig. 2.1 A closed-loop system represented as a feedback interconnection of the systems $H_1$ and $H_2$ [21].

Since the passivity properties of the feedback components $H_1$ and $H_2$ are used to deduce the stability or the asymptotic stability of the interconnected system, it is required the feedback connection to have a well-defined state model. When both components $H_1$ and $H_2$ are dynamical systems, the closed-loop state model takes the form of (2.12) - (2.13) where

$$x = \begin{bmatrix} x_1 \\ x_2 \end{bmatrix}, \quad u = \begin{bmatrix} u_1 \\ u_2 \end{bmatrix}, \quad \text{and} \quad y = \begin{bmatrix} y_1 \\ y_2 \end{bmatrix}$$

Assuming that $f$ is locally Lipschitz, $h$ is continuous, $f(0,0) = 0$ and $h(0,0) = 0$, it can be easily verified that the interconnected system will have a well-defined state model if the equations

$$e_1 = u_1 - h_2(x_2, e_2) \tag{2.20}$$

$$e_2 = u_2 + h_1(x_1, e_1) \tag{2.21}$$

have a unique solution $(e_1, e_2)$ for every $(x_1, x_2, u_1, u_2)$. The properties $f(0,0) = 0$ and $h(0,0) = 0$ follow from $f_i(0,0) = 0$ and $h_i(0,0) = 0$. It is also easy to see that (2.20) and (2.21) will always have a unique solution if $h_1$ is independent of $e_1$ or $h_2$ is independent of $e_2$. In this case, the functions $f$ and $h$ of the closed-loop state model inherit the smoothness properties of the functions $f_i$ and $h_i$ of the feedback components. In particular, if $f_i$ and $h_i$ are locally Lipschitz, so are $f$ and $h$.

When one component of the interconnected system, i.e. $H_1$, is a dynamical system, while the other one is a memoryless function, the closed loop state model takes the form

$$\dot{x} = f(t,x,u) \tag{2.22}$$

$$y = h(t,x,u) \tag{2.23}$$

where

$$x = \begin{bmatrix} x_1 \\ x_2 \end{bmatrix}, \quad u = \begin{bmatrix} u_1 \\ u_2 \end{bmatrix}, \quad \text{and} \quad y = \begin{bmatrix} y_1 \\ y_2 \end{bmatrix}$$

Assuming that $f$ is piecewise continuous in $t$ and locally Lipschitz in $(x,u)$, $h$ is piecewise continuous in $t$ and continuous $(x,u)$, $f(t,0,0) = 0$ and $h(t,0,0) = 0$, the feedback connection will have a well-defined state model if the equations

$$e_1 = u_1 - h_2(t,e_2) \tag{2.24}$$

$$e_2 = u_2 + h_1(x_1,e_1) \tag{2.25}$$

have a unique solution $(e_1,e_2)$ for every $(x_1,t,u_1,u_2)$. This will be always the case when $h_1$ is independent of $e_1$. The case when both components are memoryless functions is less important and follows trivially as a special case when the state $x$ does not exist. In this case, the feedback connection is represented by $y = h(t,u)$.

The starting point of the analysis provided in this section is the following fundamental property.

**Theorem 2.6.1** *The feedback connection of two passive systems is passive.*

By exploiting the stability properties that are satisfied by passive systems, Theorem 2.6.1 can be used to arrive at some straightforward conclusions on the stability of any closed loop system such as the one presented in Figure 2.1. We therefore quote below the main theorems connecting the terms of Lyapunov stability and passivity for nonlinear systems.

**Theorem 2.6.2** *Consider the feedback connection of two time-invariant dynamical systems of the form* (2.17) - (2.18)*. The origin of the closed-loop system (when* $u = 0$*) is asymptotically stable if*

- *both feedback components are strictly passive*
- *both feedback components are output strictly passive and zero-state observable, or*

- *one component is strictly passive and the other one is output strictly passive and zero-state observable.*

*Furthermore, if the storage function for each component is radially unbounded, the origin is globally asymptotically stable.*

When the feedback connection has a dynamical system as one component and a memoryless function as the other component, we can resort to Lyapunov analysis using the storage function of the dynamical system as a Lyapunov function candidate. However, it is important to distinguish the analysis between time-invariant and time-varying memoryless functions. In the latter case the closed-loop system will be nonautonomous and therefore the invariance principle cannot be applied. These two cases are treated separately in the next two theorems.

**Theorem 2.6.3** *Consider the feedback connection for strictly passive, time-invariant, dynamical system of the form* (2.17) - (2.18) *with a passive (possibly time-varying) memoryless function of the form* (2.19)*. Then, the origin of the closed-loop system* (2.22) *(when* $u = 0$*) is uniformly asymptotically stable. Furthermore, if the storage function for the dynamical system is radially unbounded, the origin will be globally uniformly asymptotically stable.*

**Theorem 2.6.4** *Consider the feedback connection of a time-invariant dynamical system* $H_1$ *of the form* (2.17) - (2.18) *with a time-invariant memoryless function* $H_2$ *of the form* (2.19)*. Suppose that* $H_1$ *is zero-state observable and has a positive definite storage function, which satisfies*

$$e_1^T y_1 \geq \dot{V}_1 + y_1^T p_1(y_1) \tag{2.26}$$

*and that* $H_2$ *satisfies*

$$e_2^T y_2 \geq e_2^T \varphi_2(e_2) \tag{2.27}$$

*Then, the origin of closed-loop system* (2.22) *(when* $u = 0$*)is asymptotically stable if*

$$\upsilon^T [p_1(\upsilon) + \varphi_2(\upsilon)] > 0, \quad \forall \upsilon \neq 0 \tag{2.28}$$

*Furthermore, if* $V_1$ *is radially unbounded, the origin will be globally asymptotically stable.*

# Chapter 3

# Related Literature

As discussed in Chapter 1, this thesis introduces a novel decentralized approach for stability analysis and control design in existing complex power systems. It is, therefore, necessary to present here some information regarding power system stability and the developments that have been made lately in the recent literature. In this context, Chapter 3 first provides a detailed explanation of the notion of power system stability and then describes how it is classified to effectively address the complex instability phenomena occurring across a power grid. The current chapter also reviews the existing approaches for power system stability analysis, including useful insights about their applicability and effectiveness. Finally, some preliminaries regarding the modeling used within the majority of these studies are also provided to improve the readability of this manuscript.

## 3.1 Introduction to power system stability

### 3.1.1 The notion of power system stability

Power system stability has been widely recognized as one of the most significant open problems in power systems literature. The importance of power system stability lies in the fact that it plays a significant role in the secure and reliable system operation [42], especially during the last decades that power systems have been through radical structural and operational changes. Its study dates back in the 1920s, where engineers wanted to ensure the reliable operation of parallel-connected AC generators [43, 44]. Recently, the stability of power systems has gained increased attention as a result of many major blackouts. These blackouts were the result of a variety of power system instability phenomena and led to serious technical and financial problems [45, 46].

Historically, the dominant stability problem on most systems was caused by various transient instability phenomena which in turn gained the focus of the industry's attention concerning system stability. As power systems have evolved through the continuing growth in interconnections, the use of new technologies and controls, and the increased operation in highly stressed conditions, different forms of system instability have emerged. For example, phenomena related to voltage stability, frequency stability and inter-area oscillations have now become greater concerns than in the past [47].

Before presenting in detail the above types of instability and how they are interrelated, is essential to provide an accurate definition of power system stability. Such a definition was presented in [47] and is provided here unchanged:

*'Power system stability is the ability of an electric power system, for a given initial operating condition, to regain a state of operating equilibrium after being subjected to a physical disturbance, with most system variables bounded so that practically the entire system remains intact'.*

Considering that the power system is a highly nonlinear system that operates under constantly changing conditions, the above definition implies that the stability of the system depends on the initial operating condition as well as the nature of the disturbance. Thus, power system stability is a property of the system motion around an equilibrium set, i.e., the initial operating condition.

### 3.1.2 Time scales of power system dynamic phenomena

Until the early 2010s, power system stability studies primarily dealt with the analysis of fairly slow, electromechanical phenomena. As rotating machines were the primary source of generation, the dynamic behavior of power systems was predominantly determined by the dynamic performance of synchronous generators and their controls as well as the dynamic performance of the loads. Fast transients related to the network and other fast-response devices were considered out of scope and thus neglected. Moreover, for the purposes of stability analysis in the time frame of interest, all fast electromagnetic transients were omitted as they typically decay rapidly [48]. A key aspect of these simplifications is the assumption that voltage and current waveforms are dominated by the fundamental frequency component of the system (50 or 60 Hz). This assumption allowed the modeling of the electrical network using the steady-state voltage and current phasors, which is also known as a quasi-static phasor modeling approach [49].

Nevertheless, during the last years, electric power systems have experienced a rapid integration of converter interfaced technologies. Among these new technologies are wind and photovoltaic generation, energy storage devices, FACTS devices, HVDC lines and power

electronic interfaced loads. With such an increasing integration of converter interfaced technologies, the dynamic response of power systems became faster and arose new serious stability concerns which need to be appropriately characterized, classified and defined [50].

In this context, it is necessary to present here the various classes of dynamic phenomena in power systems. As will be discussed in the following paragraphs, this categorization is very helpful in classifying stability for a system that is subjected to disturbances varying between a few microseconds and several seconds. In particular, an electric power system may encounter four types of dynamic phenomena, i.e., the wave phenomena, the electromagnetic phenomena, the electromechanical phenomena and the thermodynamic phenomena. The time scales of these phenomena are presented in Figure 3.1. Moreover, Figure 3.2 depicts the time scales for various classes of events occurring in power systems. As can be observed, the time scale related to the converter interfaced technologies ranges from a few microseconds to several milliseconds in contrast to synchronous generators whose dynamic response is significantly slower. Taking into account the proliferation of converter interfaced devices, faster dynamics will, therefore, gain more prominence when analyzing the future power grids and the traditional power system modelling approaches shall be revisited.

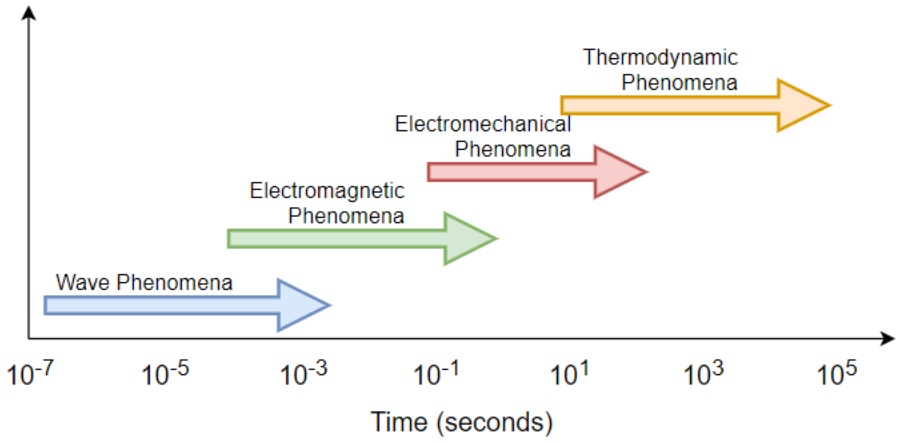


Fig. 3.1 Time scales of power system dynamic phenomena [50].

### 3.1.3 Classification of power system stability

A power grid constitutes a high-order multi-variable system whose dynamic response is influenced by a variety of devices with different characteristics and response rates. As discussed above, stability is a condition of equilibrium between opposing forces [47, 50]. Depending on the network topology, system operating condition and the occurring disturbance, these opposing forces may face a sustained imbalance leading to different forms of instability.

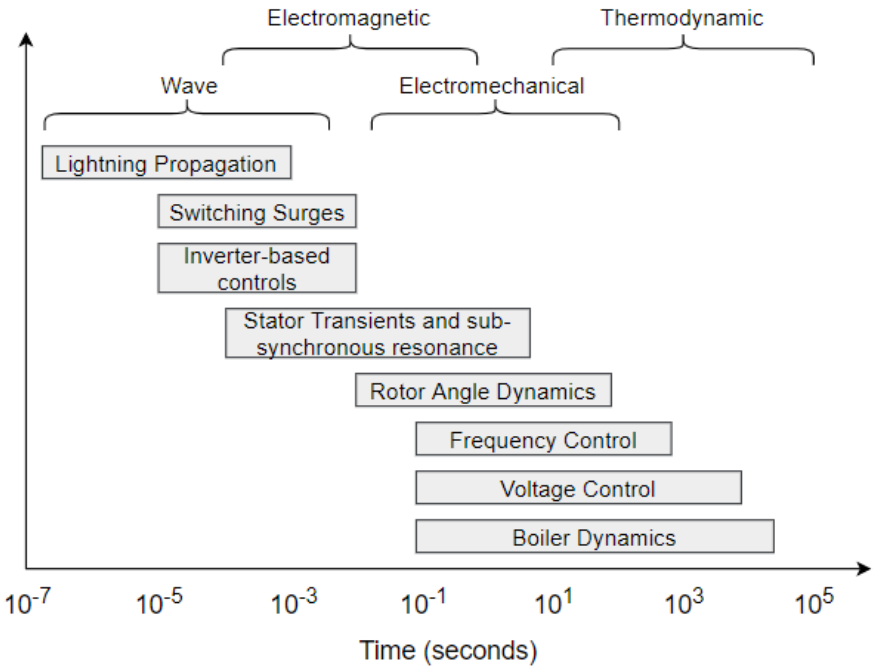


Fig. 3.2 Power system time scales [50].

Although stability is a single problem, the various forms of instabilities that a power system may undergo cannot be properly understood and analyzed. Considering the high dimensionality and complexity of stability problems, several simplifying assumptions are necessary to analyze specific types of problems using an appropriate degree of detail of system representation and appropriate analytical techniques. Stability analysis in power systems is greatly facilitated by the classification of stability into appropriate categories [48]. Classification is also essential for meaningful practical analysis and resolution of power system stability problems. According to [47, 48], power system stability is classified based on the following considerations:

- The physical nature of the resulting mode of instability as indicated by the main system variable in which instability can be observed.
- The size of the disturbance considered, which influences the method of calculation and prediction of stability.
- The devices, processes, and the time span that must be taken into consideration to assess stability.

Figure 3.3 gives the overall picture of the power system stability problem which is distinguished into the following categories:

1. *Resonance stability* refers to the ability of the power system to overcome the sub-synchronous oscillations that often occur across the grid. This sub-synchronous resonance may be associated with an electromechanical resonance or entirely electrical resonance and can manifest in two possible forms: (i) due to a resonance between series compensation and the mechanical torsional frequencies of the generator shaft and (ii) due to a resonance between series compensation and the electrical characteristics of the generator [50].

2. *Converter-driven stability* refers to the ability of the power system to maintain its stable operation and damp the occurring oscillations when a large amount of converter interfaced devices are connected across the grid. As the typical converter interface devices rely on control loops and algorithms with fast response times, their timescale becomes wider and in many cases, results in cross-couplings with both the electromechanical dynamics of the machines and the electromagnetic transients of the network. These interactions may lead to unstable power system oscillations over a wide frequency range. Consequently, as shown in Figure 3.3, slow and fast interactions are differentiated based on the frequencies of the observed phenomena [50].

3. *Rotor angle stability* refers to the ability of synchronous machines of an interconnected power system to remain synchronized after being subjected to a disturbance. It depends on the ability to maintain or restore equilibrium between electromagnetic torque and mechanical torque of each synchronous machine in the system. Instability that may result occurs in the form of increasing angular swings of some generators which in turn may lead to their loss of synchronism with other generators. Rotor angle stability is divided into two sub-categories based on the disturbance that occurs across the network. Particularly, small-disturbance (or small-signal) rotor angle stability is concerned with the ability of the power system to maintain synchronism under small disturbances. The disturbances are considered to be sufficiently small that linearization of system equations is permissible for purposes of analysis [47, 51]. The time frame of interest in small-disturbance stability studies is on the order of 10 to 20 seconds following a disturbance. On the other hand, large-disturbance rotor angle stability or transient stability, is concerned with the ability of the power system to maintain synchronism when subjected to a severe disturbance. The resulting system response involves large excursions of generator rotor angles and is influenced by the nonlinear power-angle relationship. The time frame of interest in transient stability studies is usually 3 to 5 seconds following the disturbance. It may extend to 10–20 seconds for very large systems with dominant inter-area swings.

4. *Voltage stability* refers to the ability of a power system to maintain steady voltages at all buses in the system after being subjected to a disturbance from a given initial operating condition. It depends on the ability to maintain or restore equilibrium between load demand and load supply. Instability that may result occurs in the form of a progressive fall or rise of voltages of some buses. Similarly to rotor angle stability, voltage stability is also divided into two categories based on the disturbance that occurs across the network. More specifically, the large-disturbance voltage stability refers to the system's ability to maintain steady voltages following large disturbances such as system faults, loss of generation, or circuit contingencies. On the contrary, small-disturbance voltage stability refers to the system's ability to maintain steady voltages when subjected to small perturbations such as incremental changes in system load. Based on the time frame that is examined voltage stability can be also distinguished into to short-term or long-term. Short-term voltage stability involves dynamics of fast acting load components such as induction motors, electronically controlled loads, and HVDC converters while long-term voltage stability involves slower acting equipment such as tap-changing transformers, thermostatically controlled loads, and generator current limiters [47].

5. *Frequency stability* refers to the ability of a power system to maintain steady frequency following a severe system upset resulting in a significant imbalance between generation and load. It depends on the ability to maintain or restore equilibrium between system generation and load, with minimum unintentional loss of load. Instability that may result occurs in the form of sustained frequency swings leading to tripping of generating units and/or loads. As identified in Figure 3.3, frequency stability may be a short-term phenomenon or a long-term phenomenon based on the time that frequency excursions evolve [47].

Note that the stability classes 'Converter-driven Stability' and 'Resonance Stability' were recently introduced in [50]. Their addition was motivated by the increased use of converter interfaced devices and resulted in a significant extension of the time scale of interest (down to electromagnetic transients) for power system stability. Moreover, all the dynamic phenomena considered in the original classification presented in [47], are accurately modelled using the quasi-static approach. Nevertheless, this simplified modeling approach does not apply to the converter-driven and resonance stability classes, with the possible exception of the slow-interaction of converter-driven stability [50]. The applicability of this approach is limited since, in this time frame of interest, the system variables are not dominated by the fundamental frequency component. Thus, the employed dynamic models are unable to accurately capture the dynamic response of the system.

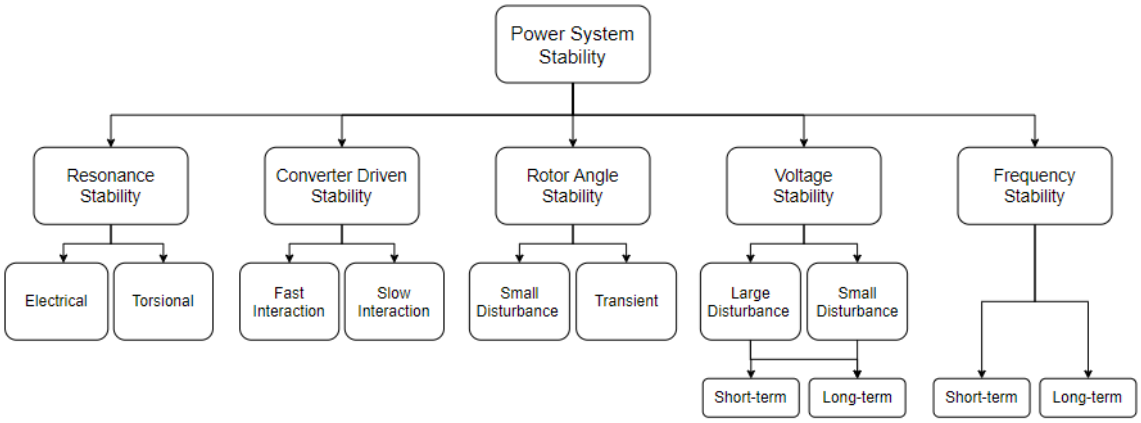


Fig. 3.3 Classification of power system stability [47].

An alternative classification of power system stability studies can be found in [52]. In particular, stability studies are classified into three types depending on the nature and order of magnitude of the disturbance. These types are:

1. Steady-state stability
2. Transient stability
3. Dynamic stability

Steady-state stability is considered to be the ability of the power system to maintain or restore synchronism after encountering slow and small disturbances. It concerns the stability of the locus of essentially steady-state operating points of the system. Transient stability, on the other hand, involves major disturbances such as loss of generators, line switching, faults and sudden load changes. The objective of transient stability studies is to determine whether or not the system will remain in synchronism following such disturbances. Finally, dynamic stability is considered to be the ability of the power system to regain synchronism after encountering small disturbance within a long time frame. It also concerns like steady-state stability studies, the stability of the locus of the steady-state operating points of the system.

## 3.2 Overview of power system stability analysis approaches

The current section briefly reviews the stability analysis approaches dealing mostly with the electromechanical phenomena that occur across the power network. These approaches are distinguished into two categories, i.e. the centralized and the decentralized approaches. This classification relies on the information required for their application. More specifically,

the application of a centralized approach requires the explicit knowledge of the network topology and the devices that are online at the time when the stability analysis is performed. On the other hand, in decentralized approaches, the derived stability results are independent of the network topology and the operating condition of remote grid-connected devices. The stability analysis is performed using local conditions that are capable of showing whether the utilization of the component of interest may lead to instability or improve the system's dynamic response.

### 3.2.1 Centralized approaches

As mentioned above, this thesis deals with the stability of power systems after small disturbances considering dynamics that evolve up to a few seconds following the disturbance. Thus, the following paragraphs present an overview of two transient stability approaches, i.e. the small signal stability analysis and the direct stability analysis. Both methods use elements/tools from Lyapunov's Stability to draw useful conclusions about the stability of the power system. In contrast to small signal stability which is an application of Lyapunov's Indirect Method, the direct stability approaches rely upon Lyapunov's Direct Method presented in Chapter 2. Furthermore, they both employ a state-space representation for the power system and are considered to be centralized since the deduction of stability guarantees for the whole system requires the explicit knowledge of the network topology and each device that is connected to it.

#### Review of centralized stability approaches

The power system is described by a set of $n$ first order nonlinear ODEs of the following form:

$$\dot{x}_i = f_i(x_1, x_2, \ldots, x_n; u_1, u_2, \ldots, u_r; t) \quad i = 1, 2, \ldots n \tag{3.1}$$

where $n$ is the order of the system and $r$ is the number of inputs. The above set of ODEs can be written in the following compact vector-matrix form:

$$\dot{x} = f(x, u, t) \tag{3.2}$$

where $x^T = [x_1, x_2, \ldots, x_n]$, $u^T = [u_1, u_2, \ldots, u_r]$ and $f^T = [f_1, f_2, \ldots, f_n]$. The column vector $x$ is referred to as the state vector, and its entries $x_i$ as state variables The column vector $u$ and the variable $t$ denote the vector of the inputs of the system and the time, respectively. As mentioned in Chapter 2, if the time derivatives of the state variables are not explicit functions

of time, the system is said to be autonomous and the equation (3.2) simplifies to:

$$\dot{x} = f(x,u). \tag{3.3}$$

In many cases, it could be useful to study certain output variables which can be observed on the system. These may be expressed in terms of the state and the input variables in the following form:

$$\dot{y} = g(x,u). \tag{3.4}$$

where $y^T = [y_1, y_2, \ldots, y_m]$ and $g^T = [g_1, g_2, \ldots, g_m]$. The column vector $y$ is the vector of outputs and $g$ is a vector of nonlinear functions relating the states and the inputs to the outputs of the system.

In a small signal stability analysis, the state-space model of the power system is linearized about an equilibrium point. The system (3.3)-(3.4) can be therefore written in the following compact form:

$$\begin{aligned} \Delta\dot{x} &= A\Delta x + B\Delta u \\ \Delta y &= C\Delta x + D\Delta u \end{aligned} \tag{3.5}$$

where:

- $A \in \mathbb{R}^{n\times n}$ is the state matrix of the system,
- $B \in \mathbb{R}^{n\times r}$ is the control or input matrix of the system
- $C \in \mathbb{R}^{m\times n}$ is the output matrix of the system and
- $D \in \mathbb{R}^{m\times r}$ is the (feedforward) matrix of the system which defines the proportion of input which appears directly in the output.

The above matrices are derived from equations (3.3)-(3.4) as described in Section 2.5.3.

The system (3.5) is then employed to deduce system-wide stability results considering that the power system is subjected only to small perturbations about the equilibrium. Note that small signal stability analysis is not applicable when large disturbances are considered as the whole analysis is carried out on a linearized system about certain operating conditions. Following the analysis presented in Chapter 2, the stability of the system can be determined by the eigenvalues of the state matrix $A$ as follows:

1. A real eigenvalue corresponds to a non-oscillatory mode. A negative eigenvalue represents a decaying mode. The larger its magnitude, the faster the decay. A positive real eigenvalue represents aperiodic instability.

2. Complex eigenvalues occur in conjugate pairs and each pair corresponds to an oscillatory mode. The real component of the eigenvalues gives the damping, and the imaginary component gives the frequency of oscillation. A negative real part represents a damped oscillation whereas a positive real part represents oscillation of increasing amplitude. Thus, for a complex pair of eigenvalues:

$$\lambda = \sigma \pm j\omega \tag{3.6}$$

the frequency of oscillation in Hz is given by

$$f = \frac{\omega}{2\pi} \tag{3.7}$$

while the damping ratio is given by

$$\zeta = \frac{-\sigma}{(\sigma^2 + \omega^2)^{1/2}}. \tag{3.8}$$

The damping ratio $\zeta$ determines the rate of decay of the amplitude of the oscillation.

Direct methods can also be used to determine the transient stability of power systems without explicitly obtaining the solutions of the differential equations governing the dynamic behavior of the system. In contrast to small signal stability analysis approaches, these methods do not require any linearization to determine the stability of systems governed by differential equations (equations (3.3)-(3.4)). On the contrary, based on Lyapunov's direct method (Section 2.5.4), it is necessary to derive an appropriate Lyapunov function, namely the Transient Energy Function (TEF), which is employed in the sequel to determine if the trajectories of the power system converge to an equilibrium of the system. More specifically, TEFs shall be differentiable, positive definite functions with $\dot{V}(x) < 0$ over an open region to guarantee the asymptotic stability of the interconnected system. Examples of such TEFs along with details of their derivation can be found in [42, 53–56]. Direct methods can, therefore, provide important information about the behavior of the system when the latter is subjected to larger disturbances. They can also give useful insights for the stability margins and the robustness of the system.

### Evaluation of centralized stability approaches

During the last decades, the analysis of power systems relied mainly on the above centralized stability analysis approaches as their application could give useful information regarding the stability and the robustness of the system. However, despite their wide use among the power engineering community, these approaches have several important disadvantages that

could be crucial for the analysis of future, fast-growing power grids. The most important are summarized as follows:

Small Signal Stability Approaches:

- Their stability guarantees are limited to certain operating conditions and are applicable only when the power system is subjected to small disturbances. Even though they allow the use of higher-order dynamical models to represent the power system components, they can provide accurate stability results only when the trajectories of the system are close to its initial operating point (equilibrium).

- The form of existing power systems (large-scale, interconnected systems) hampers their use as the linearization process and the eigenanalysis of such systems are time-consuming and require large computing resources. Although several techniques have been proposed in recent literature to improve both the time and the resources needed for their application, they still remain time-consuming procedures [57].

Direct Stability Approaches:

- The derivation of an appropriate TEF (Lyapunov function) constitutes a difficult task, especially when dealing with large-scale, interconnected systems.

- To simplify the elaborated analysis, engineers often resort to simple dynamical models that cannot accurately capture the dynamic response of the system. Such simplification could also lead to very conservative results that can be misleading regarding the stability, the reliability and the robustness of the system.

### 3.2.2 Decentralized approaches

The continuous expansion of existing power networks and the introduction of large numbers of DGs led power engineering community to seek for alternative ways to determine stability. In particular, their interest focused on techniques and conditions that can guarantee the stability of a system in a completely decentralized manner without the need for the explicit knowledge of the system topology and its online devices. In this respect, throughout the following paragraphs, the most significant methods for decentralized stability analysis are being introduced. As the technical content of this thesis relies on passivity-based techniques, an exclusive reference is made on similar passivity-based approaches presented in the recent literature. The advantages and disadvantages of these decentralized stability analysis methods are assessed at the end of the section.

### Review of decentralized stability approaches

Decentralized stability approaches rely on the concept of input-output stability where an input-output model relates the output of the system directly to the input. Such an approach can be employed without necessarily knowing the internal structure that is represented by the state equation [21]. The system is viewed as a black box that can be accessed only through its input and output terminals. The foundation of this input-output approach to nonlinear systems can be found in the 1960's work of Sandberg and Zames [58, 59].

In power engineering, the power network and the power system components can be modeled as input-output dynamical systems that are interconnected in a certain, negative feedback formation. The way that these sub-systems interact in combination with their characteristics is further exploited for the deduction of completely decentralized stability results that ensure the stability of the interconnected system. The elaborated analysis relies on decentralized conditions that are derived from several features of nonlinear systems analysis such as Lyapunov stability, L2 stability as well as other optimal and robust control design techniques [60–62]. Some of the most important recent works where various decentralized approaches for stability analysis and control design are proposed can be found in [63–73].

Another key structural property that can be employed in a decentralized power system stability analysis is the notion of passivity. Passivity has been one of the cornerstones of nonlinear control theory since it can facilitate the stability analysis of large-scale interconnected systems and the design of effective and robust control mechanisms [19]. Its main advantage lies in the fact that every passive system is Lyapunov stable while passivity-based conditions can be used to determine the stability of large systems and decentralized subsystems according to the way they are interfaced [19–21]. It can also allow the adoption of more accurate, higher-order dynamics and the deduction of decentralized results when used appropriately [74]. The application of passivity within power system studies dates back to the '80s, where passivity-based techniques were used to study the effect of AVRs on power systems [75]. More recently, the notion of passivity was widely used in power system studies via the framework of port-Hamiltonian systems (described in [76]). Examples of this approach include [77–79] as well as more recent works as in [28, 30, 31, 35, 80–86].

### Evaluation of decentralized stability approaches

Similarly to the centralized stability approaches, the decentralized ones have both important advantages and disadvantages. These advantages and disadvantages which are related to the reliability, the accuracy and the complexity of these methods, are summarized as follows:

Advantages:

- Significant stability results for the whole power system can be derived in a decentralized manner. This could provide to the system operators the necessary "plug and play" capabilities to confront the continuously increasing introduction of DGs.

- The derived stability guarantees are independent of the system structure and topology. Such dependency could lead to computationally intractable studies as the current networks constitute large-scale, interconnected systems that consist of numerous distributed components.

Disadvantages:

- Decentralized methods for stability analysis of large-scale systems often require the employment of complex mathematical tools. Apart from the complexity, this could also lead to the simplification of the analysis through the adoption of simpler dynamical models for power system components. Such modeling, however, could add conservatism to the derived stability results.

- The representation of the power network as a system of arbitrary topology could also lead to significant simplifications which in turn could affect the effectiveness and the reliability of the proposed method. Such simplifications are the consideration of lossless lines [28, 64, 80, 87] or a static representation of the currents flowing across the grid [82, 86, 88–90].

## 3.3 Power system modeling in stability analysis studies

The stability analysis approach presented in this thesis relies on the representation of power systems as an interconnection of dynamical systems in an appropriate frame of reference. To introduce this framework and help the reader understand the modeling employed in power system stability studies more generally, it is necessary to present here some basic preliminaries that are relevant to this context. It should be noted here that the following paragraphs refer to the quasi-static phasor modeling.

### 3.3.1 Alternating Current (AC) three phase sources

Power systems are networks consisting of devices that generate, transmit and distribute electrical energy to consumers. Since the majority of power systems and their components

rely upon three-phase AC power [91], in this paper we will use the notation

$$x_{ABC} = [x_A(t)\ x_B(t)\ x_C(t)]^T$$

to represent three-phase AC signals $x_{ABC} : \mathbb{R}^+ \to \mathbb{R}^3$. In particular, three-phase voltages and currents will be denoted as

$$v_{ABC} = [v_A(t)\ v_B(t)\ v_C(t)]^T \text{ and } i_{ABC} = [i_A(t)\ i_B(t)\ i_C(t)]^T \tag{3.9}$$

respectively.

**Assumption 3.3.1** *The power networks considered throughout this thesis consist of symmetric, balanced, positive-sequence, three-phase AC generation sources.*

Since power systems are designed to be symmetric and balanced, the above assumption is often accurate, especially when analysis is carried out at the transmission level. Assumption 3.3.1 results in three symmetric waveforms which have $120^o$ phase difference between each other, i.e.

$$x_{ABC} = \begin{bmatrix} x_A(t) \\ x_B(t) \\ x_C(t) \end{bmatrix} = \sqrt{2}|x| \begin{bmatrix} \cos(\gamma_x(t)) \\ \cos(\gamma_x(t) - \frac{2\pi}{3}) \\ \cos(\gamma_x(t) + \frac{2\pi}{3}) \end{bmatrix} \tag{3.10}$$

where $|x| \in \mathbb{R}^+$ is the amplitude and $\gamma_x \in [0, 2\pi)$ is the phase of the waveform. The fact that the three phases are balanced results in

$$x_A(t) + x_B(t) + x_C(t) = 0 \tag{3.11}$$

Furthermore, problems in symmetric and balanced power systems can be dealt with by using only the phase A and then deduce the results for phases B and C from (3.10).

### 3.3.2 Phasor representation

To simplify power system analysis, it is usually convenient to use the phasor representation of voltages and currents rather than their sinusoidal form (3.10). The phasor representation is defined as follows [92]:

**Definition 3.3.1** *A phasor is a complex number representing a sinusoidal signal*

$$x(t) = |x|\cos(\gamma_x(t)) = |x|\cos(\omega t + \phi_x) \tag{3.12}$$

*whose amplitude $|x|$, frequency $\omega$ and phase angle $\phi_x$ can be time varying quantities. Using the quantity $\bar{X}$ to indicate the phasor, the polar phasor representation of the signal* (3.12) *is given by:*

$$\bar{X} = |x|e^{j\gamma_x(t)} = |x|\angle\gamma_x(t). \tag{3.13}$$

*We can also obtain its rectangular representation by using Euler's identity as follows:*

$$\bar{X} = |x|e^{j\gamma_x(t)} = |x|\big(\cos(\gamma_x(t)) + j\sin(\gamma_x(t))\big). \tag{3.14}$$

*A simplification often made is the consideration of a constant $\omega = \omega_s = 2\pi f_s$ where $f_s$ denotes the synchronous frequency of a power grid (50 or 60 Hz). Phasors can be therefore represented by:*

$$\bar{X} = |x|e^{j\phi_x} = |x|\angle\phi_x. \tag{3.15}$$

*Note that $\phi_x$ can be a time varying quantity that models variations in frequency.*

### 3.3.3 (0,d,q) or Clarke-Park transformation

A key tool to facilitate power systems analysis is (0,d,q) or Park's transformation. The sinusoidal waveforms (3.10), describing either voltages or currents, introduce significant complexity in the analysis. Therefore, to simplify these equations, (0,d,q) or Park's transformation is used to map the system's components into three axis that rotate at a specific velocity $\omega$, namely, the 0-axis, the d-axis and the q-axis. Following [48, 91, 93, 94], the Park's transformation is defined by:

$$\begin{bmatrix} x_0 \\ x_d \\ x_q \end{bmatrix} = \sqrt{\frac{2}{3}} \underbrace{\begin{bmatrix} \frac{1}{\sqrt{2}} & \frac{1}{\sqrt{2}} & \frac{1}{\sqrt{2}} \\ \cos\rho(t) & \cos(\rho(t) - \frac{2\Pi}{3}) & \cos(\rho(t) + \frac{2\Pi}{3}) \\ \sin\rho(t) & \sin(\rho(t) - \frac{2\Pi}{3}) & \sin(\rho(t) + \frac{2\Pi}{3}) \end{bmatrix}}_{P} \begin{bmatrix} x_A \\ x_B \\ x_C \end{bmatrix} \tag{3.16}$$

where $P$ is the transformation matrix relating the $abc$ and $0dq$ vectors. The new $0dq$ variables are also called Park's variables. Furthermore, the Park's transformation is orthogonal, i.e. $P^{-1} = P^T$. Under Assumption 3.3.1, which yields the zero sum of both the voltages and currents of the three phases, the 0-component in (3.16) is equal to zero and is therefore neglected. Considering that the 0-component can be neglected, we substitute equation (3.10) into (3.16) to get

$$x_{dq} = \sqrt{3}|x| \begin{bmatrix} \cos(\gamma_x(t) - \rho(t)) \\ \sin(\gamma_x(t) - \rho(t)) \end{bmatrix} \tag{3.17}$$

which is essentially a projection of phasors onto axes rotating with frequency $\omega = \dot{\rho}$. Similarly to the *abc* components, the *dq* components can also be expressed as complex numbers onto these rotating axes, i.e. $X_{dq} = X_q + jX_d$. This representation will be referred to as the phasor representation of $x$ in a frame of reference rotating with frequency $\dot{\rho}$.

Note also that $\bar{X}$ in (3.15) is the phasor representation in a frame of reference rotating with a constant frequency $\omega_s$. The latter will be referred to as the *system reference frame*.

### 3.3.4 Power Network Structure

A power network with arbitrary topology can be described by a connected and undirected graph $(\mathscr{N}, \mathscr{E})$, where $\mathscr{N} = \{1, 2, \dots |\mathscr{N}|\}$ is the set of buses and $\mathscr{E} \subset \mathscr{N} \times \mathscr{N} = \{1, 2, \dots |\mathscr{E}|\}$ the set of lines connecting them. The network structure can be represented by its corresponding incidence matrix $E \in \mathbb{R}^{|\mathscr{N}| \times |\mathscr{E}|}$, similarly to [86]. By arbitrarily labeling the ends of the line $l$ with a $+$ and a $-$, the matrix $E$ is given by

$$E_{il} = \begin{cases} +1 & \text{if } i \text{ is the positive end of } l \\ -1 & \text{if } i \text{ is the negative end of } l \\ 0 & \text{otherwise.} \end{cases} \tag{3.18}$$

We also use $l = (i, j)$ to denote the link connecting the network buses i and j through the line $l$ and $l \to i$ to denote that the line $l$ is connected to bus $i$. For the formulation of a dynamical model to represent the network, it is now necessary to make the following assumptions regarding the network lines and the system frequency.

**Assumption 3.3.2** *Network lines can be accurately represented by symmetric RLC elements ($\Pi$-equivalent).*

**Assumption 3.3.3** *The network frequency $\omega$, is almost constant at synchronous value $\omega_s$ (50 or 60 HZ), i.e. $\omega - \omega_s \approx 0$.*

Assumption 3.3.2 states that any line can be represented by the traditional $\Pi$-equivalent as illustrated in Figure 3.4, similarly to the majority of the related literature [93]. Moreover, in Assumption 3.3.3, it is considered that the variations of the network frequency are very small which is also a mild assumption considering that the maximum frequency deviation in the European Network of Transmission System Operators for Electricity (ENTSO-E) system is $200mHz$ ($\pm 0.4\%$) [95].

It is also necessary to introduce here the diagonal matrices $R$, $L$ and $C \in \mathbb{R}^{|\mathscr{E}| \times |\mathscr{E}|}$ which contain the resistance, the inductance and the capacitance of each line across the network.

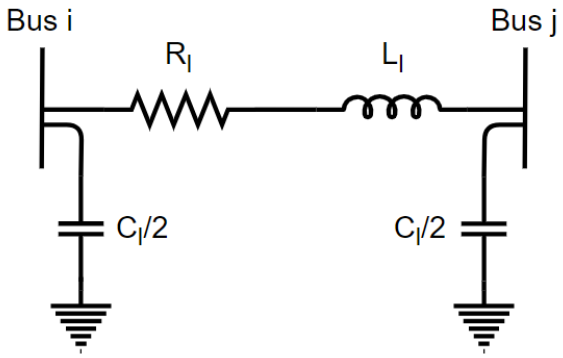


Fig. 3.4 Lumped circuit model ($\pi$-equivalent) representation of a network line from bus $i$ to bus $j$.

We get:

$$R_{ml} = \begin{cases} R_l & \text{if } m = l \\ 0 & \text{otherwise} \end{cases} \tag{3.19}$$

$$L_{ml} = \begin{cases} L_l & \text{if } m = l \\ 0 & \text{otherwise} \end{cases} \tag{3.20}$$

and

$$C_{ml} = \begin{cases} C_l & \text{if } m = l \\ 0 & \text{otherwise} \end{cases} \tag{3.21}$$

where $R_l$,$L_l$ and $C_l$ denote the resistance, the inductance and the capacitance of the line $l$ respectively. Note that $C_l$ could be considered equal to zero when $l$ corresponds to a Low Voltage (LV) distribution line of the system.

### 3.3.5 Network Equations

The equations describing the network are derived based on the formulation described in [88]. The following assumption for line dynamics is, therefore, considered.

**Assumption 3.3.4** *Line dynamics evolve on a much faster timescale than the dynamics of the generation sources and the loads.*

Assumption 3.3.4 states that network lines reach steady state much earlier than the generators and the loads[1]. Thus, the power network can be modeled by the static network

[1] As we are about to show in Chapter 4, Assumption 3.3.4 is valid when the system's inertia is high. In low-inertia power grids the response of the network and the bus dynamics is comparable - in terms of time.

current flows given by the nodal set of equations:

$$\bar{I} = Y_n \bar{V} = (G_n + jB_n)\bar{V}. \tag{3.22}$$

$Y_n \in \mathbb{C}^{|\mathscr{N}|\times|\mathscr{N}|}$, and $G_n$, $B_n \in \mathbb{R}^{|\mathscr{N}|\times|\mathscr{N}|}$ are the network's admittance, conductance and susceptance matrices respectively. $\bar{I} \in \mathbb{C}^{|\mathscr{N}|}$ and $\bar{V} \in \mathbb{C}^{|\mathscr{N}|}$ denote the net injected current and the bus voltage vectors of the power grid in their phasor representation. The derivation of the nodal admittance matrix (3.22) is extensively described in [91] and is based on the fact that the transmission lines are modeled by their Π-equivalent model according to Assumption 3.3.2.

**Remark 3.3.1** *$G_n$ and $B_n$ are real, $|\mathscr{N}| \times |\mathscr{N}|$, sparse symmetric matrices and they do not include loads or FACTS devices and line compensation components.*

The components of net injected current and bus voltage vectors can equivalently be expressed in either their rectangular or polar complex form. However, it is convenient here to express these in the same form as the elements of the nodal admittance matrix, that is, the rectangular form. Considering a steady state network frequency $\omega_s$, the net injected currents and bus voltages can be written using the phasor representation in (3.15) as

$$\bar{I}_i = I_i \angle \phi_{I,i} = I_i \cos\phi_{I,i} + jI_i \sin\phi_{I,i} = I_{a,i} + jI_{b,i} \tag{3.23}$$

and

$$\bar{V}_i = V_i \angle \phi_{V,i} = V_i \cos\phi_{V,i} + jV_i \sin\phi_{V,i} = V_{a,i} + jV_{b,i} \tag{3.24}$$

respectively, for all $i \in \mathscr{N}$. We now define the vectors $I_a = [I_{a,1}\ I_{a,2}\ \ldots\ I_{a,|\mathscr{N}|}]$, $I_b = [I_{b,1}\ I_{b,2}\ \ldots\ I_{b,|\mathscr{N}|}]$, $V_a = [V_{a,1}\ V_{a,2}\ \ldots\ V_{a,|\mathscr{N}|}]$ and $V_b = [V_{b,1}\ V_{b,2}\ \ldots\ V_{b,|\mathscr{N}|}] \in \mathbb{R}^{|\mathscr{N}|}$. The net injected current and the bus voltage vectors can therefore be written as:

$$\bar{I} = I_a + jI_b \text{ and } \bar{V} = V_a + jV_b \tag{3.25}$$

respectively. By substituting equations (3.25) into (3.22) we get:

$$\bar{I} = I_a + jI_b = (G_n V_a - B_n V_b) + j(B_n V_a + G_n V_b). \tag{3.26}$$

Equation (3.26) is then used to deduce the equations for the net injected current components, $I_{a,i}$ and $I_{b,i}$, at each bus $i = 1, 2, \ldots, |\mathscr{N}|$, i.e., we get:

$$I_{a,i} = \sum_{j=1}^{|\mathscr{N}|} (G_{ij}V_{a,j} - B_{ij}V_{b,j}) \text{ and } I_{b,i} = \sum_{j=1}^{|\mathscr{N}|} (B_{ij}V_{a,j} + G_{ij}V_{b,j}). \tag{3.27}$$

Note that in the network equations (3.22) - (3.27), the current and voltage phasors $\bar{I}, \bar{V}$ are represented in the *system reference frame*, i.e. a common reference frame rotating at the synchronous frequency $\omega_s$. The network admittance matrix in (3.22) is also evaluated at $\omega_s$. This is a common approach in the literature, and as discussed in [88], it is a valid approximation, under the assumption that line dynamics are much faster than machine dynamics.

It is also important to consider the transition from the system reference frame to the local $(d,q)$ or the *machine reference frame* and vice versa. We thus define the angle $\delta_i \in [0, 2\pi)$ denoting the phase difference between the local machine reference frame at bus i, with phase angle $\rho_i(t)$, and the system reference frame which rotates at synchronous frequency $\omega_s$, i.e.

$$\delta_i = \int_0^t (\dot{\rho}_i(\tau) - \omega_s)\, d\tau \;\Rightarrow\; \dot{\delta}_i = \dot{\rho}_i(t) - \omega_s = \omega_i - \omega_s \tag{3.28}$$

The relative position of the two systems of coordinates is illustrated in Figure 3.5 and the relationship between them is given by:

$$V_{dq,i} = T(\delta_i)\bar{V}_i \Leftrightarrow \begin{bmatrix} V_{q,i} \\ V_{d,i} \end{bmatrix} = \begin{bmatrix} \cos\delta_i & \sin\delta_i \\ -\sin\delta_i & \cos\delta_i \end{bmatrix} \begin{bmatrix} V_{a,i} \\ V_{b,i} \end{bmatrix} \tag{3.29}$$

where the transformation matrix $T(\delta_i)$ denotes the mapping of the phasor components in the system reference frame to the dq-components for bus i. The transformation $T$ is also orthogonal ($T^{-1} = T^T$), and its inverse transformation can be written as:

$$\bar{V}_i = T^{-1}(\delta_i)V_{dq,i} \Leftrightarrow \begin{bmatrix} V_{a,i} \\ V_{b,i} \end{bmatrix} = \begin{bmatrix} \cos\delta_i & -\sin\delta_i \\ \sin\delta_i & \cos\delta_i \end{bmatrix} \begin{bmatrix} V_{q,i} \\ V_{d,i} \end{bmatrix}. \tag{3.30}$$

Equivalently, for the net current injection components we get

$$I_{dq,i} = T(\delta_i)\bar{I}_i \Leftrightarrow \begin{bmatrix} I_{q,i} \\ I_{d,i} \end{bmatrix} = \begin{bmatrix} \cos\delta_i & \sin\delta_i \\ -\sin\delta_i & \cos\delta_i \end{bmatrix} \begin{bmatrix} I_{a,i} \\ I_{b,i} \end{bmatrix} \tag{3.31}$$

$$\bar{I}_i = T^{-1}(\delta_i)I_{dq,i} \Leftrightarrow \begin{bmatrix} I_{a,i} \\ I_{b,i} \end{bmatrix} = \begin{bmatrix} \cos\delta_i & -\sin\delta_i \\ \sin\delta_i & \cos\delta_i \end{bmatrix} \begin{bmatrix} I_{q,i} \\ I_{d,i} \end{bmatrix} \tag{3.32}$$

Now, the network equations (3.26) are expressed in each generator's reference frame to obtain the general network relationships. By substituting (3.30) and (3.32) into (3.27) we

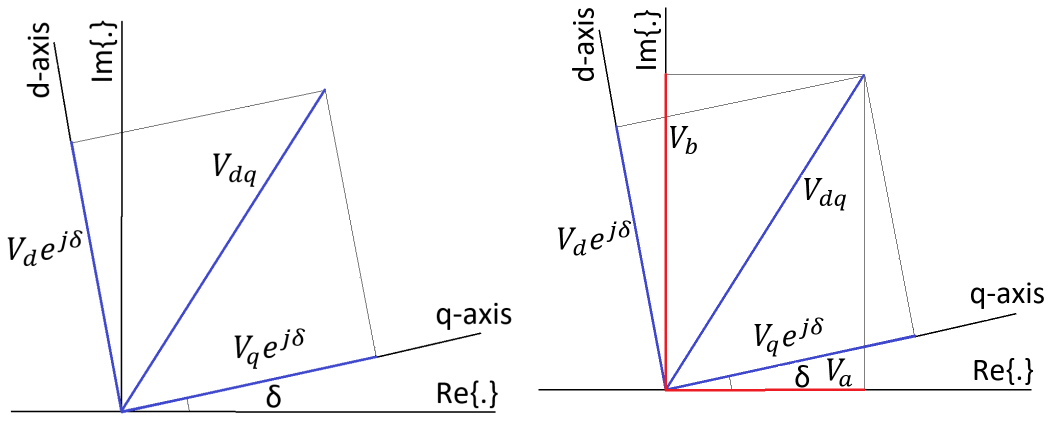


(a) The geometry of dq-components on the system's complex plane.

(b) The decomposition of dq-components in both the system and the machine reference frames.

Fig. 3.5 Relative position of the machine reference frame with respect to the system reference frame [91].

get:

$$\begin{aligned} I_{q,i} &= \sum_{j=1}^{|\mathcal{N}|} \Big[ V_{q,j} \Big( G_{ij}\cos(\eta_{ij}) + B_{ij}\sin(\eta_{ij}) \Big) + V_{d,j} \Big( G_{ij}\sin(\eta_{ij}) - B_{ij}\cos(\eta_{ij}) \Big) \Big] \\ I_{d,i} &= \sum_{j=1}^{|\mathcal{N}|} \Big[ V_{q,j} \Big( -G_{ij}\sin(\eta_{ij}) + B_{ij}\cos(\eta_{ij}) \Big) + V_{d,j} \Big( G_{ij}\cos(\eta_{ij}) + B_{ij}\sin(\eta_{ij}) \Big) \Big] \end{aligned} \tag{3.33}$$

where, for ease of notation, angle differences are written as $\eta_{ij} = \delta_i - \delta_j$.

# Chapter 4

# Multi-variable network formulation

The current chapter contains the main technical content of this thesis. In particular, it introduces the multi-variable network formulation used within the proposed framework for decentralized stability analysis and control. As will be discussed in the sequel, when network equations are formulated as a multi-input/multi-output system expressed in the system reference frame, the passive nature of the network is revealed. This result is derived without neglecting the lossy and the dynamic nature of the network lines. The passivity property of the network will then be used in Chapter 5 for the derivation of useful stability guarantees for the interconnected system. Furthermore, an extensive discussion is provided regarding the advantages and the opportunities offered by the proposed network models. Both representations are finally verified through a numerical application on the Kundur four-machine two-area test system and several dynamic simulations on a simple four-area test system [31, 32, 34].

## 4.1 Static network representation

### 4.1.1 Multi-input/multi-output formulation

As discussed in Chapter 3, the power network is usually represented by the nodal set of equations (3.22), which can be also written in the rectangular form (3.26). For the formulation of the network model that will be used within the proposed stability analysis approach, we separate the real and the imaginary part of equation (3.26) to form the following $(2\times|\mathscr{N}|)$-input/$(2\times|\mathscr{N}|)$-output system

$$\begin{bmatrix} I_a \\ I_b \end{bmatrix} = \begin{bmatrix} G_n & -B_n \\ B_n & G_n \end{bmatrix} \begin{bmatrix} V_a \\ V_b \end{bmatrix} = H_{2n} \begin{bmatrix} V_a \\ V_b \end{bmatrix} = g^N([V_a^T \; V_b^T]) \tag{4.1}$$

where $H_{2n}$ denotes the matrix relating vectors $[V_a^T \; V_b^T]^T$ with vectors $[I_a^T \; I_b^T]^T$. The vector function $g^N : \mathbb{R}^{2|\mathcal{N}|} \to \mathbb{R}^{2|\mathcal{N}|}$ provides an alternative notation to comply with the definitions that will be used in the forthcoming chapters. A graphical illustration of the multi-input/multi-output network model (4.1) is provided in Fig. 4.1.

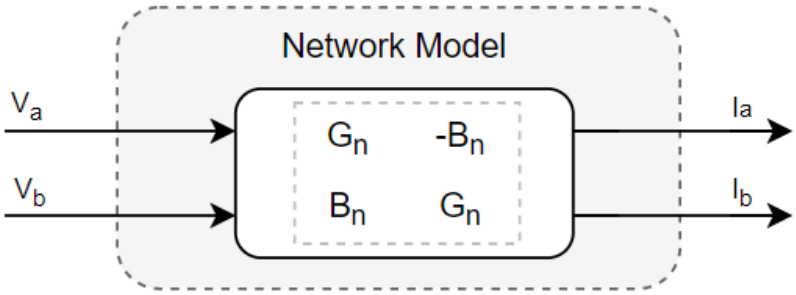


Fig. 4.1 The network equations represented as a $(2 \times |\mathcal{N}|)$-input/$(2 \times |\mathcal{N}|)$-output system.

### 4.1.2 Passivity of the static network model

The passivity properties that are revealed through the aforementioned modeling are examined in the following paragraphs. Taking into account that Assumption 3.3.4 holds, the following lemma is provided. This lemma relies upon the fundamental passivity Definition 2.6.1 provided in Chapter 2 [21]. Therefore, the static network model (4.1) is passive if and only if the inequality within Definition 2.6.1 is satisfied, i.e.

$$u^T y = [V_a^T \; V_b^T] \begin{bmatrix} I_a \\ I_b \end{bmatrix} \geq 0 \tag{4.2}$$

for all $V_a, V_b, I_a, I_b \in \mathbb{R}^{|\mathcal{N}|}$.

**Lemma 4.1.1** *The network system defined in (4.1) with inputs the vectors of bus voltage components $[V_a^T \; V_b^T]^T$ and outputs the vectors of net injected current components $[I_a^T \; I_b^T]^T$ is passive.*

**Proof of Lemma 4.1.1** *By substituting the network equations (4.1) in inequality (4.2) we get*

$$\begin{aligned} u^T y =& [V_a^T \; V_b^T] H_{2n} \begin{bmatrix} V_a \\ V_b \end{bmatrix} = [V_a^T \; V_b^T] \begin{bmatrix} G_n & -B_n \\ B_n & G_n \end{bmatrix} \begin{bmatrix} V_a \\ V_b \end{bmatrix} \\ =& V_a^T G_n V_a + V_b^T G_n V_b \geq 0 \end{aligned} \tag{4.3}$$

*for all $V_a$, $V_b \in \mathbb{R}^{|\mathscr{N}|}$. The inequality (4.3) reveals that the passivity of the network is ensured when the composite matrix $H_{2n}$ or equivalently its diagonal elements $G_n$, are positive semidefinite matrices.*

*$G_n \in \mathbb{R}^{|\mathscr{N}|\times|\mathscr{N}|}$ is a square, sparse symmetric matrix with non negative diagonal and negative off-diagonal elements, i.e., $G_{ii} \geq 0$ and $G_{ij} \leq 0 \; \forall \; i, \; j = 1,2,\ldots,|\mathscr{N}|$. It is also diagonally dominant as the following equation holds:*

$$G_{ii} = -\sum_{j\neq i}^{|\mathscr{N}|} G_{ij} \Rightarrow |G_{ii}| = \sum_{j\neq i}^{|\mathscr{N}|} |G_{ij}| \quad (i,j) \in \mathscr{E} \tag{4.4}$$

*In order to prove the positive semidefiniteness of the matrix $G_n$, we now define the Gershgorin discs $D_i(G_{ii},R_i), \; i = 1,2,\ldots,|\mathscr{N}|$. $D_i$ is a closed disc centered at $(G_{ii},0)$, with radius $R_i = \sum_{i\neq j}|G_{ij}|$. As stated above the matrix $G_n$ has positive diagonal elements and is also diagonally dominant. Subsequently, its Gershgorin discs lie in the right half plane, have center on the real axis and are tangent to the imaginary axis since $G_{ii} - R_i = 0, \; \forall \; i = 1,2,\ldots,|\mathscr{N}|$. According to the Gershgorin circle theorem [96], the eigenvalues of the matrix $G_n$ lie within its Gershgorin discs, corresponding to its columns (or equivalently to its rows). Thus, $G_n$ has eigenvalues with non negative real parts which immediately leads to the fact that it is positive semidefinite [96]. Condition (4.2) is therefore satisfied.* □

**Remark 4.1.1** *As shown within the proof of Lemma 4.1.1, the condition (4.2) always holds and the passivity of the network system is ensured regardless of its topology. Specifically, due to the form of the composite matrix $H_{2n}$, the positive semi-definiteness of the network's conductance matrix $G_n$ is sufficient for condition (4.2) to be satisfied. $G_n$ in turn, is always positive semi-definite since it has positive diagonal elements and is diagonally dominant.*

**Remark 4.1.2** *As will be discussed in the following paragraphs, the majority of the recent literature dealing with power system stability in general network topologies adopts lossless networks, i.e. $G_n = 0$. The main reason for considering such simplification lies in the fact that when the analysis is carried out in dq-coordinates, the passivity property holds only for lossless networks. For the proposed approach, under such assumption condition (4.2) becomes*

$$u^T y = [V_a^T \; V_b^T] \begin{bmatrix} 0 & -B_n \\ B_n & 0 \end{bmatrix} \begin{bmatrix} V_a \\ V_b \end{bmatrix} = 0 \tag{4.5}$$

*Note that the network's passivity follows here easily from the skew-symmetry of the matrix $H_{2n}$.*

## 4.2 Dynamic network representation

### 4.2.1 Multi-input/multi-output formulation

The previous static network model is now extended to include the dynamic nature of network lines and thus to improve the fidelity and accuracy of the stability analysis of power systems. For the derivation of a dynamic, multi-variable network representation, we introduce the differential equations describing the current components at the series impedances and the voltage components at the shunt capacitances of each line $l \in \mathscr{E}$ of the network. These differential equations are subsequently used along with the network's incidence matrix to formulate a dynamical representation for the power network. The proposed network model depicted in Figure 4.2, constitutes a multi-input/multi-output dynamical system with inputs the components of the bus voltages and outputs the components of the net injected current at every bus $i \in \mathscr{N}$ of the grid. As observed, the proposed network formulation consists of two subsystems, i.e. the branch and capacitance dynamics, connected in a negative feedback formation. It should also be noted that all variables/states of the proposed network model are expressed on a *common system reference frame*, i.e. two common axes that rotate at a specific angular velocity $\omega$ [93].

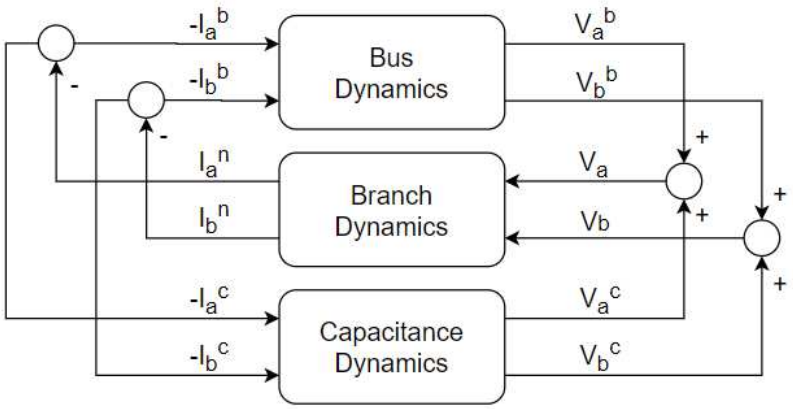


Fig. 4.2 The power network represented as an interconnection of input/output systems associated with the bus and network dynamics, respectively [31].

Firstly, we define the phasors of the current of line $l \in \mathscr{E}$ and the voltage of bus $i \in \mathscr{N}$ in their rectangular form as follows:

$$\hat{I}_l = I_{a,l} + jI_{b,l} \text{ and } \hat{V}_i = V_{a,i} + jV_{b,i} \tag{4.6}$$

where $I_{a,l}$ and $I_{b,l}$ are the current components of line $l$ and $V_{a,i}$ and $V_{b,i}$ are the voltage components of bus $i$. Based on the phasor representation provided in [97], the state equations

of the line current of line $l$ are given by:

$$L_l \dot{I}_{a,l} = -R_l I_{a,l} - \omega L_l I_{b,l} + (V_{a,i} - V_{a,j}) \tag{4.7}$$
$$L_l \dot{I}_{b,l} = -R_l I_{b,l} + \omega L_l I_{a,l} + (V_{b,i} - V_{b,j}) \tag{4.8}$$

where $V_{a,i}$, $V_{b,i}$, $V_{a,j}$ and $V_{b,j}$ are the voltage components at buses $i$ and $j$ which are connected through line $l$. Considering that Assumption 3.3.3 holds (that is $\omega \approx \omega_s$), the differential equations can be further simplified as follows:

$$L_l \dot{I}_{a,l} = -R_l I_{a,l} - \omega_s L_l I_{b,l} + (V_{a,i} - V_{a,j}) \tag{4.9}$$
$$L_l \dot{I}_{b,l} = -R_l I_{b,l} + \omega_s L_l I_{a,l} + (V_{b,i} - V_{b,j}). \tag{4.10}$$

The net injected current components at each bus of the grid are now defined by employing the incidence matrix $E$. The net injected current components at bus $i$ are therefore given by the following set of equations:

$$I^n_{a,i} = \sum_{l=1}^{|\mathscr{E}|} E_{il} I_{a,l} \text{ and } I^n_{b,i} = \sum_{l=1}^{|\mathscr{E}|} E_{il} I_{b,l} \tag{4.11}$$

which are the Kirchoff's Current Law equations at each bus of the grid. By introducing the vectors $I_a = [I_{a,1}\ I_{a,2}\ \dots\ I_{a,|\mathscr{E}|}]^T$, $I_b = [I_{b,1}\ I_{b,2}\ \dots\ I_{b,|\mathscr{E}|}]^T$, $I^n_a = [I^n_{a,1}\ I^n_{a,2}\ \dots\ I^n_{a,|\mathscr{N}|}]^T$, $I^n_b = [I^n_{b,1}\ I^n_{b,2}\ \dots\ I^n_{b,|\mathscr{N}|}]^T$, $V_a = [V_{a,1}\ V_{a,2}\ \dots\ V_{a,|\mathscr{N}|}]^T$ and $V_b = [V_{b,1}\ V_{b,2}\ \dots\ V_{b,|\mathscr{N}|}]^T$, the branch dynamics can be represented by the following dynamical system with inputs the vectors of bus voltage components $V_a$ and $V_b$, states the vectors of line current components $I_a$ and $I_b$, and outputs the vectors of net injected current components $I^n_a$ and $I^n_b$:

$$\begin{bmatrix} \dot{I}_a \\ \dot{I}_b \end{bmatrix} = \begin{bmatrix} K_A & \omega_s I^{\mathscr{E}} \\ -\omega_s I^{\mathscr{E}} & K_A \end{bmatrix} \begin{bmatrix} I_a \\ I_b \end{bmatrix} + \begin{bmatrix} K_B & 0 \\ 0 & K_B \end{bmatrix} \begin{bmatrix} V_a \\ V_b \end{bmatrix} \tag{4.12}$$
$$\begin{bmatrix} I^n_a \\ I^n_b \end{bmatrix} = \begin{bmatrix} K_C & 0 \\ 0 & K_C \end{bmatrix} \begin{bmatrix} I_a \\ I_b \end{bmatrix} \tag{4.13}$$

The matrices $K_A \in \mathbb{R}^{|\mathscr{E}|\times|\mathscr{E}|}$ , $K_B \in \mathbb{R}^{|\mathscr{E}|\times|\mathscr{N}|}$ and $K_C \in \mathbb{R}^{|\mathscr{N}|\times|\mathscr{E}|}$ can be deduced from the set of differential equations (4.9)-(4.11) as follows:

$$K_A = -L^{-1}R \tag{4.14}$$

$$K_B = L^{-1}E^T \tag{4.15}$$

and

$$K_C = E \tag{4.16}$$

where $I^{\mathscr{E}}$ is the $\mathbb{R}^{|\mathscr{E}|\times|\mathscr{E}|}$ identity matrix. As can be seen from the above formulation, branch dynamics constitute a $2|\mathscr{N}|$-input$\times 2|\mathscr{N}|$-output Linear Time Invariant (LTI) system with state-space representation $\Sigma^n = \{A^n, B^n, C^n, 0^n\}$ where:

$$A^n = \begin{bmatrix} K_A & \omega_s I^{\mathscr{E}} \\ -\omega_s I^{\mathscr{E}} & K_A \end{bmatrix},\ B^n = \begin{bmatrix} K_B & 0 \\ 0 & K_B \end{bmatrix} \text{ and } C^n = \begin{bmatrix} K_C & 0 \\ 0 & K_C \end{bmatrix}. \tag{4.17}$$

On the other hand, capacitance dynamics are derived using the following state equations of the voltage components at the shunt capacitance of line $l \to i$:

$$\frac{C_{l\to i}}{2}\dot{V}^c_{a,i} = \omega_s \frac{C_{l\to i}}{2} V^c_{b,i} - I^c_{a,i} \tag{4.18}$$

$$\frac{C_{l\to i}}{2}\dot{V}^c_{b,i} = -\omega_s \frac{C_{l\to i}}{2} V^c_{a,i} - I^c_{b,i}. \tag{4.19}$$

$I^c_{a,i}$ and $I^c_{b,i}$ denote the components of the current absorbed by the shunt capacitance $C_{l\to i}$ at bus $i$. Using the differential equations (4.18) - (4.19), capacitance dynamics can now be expressed in the following compact matrix form:

$$\begin{bmatrix} \dot{V}^c_a \\ \dot{V}^c_b \end{bmatrix} = \begin{bmatrix} 0 & \omega_s I^{\mathscr{N}} \\ -\omega_s I^{\mathscr{N}} & 0 \end{bmatrix} \begin{bmatrix} V^c_a \\ V^c_b \end{bmatrix} - \begin{bmatrix} \mathscr{C}^{-1} & 0 \\ 0 & \mathscr{C}^{-1} \end{bmatrix} \begin{bmatrix} I^c_a \\ I^c_b \end{bmatrix} \tag{4.20}$$

$V^c_a$, $V^c_b$, $I^c_a$ and $I^c_b$ denote the vectors of voltage and absorbed current components at the shunt capacitances connected to every bus $i = 1, 2, \ldots, |\mathscr{N}|$ of the network, respectively. Furthermore, the matrix $I^{\mathscr{N}} \in \mathbf{R}^{\mathscr{N}\times\mathscr{N}}$ is the corresponding identity matrix while $\mathscr{C}$ can be deduced from equations (4.18) - (4.19) as follows:

$$\mathscr{C} = \frac{1}{2} E C E^T I^{\mathscr{N}}. \tag{4.21}$$

It should be highlighted here that similarly to branch dynamics, the capacitance dynamics are derived based on Assumption 3.3.3 which states that voltages and currents are dominated by the fundamental frequency component.

### 4.2.2 Passivity of the dynamic network model

The passivity properties revealed for the network through the adoption of such a dynamical multi-variable formulation, are examined in the following paragraphs. We, therefore, provide the following lemma which relies on the fundamental passivity Definition 2.6.2 [21].

**Lemma 4.2.1** *The branch dynamics defined in* (4.12)-(4.13) *with inputs the vectors of bus voltage components $V_a$ and $V_b$, states the vectors of line current components $I_a$ and $I_b$, and outputs the vectors of net injected current components $I_a^n$ and $I_b^n$ constitute a passive $2|\mathcal{N}|$-input$\times 2|\mathcal{N}|$-output system.*

**Proof of Lemma 4.2.1** *In order to prove that the dynamical system* (4.12)-(4.13) *is passive, the following storage function is used:*

$$\mathscr{V}^N(I_a, I_b) = \frac{1}{2}\begin{bmatrix} I_a^T & I_b^T \end{bmatrix}\begin{bmatrix} L & 0 \\ 0 & L \end{bmatrix}\begin{bmatrix} I_a \\ I_b \end{bmatrix}. \tag{4.22}$$

*The derivative of the above storage function with respect to time is therefore given by:*

$$\begin{aligned} \dot{\mathscr{V}}^N &= \begin{bmatrix} I_a^T & I_b^T \end{bmatrix}\begin{bmatrix} L & 0 \\ 0 & L \end{bmatrix}\begin{bmatrix} \dot{I}_a \\ \dot{I}_b \end{bmatrix} \\ &= \begin{bmatrix} I_a^T & I_b^T \end{bmatrix}\begin{bmatrix} -R & \omega_s L \\ -\omega_s L & -R \end{bmatrix}\begin{bmatrix} I_a \\ I_b \end{bmatrix} + \begin{bmatrix} I_a^T & I_b^T \end{bmatrix}\begin{bmatrix} E^T & 0 \\ 0 & E^T \end{bmatrix}\begin{bmatrix} V_a \\ V_b \end{bmatrix} \\ &= -I_a^T R I_a - I_b^T R I_b + \begin{bmatrix} I_a^{nT} & I_b^{nT} \end{bmatrix}\begin{bmatrix} V_a \\ V_b \end{bmatrix} \end{aligned} \tag{4.23}$$

*Since the network's resistance matrix R is a positive definite matrix, equation* (4.23) *satisfies $\dot{\mathscr{V}}^N \leq u^T y$ which completes the proof.* □

**Lemma 4.2.2** *The capacitance dynamics defined in* (4.20) *with inputs the vectors of current components $-I_a^c$ and $-I_b^c$ and states/outputs the vectors of voltage components $V_a^c$ and $V_b^c$ constitute a lossless $2|\mathcal{N}|$-input$\times 2|\mathcal{N}|$-output system.*

**Proof of Lemma 4.2.2** *For the proof of the Lemma 4.2.2, we use the following storage function for the capacitance dynamics* (4.20)*:*

$$\mathscr{V}^C(V_a^c, V_b^c) = \frac{1}{2}\begin{bmatrix} V_a^{cT} & V_b^{cT} \end{bmatrix}\begin{bmatrix} \mathscr{C} & 0 \\ 0 & \mathscr{C} \end{bmatrix}\begin{bmatrix} V_a^c \\ V_b^c \end{bmatrix}. \tag{4.24}$$

*The time derivative of the storage function* (4.24) *is therefore given by:*

$$\begin{aligned}\dot{\mathscr{V}}^C &= \begin{bmatrix} V_a^{cT} & V_b^{cT} \end{bmatrix} \begin{bmatrix} \mathscr{C} & 0 \\ 0 & \mathscr{C} \end{bmatrix} \begin{bmatrix} \dot{V}_a^c \\ \dot{V}_b^c \end{bmatrix} \\ &= \begin{bmatrix} V_a^{cT} & V_b^{cT} \end{bmatrix} \begin{bmatrix} 0 & \omega_s \mathscr{C} \\ -\omega_s \mathscr{C} & 0 \end{bmatrix} \begin{bmatrix} V_a^c \\ V_b^c \end{bmatrix} + \begin{bmatrix} V_a^{cT} & V_b^{cT} \end{bmatrix} \begin{bmatrix} I^{\mathscr{N}} & 0 \\ 0 & I^{\mathscr{N}} \end{bmatrix} \begin{bmatrix} -I_a^c \\ -I_b^c \end{bmatrix} \\ &= \begin{bmatrix} V_a^{cT} & V_b^{cT} \end{bmatrix} \begin{bmatrix} -I_a^c \\ -I_b^c \end{bmatrix}.\end{aligned} \tag{4.25}$$

*From* (4.25)*, we observe that* $\dot{\mathscr{V}}^C = u^T y$ *which implies that capacitance dynamics constitute a lossless system.* □

**Remark 4.2.1** *The passivity of any power network with arbitrary topology can also be shown through the use of the Positive-real Lemma for LTI systems [19, 21, 98]. Particularly, the Positive-real lemma which is the representation of Kalman-Yakubovich-Popov (KYP) condition using a Linear Matrix Inequality (LMI), states that a stable LTI system with minimal state representation* $\Sigma = \{A, B, C, D\}$ *is passive if and only if there exists a positive definite matrix P such that the following inequality holds:*

$$\begin{bmatrix} A^T P + PA & PB - C^T \\ B^T P - C & -D - D^T \end{bmatrix} < 0. \tag{4.26}$$

*The above inequality was verified for branch dynamics which constitute a stable LTI system as the state matrix of this system is negative definite and thus, its eigenvalues lie in the left half of the complex plane [32]. This verification was carried out in Section 4.4 through a numerical application on the Kundur's Four-Machine Two-Area test system by considering that matrix* $P^n = P^{nT} \in \mathbb{R}^{2|\mathscr{E}| \times 2|\mathscr{E}|}$ *is given by:*

$$P^n = \begin{bmatrix} L & 0 \\ 0 & L \end{bmatrix} \tag{4.27}$$

**Remark 4.2.2** *A similar network representation that takes into account the network's dynamic behavior and leads to identical results as those presented in Lemmas 4.2.1 - 4.2.2, is provided in [35]. The difference between the two dynamical formulations lies in the fact that the network system in [35] has inputs the vectors of net injected current components and outputs the vectors of the bus voltages, i.e.* $u^T = [I_a^{nT}\ I_b^{nT}]$ *and* $y^T = [V_a^T\ V_b^T]$.

## 4.3 Discussion

As mentioned before, the main difference between the proposed approach and the recent literature is that the analysis is carried out in the system reference-frame instead of each local machine reference-frame. Even though this change of reference frame does not have an effect in centralized stability approaches, it provides important benefits when stability is deduced using decentralized conditions. In particular, as will be shown in the following chapters, a local passivity property at the bus dynamics in this reference frame is sufficient to deduce stability in a general network, without having to resort to important simplifications on the network lines. Such simplifications are usually necessary when the analysis is carried out using the local $dq$ coordinates due to the different bus frequencies and the voltage angles that are appearing in the network equations [35]. Consequently, both the active and the reactive power flows across the network are taken into account while the bus voltage magnitudes are not considered to remain constant when a sudden generation or load disturbances appear across the power grid.

More specifically, the transformation into the system reference-frame leads to simpler network equations. By comparing equations (3.27) with equations (3.33), it is easy to discern the complexity added when the analysis is carried out in the local machine reference-frame due to the existence of the sinusoids. This was the main reason why several simplifications were considered in the stability analysis for power networks within the recent literature. Such an important simplification was the adoption of lossless power networks where equations (3.33) are reduced to

$$\begin{aligned} I_{q,i} &= \sum_{j=1}^{|\mathcal{N}|} \Big[ B_{ij} V_{q,j} \sin(\eta_{ij}) - B_{ij} V_{d,j} \cos(\eta_{ij}) \Big] \\ I_{d,i} &= \sum_{j=1}^{|\mathcal{N}|} \Big[ B_{ij} V_{q,j} \cos(\eta_{ij}) + B_{ij} V_{d,j} \sin(\eta_{ij}) \Big]. \end{aligned} \tag{4.28}$$

Commonly, the previous equations are further simplified by assuming that $V_{d,i} = 0 \; \forall \; i \in \mathcal{N}$, which leads to the following simpler and less accurate form:

$$I_{q,i} = \sum_{j=1}^{|\mathcal{N}|} \Big[ B_{ij} V_{q,j} \sin(\eta_{ij}) \Big] \text{ and } I_{d,i} = \sum_{j=1}^{|\mathcal{N}|} \Big[ B_{ij} V_{q,j} \cos(\eta_{ij}) \Big]. \tag{4.29}$$

In order to avoid counting in the generator's transient reactances and thus to facilitate the analysis, several works such as [64, 66, 86, 99] also considered that the q-axis bus voltage is equal to the q-axis transient emf, i.e. $V_{q,i} = E'_{q,i}$ (see also Chapter 5).

Moreover, the proposed dynamic network representation allows us to take into account the network's dynamic behaviour. Such a network representation becomes crucial due to the constantly increasing penetration of converter interfaced devices in existing power grids. More specifically, as indicated in Chapter 3, the dynamics of the converter interfaced devices are on similar time scales as the line dynamics while their controls are also significantly faster [11, 50]. The response of converters, in turn, affects the overall dynamic response of the system while requiring more accurate modelling to be sufficiently captured.

## 4.4 Assessment of the proposed network formulations

This section evaluates the applicability and the accuracy of the proposed network formulations through several numerical applications and dynamic simulations. These applications and simulations are carried out on the Kundur Four Machine Two Areas test system and a simple four-area test system, respectively.

### 4.4.1 Numerical applications

The proposed network formulations are verified through two numerical applications on the Four Machine Two Areas Kundur test system presented in Figure 4.3 [48]. Note that the boxed numbers represent buses, while the numbers outside the boxes indicate transmission lines. The topology of this test system is used for the derivation of both the static and the dynamic network representations (models (4.1) and (4.12)-(4.13), respectively). It should also be noted that for the derivation of the dynamic network representation we only consider the branch dynamics as the shunt capacitances of the test system are omitted.

For the derivation of the static network representation, we calculate its nodal admittance matrix $Y_n$ using the following formula:

$$Y_n = G_n + jB_n = \begin{cases} Y_{ii} = \sum_{k=1}^{n} y_{ik} & \\ Y_{ij} = Y_{ji} = -y_{ij} & (i,j) \in \mathscr{E} \\ Y_{ij} = Y_{ji} = 0 & \text{otherwise.} \end{cases} \tag{4.30}$$

The loads at buses 3 and 7 are not included in the calculation of the nodal admittance matrix. As we can observe from (4.31) and (4.32), the matrices $G_n$ and $B_n$ are positive semidefinite and negative semidefinite, respectively. This verifies that the network of this test system is passive as shown in the previous analysis.

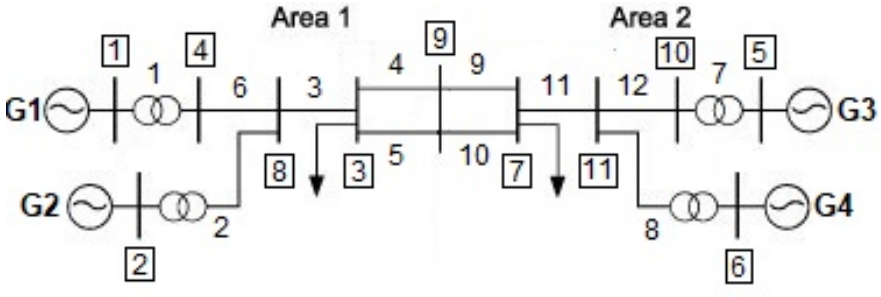


Fig. 4.3 Single line diagram of the Four Machine Two-Areas Kundur test system [48].

$$G_n = \begin{bmatrix} 0 & 0 & 0 & 0 & 0 & 0 & 0 & 0 & 0 & 0 & 0 \\ 0 & 0 & 0 & 0 & 0 & 0 & 0 & 0 & 0 & 0 & 0 \\ 0 & 0 & 0 & 0 & 0 & 0 & 0 & 0 & 0 & 0 & 0 \\ 0 & 0 & 0 & 0 & 0 & 0 & 0 & 0 & 0 & 0 & 0 \\ 0 & 0 & 0 & 0 & 0.44 & -0.44 & 0 & 0 & 0 & 0 & 0 \\ 0 & 0 & 0 & 0 & -0.44 & 1.54 & -1.1 & 0 & 0 & 0 & 0 \\ 0 & 0 & 0 & 0 & 0 & -1.1 & 1.3 & -0.2 & 0 & 0 & 0 \\ 0 & 0 & 0 & 0 & 0 & 0 & -0.2 & 0.4 & -0.2 & 0 & 0 \\ 0 & 0 & 0 & 0 & 0 & 0 & 0 & -0.2 & 1.3 & -1.1 & 0 \\ 0 & 0 & 0 & 0 & 0 & 0 & 0 & 0 & -1.1 & 1.54 & -0.44 \\ 0 & 0 & 0 & 0 & 0 & 0 & 0 & 0 & 0 & -0.44 & 0.44 \end{bmatrix} pu \tag{4.31}$$

$$B_n = \begin{bmatrix} -j6.65 & 0 & 0 & 0 & j6.65 & 0 & 0 & 0 & 0 & 0 & 0 \\ 0 & -j6.65 & 0 & 0 & 0 & j6.65 & 0 & 0 & 0 & 0 & 0 \\ 0 & 0 & -j6.65 & 0 & 0 & 0 & 0 & 0 & 0 & 0 & j6.65 \\ 0 & 0 & 0 & -j6.65 & 0 & 0 & 0 & 0 & 0 & j6.65 & 0 \\ j6.65 & 0 & 0 & 0 & -j11.05 & j4.4 & 0 & 0 & 0 & 0 & 0 \\ 0 & j6.65 & 0 & 0 & j4.4 & j22.02 & j11 & 0 & 0 & 0 & 0 \\ 0 & 0 & 0 & 0 & 0 & j11 & -j13 & j2 & 0 & 0 & 0 \\ 0 & 0 & 0 & 0 & 0 & 0 & j2 & -j4 & j2 & 0 & 0 \\ 0 & 0 & 0 & 0 & 0 & 0 & 0 & j2 & -j13 & j11 & 0 \\ 0 & 0 & 0 & j6.65 & 0 & 0 & 0 & 0 & j11 & -j22.05 & j4.4 \\ 0 & 0 & j6.65 & 0 & 0 & 0 & 0 & 0 & 0 & j4.4 & -j11.05 \end{bmatrix} pu \tag{4.32}$$

Now, we proceed with the verification of the proposed dynamic network model. Since the shunt capacitances of the lines are neglected the dynamic network representation is derived using equations (4.12)-(4.16). The matrices $K_A$, $K_B$ and $K_C$ are therefore given in per unit system by:

$$K_A = -\text{diag}\{0,0,0.1,0.1,0.1,0.1,0,0,0.1,0.1,0.1,0.1\}$$

$$K_B = \begin{bmatrix} 59.9 & 0 & 0 & -59.9 & 0 & 0 & 0 & 0 & 0 & 0 & 0 \\ 0 & 59.9 & 0 & 0 & 0 & 0 & 0 & -59.9 & 0 & 0 & 0 \\ 0 & 0 & 100 & 0 & 0 & 0 & 0 & -100 & 0 & 0 & 0 \\ 0 & 0 & 9.1 & 0 & 0 & 0 & 0 & 0 & -9.1 & 0 & 0 \\ 0 & 0 & 9.1 & 0 & 0 & 0 & 0 & 0 & -9.1 & 0 & 0 \\ 0 & 0 & 0 & 40 & 0 & 0 & 0 & 40 & 0 & 0 & 0 \\ 0 & 0 & 0 & 0 & 59.9 & 0 & 0 & 0 & 0 & -59.9 & 0 \\ 0 & 0 & 0 & 0 & 0 & 59.9 & 0 & 0 & 0 & 0 & 0-59.9 \\ 0 & 0 & 0 & 0 & 0 & 0 & 9.1 & 0 & -9.1 & 0 & 0 \\ 0 & 0 & 0 & 0 & 0 & 0 & 9.1 & 0 & -9.1 & 0 & 0 \\ 0 & 0 & 0 & 0 & 0 & 0 & 100 & 0 & 0 & 0 & -100 \\ 0 & 0 & 0 & 0 & 0 & 0 & 0 & 0 & 0 & 40 & -40 \end{bmatrix}$$

and

$$K_C = \begin{bmatrix} 1 & 0 & 0 & 0 & 0 & 0 & 0 & 0 & 0 & 0 & 0 & 0 \\ 0 & 1 & 0 & 0 & 0 & 0 & 0 & 0 & 0 & 0 & 0 & 0 \\ 0 & 0 & 1 & 1 & 1 & 0 & 0 & 0 & 0 & 0 & 0 & 0 \\ -1 & 0 & 0 & 0 & 0 & 1 & 0 & 0 & 0 & 0 & 0 & 0 \\ 0 & 0 & 0 & 0 & 0 & 0 & 1 & 0 & 0 & 0 & 0 & 0 \\ 0 & 0 & 0 & 0 & 0 & 0 & 0 & 1 & 0 & 0 & 0 & 0 \\ 0 & 0 & 0 & 0 & 0 & 0 & 0 & 0 & 1 & 1 & 1 & 0 \\ 0 & -1 & -1 & 0 & 0 & -1 & 0 & 0 & 0 & 0 & 0 & 0 \\ 0 & 0 & 0 & -1 & -1 & 0 & 0 & 0 & -1 & -1 & 0 & 0 \\ 0 & 0 & 0 & 0 & 0 & 0 & -1 & 0 & 0 & 0 & 0 & 1 \\ 0 & 0 & 0 & 0 & 0 & 0 & 0 & -1 & 0 & 0 & -1 & -1 \end{bmatrix}$$

respectively.

The matrices (4.14) - (4.17) and (4.27) are now substituted into the inequality (4.26) in order to verify the passivity of the network when the proposed dynamic formulation is adopted (Remark 4.3.1). We get:

$$\begin{bmatrix} A^{nT}P + PA^n & 0 \\ 0 & 0 \end{bmatrix} < 0 \tag{4.33}$$

which means that the inequality (4.26) is satisfied only when

$$A^{nT}P^n + P^nA^n < 0. \tag{4.34}$$

By further expanding the left side of the inequality (4.34), we get the following inequality:

$$\begin{aligned} A^{nT}P^n + P^nA^n &= \begin{bmatrix} K_A^T L + LK_A & 0 \\ 0 & K_A^T L + LK_A \end{bmatrix} \\ &= -2\begin{bmatrix} R & 0 \\ 0 & R \end{bmatrix} < 0. \end{aligned} \tag{4.35}$$

which holds since the network's resistance matrix $R$ is positive definite. This also verifies the passivity result shown within the proof Lemma 4.2.1.

### 4.4.2 Simulations

The evaluation of the presented network models is carried out using the simple four area test system that is illustrated in Figure 4.4. This test system consists of four areas that are

connected through a typical $230kV$ transmission line of various lengths and of the following characteristics: $r = 0.0001 pu/km$, $x = 0.001 pu/km$ and $b = 0.00175 pu/km$ ($S_b = 100MVA$). For the representation of all areas, we use the classical third-order synchronous generator model and the ZIP load model [21, 93]. Moreover, generator dynamics include the models of a simple turbine governor and a simple exciter. As will be discussed in Chapter 5, both the aforementioned models can be written in an appropriate state-space form and consequently can be easily incorporated into the stability analysis using the proposed framework.

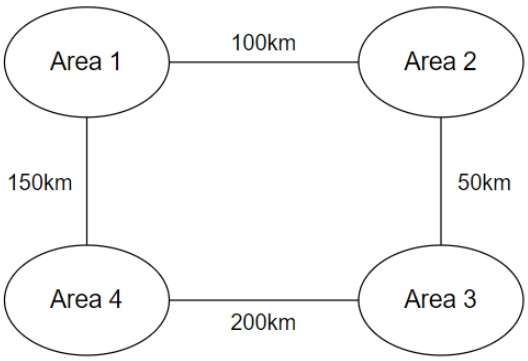


Fig. 4.4 Single line diagram of a simple four area test system.

To show the effect of such a dynamic network modeling, we consider a sudden increase of $100MW$ of load at area 2. The simulations are carried out using: (a) a lossless, (b) a static and (c) the proposed dynamic network representation. Furthermore, it is considered that during this sudden load change the test system is under the following three operating conditions: (a) low RES penetration, (b) medium RES penetration and (c) high RES penetration, that is, RES supply the 5%, 10% and 15% of system load respectively. It should also be noted that RES penetration was modeled by a constant PQ injection at the four buses which constitutes an accurate representation of grid-feeding inverters. At the same time, the synchronous generator output and size are decreased accordingly. Both the aforementioned parameters yielded in a significant reduction of the system's inertia.

The results of these simulations are illustrated in Figures 4.5 - 4.10 through the representation of the voltage and the frequency response at area 2 when either a lossless, a static and a dynamic network model are adopted for each of the three operating conditions. As one can observe from the figures, in all cases, the use of a lossless network model results in a less accurate voltage and frequency deviation since although the line resistance is significantly smaller than its inductance, it still affects the voltage and the frequency across the grid. On the other hand, both the static and dynamic network representation result in a quite similar voltage and frequency deviation. However, while the RES penetration increases, considerable

low-frequency oscillations are appearing when a dynamic network model is used. As can be seen in Figures 4.6-4.7 and 4.9-4.10 (steady-state region), these voltage and frequency oscillations are becoming larger and faster as both the line's length and the RES penetration increase. This directly leads to the conclusion that as RES share in power generation increases, power grids could be also subjected to inter-area oscillations of significant amplitude and thus, more accurate dynamical models are necessary to ensure the reliability and the robustness of the system.

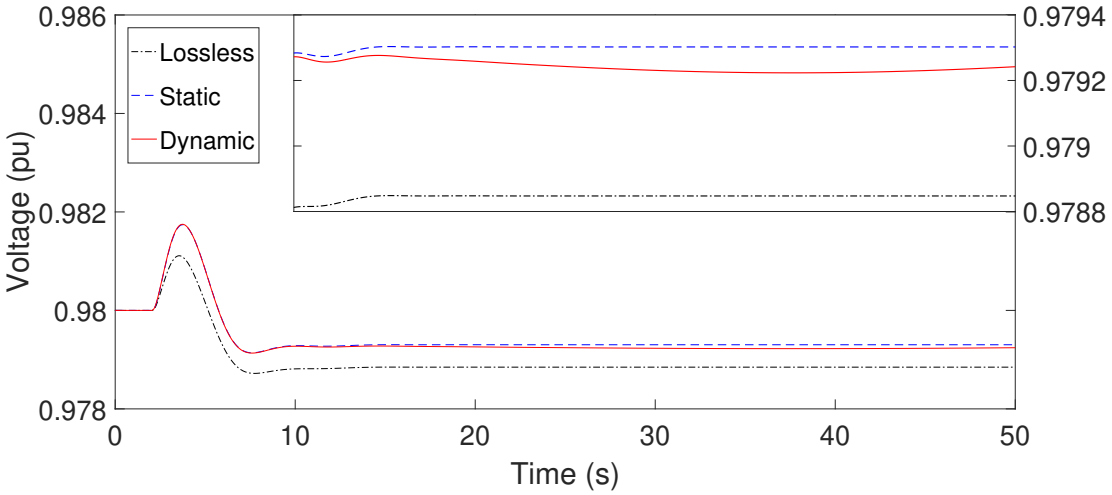


Fig. 4.5 Voltage deviation at area 2 after a sudden load increase of 100MW (low RES penetration conditions).

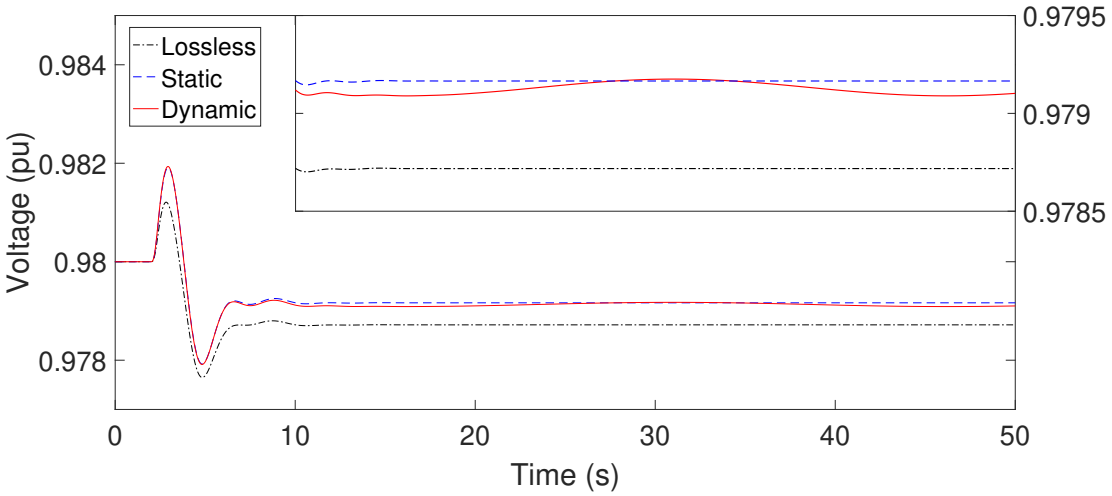


Fig. 4.6 Voltage deviation at area 2 after a sudden load increase of 100MW (medium RES penetration conditions).

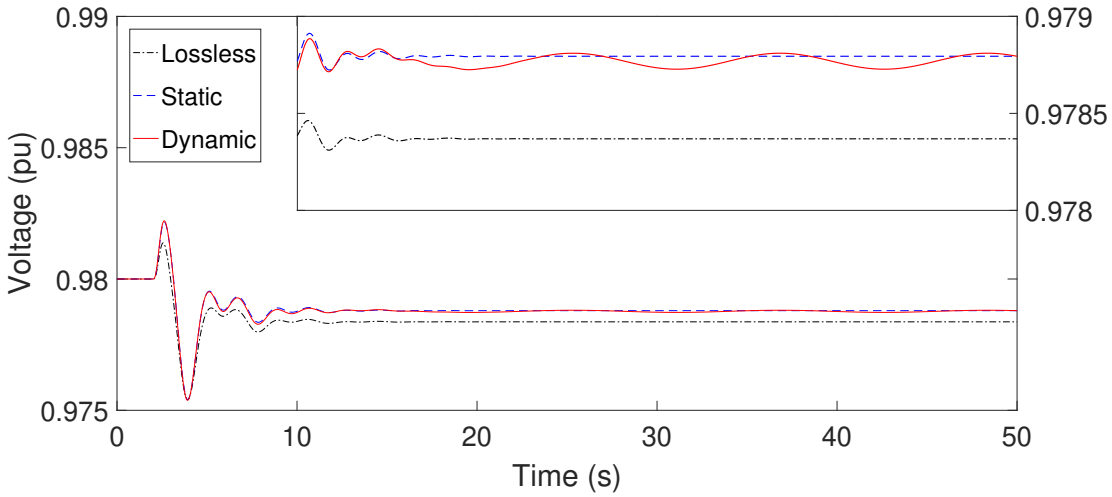


Fig. 4.7 Voltage deviation at area 2 after a sudden load increase of 100MW (high RES penetration conditions).

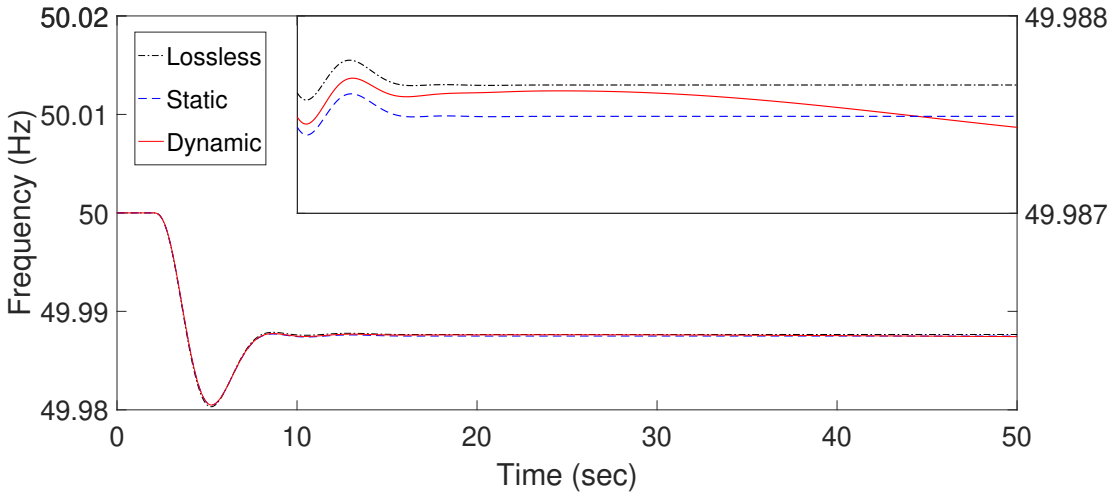


Fig. 4.8 Frequency deviation at area 2 after a sudden load increase of 100MW (low RES penetration conditions).

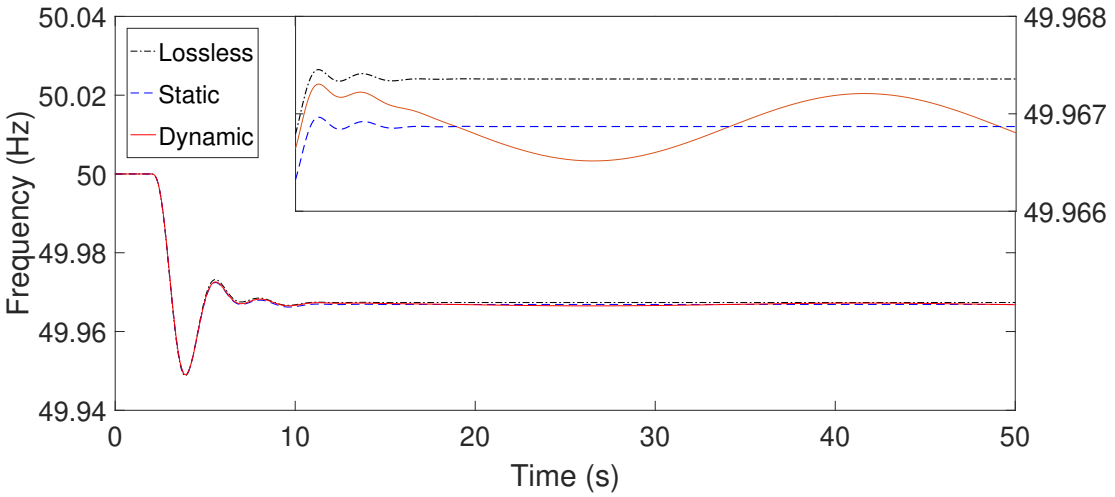


Fig. 4.9 Frequency deviation at area 2 after a sudden load increase of 100MW (medium RES penetration conditions).

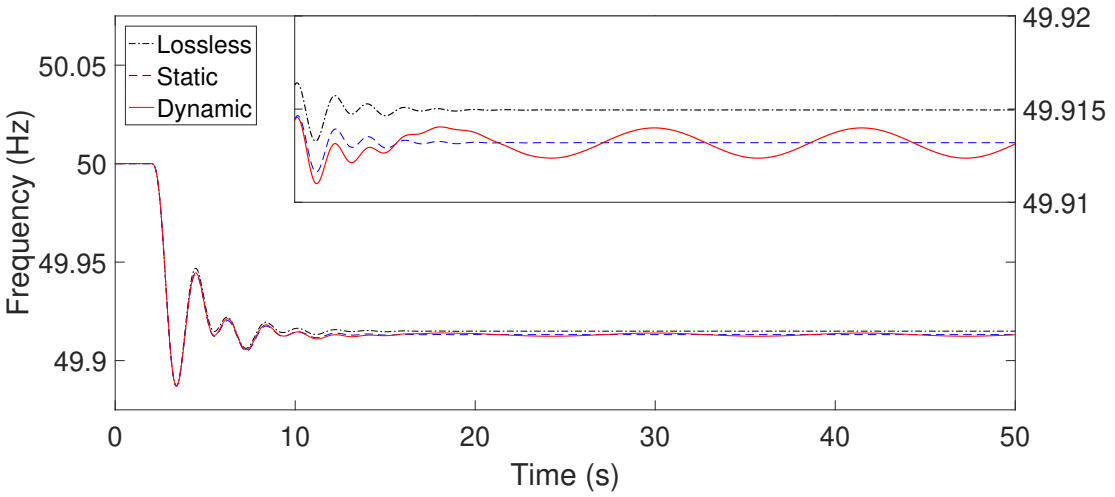


Fig. 4.10 Frequency deviation at area 2 after a sudden load increase of 100MW (high RES penetration conditions).

# Chapter 5

# Incorporation of power system components and system-wide stability results

Following the previous multi-variable network formulation, the current chapter focuses on the incorporation of the power system components into the proposed stability analysis framework and the derivation of system-wide stability results. Firstly, a broad class of dynamical systems is being introduced in Section 5.1 to facilitate the adoption of a variety of power system components and control mechanisms. Then, in Section 5.2, several local passivity conditions are presented for bus dynamics. As will be shown in the sequel, these conditions in combination with the passivity properties satisfied by the adopted network models, are sufficient to guarantee the asymptotic stability of the interconnected system in a completely decentralized manner. The significance and feasibility of these findings are finally explained through a brief discussion in Section 5.4. It should be noted here that due to the differences in either bus dynamics and the local passivity conditions, the analysis is carried out for both the static and the dynamic network representation.

## 5.1 General multi-input/multi-output formulation of bus dynamics

### 5.1.1 Static network representation

To incorporate the bus models and derive stability results for the interconnected system, both the network and the bus dynamics have to be expressed in the same reference frame, which is

chosen here as the system reference frame. In contrast to the recent literature, we, therefore, transform the bus dynamics into the system reference frame instead of each bus local $dq$-coordinates and consider that each of the $|\mathcal{N}|$ buses forms a 2-input/2-output system to fit with the network formulation described in the previous chapter. A graphical representation of the interconnected system is provided in Figure 5.1 where the multi-input/multi-output network system is connected to the aggregate bus dynamics. The bus models are expressed in the system reference frame by incorporating the mappings $T$ and $T^{-1}$ (equations (3.29)-(3.32)) into the bus dynamics. This approach is novel and allows the consideration of more relaxed conditions for the network. It also provides the necessary means for decentralized stability analysis and control.

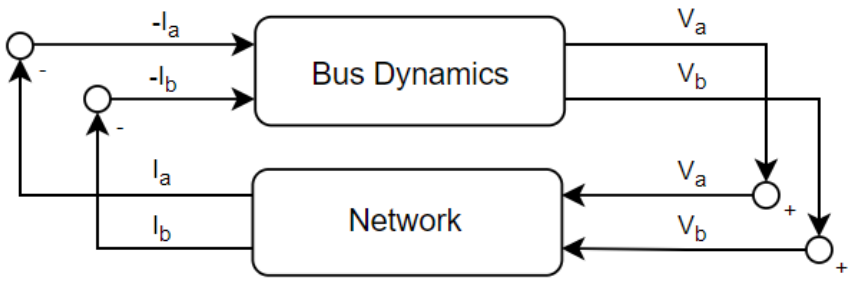


Fig. 5.1 The power network represented as an interconnection of input/output systems associated with the bus dynamics and transmission lines, respectively.

A broad class of systems is introduced now to represent the bus models. Considering that these dynamical systems have inputs the phasor components of the net current injection $(-I_{a,i}, -I_{b,i}) \in \mathbb{R}^2$, states $x_i \in X \subseteq \mathbb{R}^k$ and outputs the phasor components of the bus voltage $(V_{a,i}, V_{b,i}) \in \mathbb{R}^2$, their state-space representation is given by:

$$\begin{aligned} \dot{x}_i &= f_i(x_i, u_i) \\ y_i &= g_i(x_i, u_i) \quad i \in \mathcal{N} \end{aligned} \tag{5.1}$$

where $u_i = [-I_{a,i}, -I_{b,i}]$, $y_i = [V_{a,i}, V_{b,i}]$. The vector functions $f_i : \mathbb{R}^{k_i} \times \mathbb{R}^2 \to \mathbb{R}^{k_i}_i$ and $g_i : \mathbb{R}^{k_i} \times \mathbb{R}^2 \to \mathbb{R}^2$ are locally Lipschitz for any $i \in \mathbb{N}$. It is also highlighted here that the bus dynamics (5.1) can be of arbitrary dimension.

### 5.1.2 Dynamic network representation

The incorporation of bus dynamics into the proposed multi-variable framework can similarly be implemented as described in the above paragraphs for the static network representation [31]. More specifically, the bus models are expressed in a common system reference frame

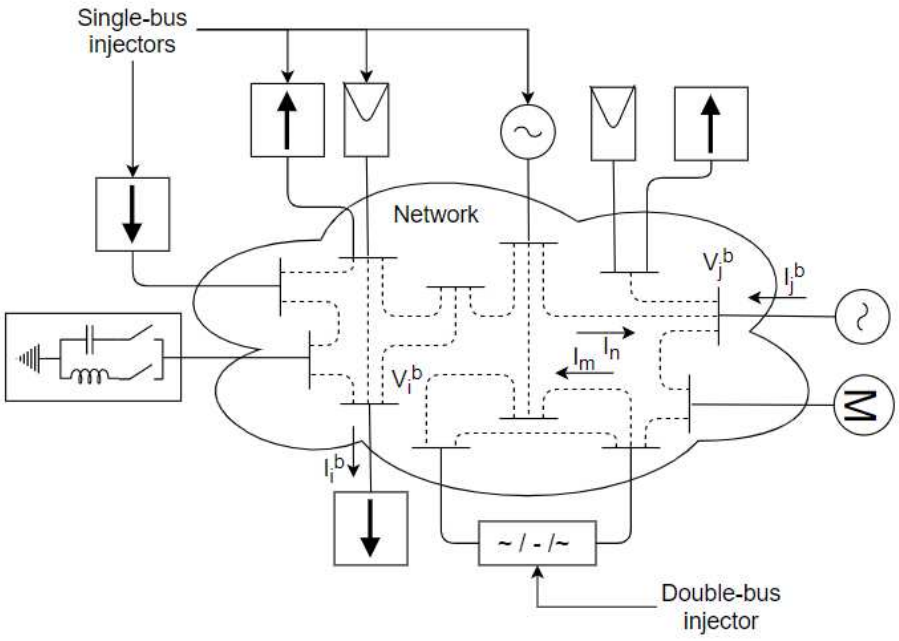


Fig. 5.2 An overview of the proposed power system configuration.

instead of their local $dq$-coordinates by incorporating the mappings (3.29) - (3.32) (Park transformation) into bus dynamics. Additionally, it is considered that each power system component constitutes a device that either produces or consumes power in normal operating conditions and can be attached to a single bus (e.g. synchronous machines, motors, wind turbines, etc.) or two buses (e.g.HVDC lines, AC/DC converters, etc.). Moreover, the power system components can be modeled by voltage sources that either inject or absorb current in the network and hereon, they will be referred to as *injectors*, as presented in [18]. Specifically, the components connected to a single bus will be denoted as *single-bus injectors* while for the components attached to two buses we will use the term *double-bus injector*. The proposed configuration can be visualized in Fig. 5.2.

Subsequently, to fit with the network formulation described in the previous chapter, it is considered that each single-bus injector forms a 2-input×2-output system while double-bus injectors are modeled by a 4-input×4-output system. Each injector is connected to the network (branch and capacitance) dynamics as illustrated in Fig. 5.1. For the representation of either the single-bus or the double-bus injectors, the following broad class of dynamical systems is now employed:

$$\begin{aligned} \dot{x} &= f(x,u) \\ y &= g(x,u). \end{aligned} \tag{5.2}$$

As observed, the dynamical model (5.2) is almost identical to (5.1). The vectors $u$, $x$ and $y$ denote the inputs, the states and the outputs of the system, respectively. The dimensions of the vectors $u$ and $y$ depend on the type of the component, that is a single-bus or a double-bus injector. In particular, a single-bus injector at bus $i$ has inputs the phasor components of the net injected currents $u = (-I^b_{a,i},\ -I^b_{b,i}) \in \mathbb{R}^2$ and outputs the phasor components of the bus voltages $y = (V^b_{a,i},\ V^b_{b,i}) \in \mathbb{R}^2$. On the other hand, a double-bus injector which is attached to buses $i$ and $j$, has inputs the phasor components of the net injected currents at buses $i$ and $j$, i.e. $u = (-I^b_{a,i},\ -I^b_{a,j},\ -I^b_{b,i},\ -I^b_{b,j}) \in \mathbb{R}^4$ and outputs the phasor components of the bus voltages at buses $i$ and $j$, i.e. $y = (V^b_{a,i},\ V^b_{a,j},\ V^b_{b,i},\ V^b_{b,j}) \in \mathbb{R}^4$. The states $x \in X \subset \mathbb{R}^n$ of the dynamical system (5.2) are of arbitrary dimension since they are directly related to the dynamical model that is employed to represent the component.

## 5.2 Necessary passivity conditions on bus dynamics

### 5.2.1 Static network representation

The current section presents certain passivity conditions on the bus dynamics, which when satisfied guarantee the asymptotic stability of the equilibria of the interconnected system (4.1) and (5.1). It should be noted that these conditions are decentralized since they are independent of network topology. Before presenting these conditions, it is first necessary to provide the following definitions for the equilibrium of the interconnected system (4.1) and (5.1) and the local input-strict passivity [21].

**Definition 5.2.1** *The constant vector $\hat{x} = [\hat{x}_1\ \hat{x}_2\ \dots\ \hat{x}_{|\mathcal{N}|}]$, $\hat{x}_i \in \mathbb{R}^{k_i}$ is an equilibrium of the interconnected system (4.1) and (5.1), if the time derivative of the states in (5.1) is equal to zero when*[1] *$x_i = \hat{x}_i,\ i \in \mathcal{N}$.*

**Definition 5.2.2** *Consider a dynamical system represented by the state space model*

$$\begin{aligned} \dot{x}_i &= f_i(x_i, u_i) \\ y_i &= g_i(x_i, u_i) \end{aligned} \tag{5.3}$$

*where $f_i : \mathbb{R}^{n_i} \times \mathbb{R}^{p_i} \to \mathbb{R}^{n_i}$ and $g_i : \mathbb{R}^{n_i} \times \mathbb{R}^{p_i} \to \mathbb{R}^{p_i}$ are locally Lipschitz. Such system is said to be locally input strictly passive about the equilibrium $(\hat{u}_i, \hat{x}_i)$, if there exist open neighborhoods $U_i$ and $X_i$ about $\hat{u}_i$, $\hat{x}_i$, respectively, a continuously differentiable function*

[1] Note that the inputs $u_i$ are also function of the states $x_1, \dots, x_{|\mathcal{N}|}$ as the system is interconnected.

$\mathscr{V}_i(x_i)$ *(called the storage function), and a function* $\phi(.)$ *such that*

$$(u_i - \hat{u}_i)^T (y_i - \hat{y}_i) \geq \dot{\mathscr{V}}_i + (u_i - \hat{u}_i)^T \phi_i(u_i - \hat{u}_i) \tag{5.4}$$

*for all* $u_i \in U_i$ *and all* $x_i \in X_i$*, where* $(u_i - \hat{u}_i)^T \phi_i(u_i - \hat{u}_i) > 0$ *for* $u_i \neq \hat{u}_i$*.*

**Remark 5.2.1** *For linear systems or systems linearized about equilibrium, the passivity property can be easily verified by means of computationally efficient methods using the KYP lemma [20]. Note here that the KYP lemma also allows to explicitly construct the storage function of the system, which for linear systems is a quadratic function of the form* $\mathscr{V}(x_i) = x_i^T P_i x_i$*, where matrix* $P_i \in \mathbb{R}^{n_i \times n_i}$ *is obtained by solving a convex optimization problem (a semidefinite program). For nonlinear systems, it can be verified either locally or globally by exploiting structural properties such as feedback interconnections of passive systems, or via an explicit construction of the storage function (see e.g. [28], [100]). An alternative way to check the passivity property for linear systems is via the positive realness of their transfer function* $G(s)$*. In particular, input strict passivity is implied if* $G(j\omega) + G^T(-j\omega)$ *is positive definite (or equivalently has positive eigenvalues) for all* $\omega \in \mathbb{R}$*.*

In the assumptions below $\hat{x}$ is an equilibrium point of the interconnected system, and $(\hat{u}_i, \hat{x}_i)$ are the corresponding constant inputs and states of the bus dynamics (5.1) at this point.

**Assumption 5.2.1** *For each* $i \in \mathscr{N}$*, each of the bus dynamical systems (5.1) satisfy a local input-strict passivity property about* $(\hat{u}_i, \hat{x}_i)$*, in the sense described in Definition 5.2.2.*

Similarly to the approach presented in [28], [101], it is assumed that the aforementioned passivity property holds without specifying the precise form of the bus dynamics. This will allow us to include in the stability analysis a broad class of bus dynamics and a variety of frequency and/or voltage control mechanisms.

Finally, to guarantee convergence, two additional conditions on the behavior of the interconnected system (4.1) and (5.1) will be required. These conditions will be used in the proof of the convergence result in Theorem 5.3.1.

**Assumption 5.2.2** *Consider the dynamics (5.1) at bus i. When* $u_i(t) = \hat{u}_i \ \forall t$*, then* $\hat{x}_i$ *is asymptotically stable, i.e. there exists neighbourhood* $\tilde{X}_i$ *about* $\hat{x}_i$ *such that for all* $x_i(0) \in \tilde{X}_i$*, we have* $x_i(t) \to \hat{x}_i$ *as* $t \to \infty$*.*

**Remark 5.2.2** *Note that this condition is trivially satisfied in many cases as generation dynamics are usually open loop stable. The condition could also be relaxed to allow for*

*integrators at some buses (used in e.g, secondary control), but this is not done here for simplicity in the presentation.*

**Assumption 5.2.3** *The storage functions $\mathscr{V}_i$ in Assumption 5.2.1 have a strict local minimum at the point $\hat{x}_i$.*

**Remark 5.2.3** *The above assumption is a technical condition often satisfied. More specifically, it means that the region, whereas the bus dynamics are passive, contains at least one stable equilibrium of the interconnected system. As extensively discussed in [19], at any stable equilibrium point, the energy stored in the system remains unchanged, i.e. the time derivative of the storage function is equal to zero. The previous statement implies that the system trajectories starting at this particular point, remain at it, as $t \to \infty$. This condition is satisfied, for example, for any linear system if the latter is observable and controllable.*

### 5.2.2 Dynamic network representation

The natural passivity properties that were revealed for the network along with the proposed system structure (the power system is represented by the negative feedback interconnection of multiple subsystems, i.e. the branch, the capacitance and the bus dynamics.) allow us to deduce significant stability results for the interconnected system by only imposing several local passivity conditions on bus dynamics. Similarly to the previous section, it is now necessary to provide here the following definitions regarding the equilibria of an interconnected system and the property of local strict passivity.

**Definition 5.2.3** *The constant vector $[\hat{x}^T \ \hat{I}_a^T \ \hat{I}_b^T \ \hat{V}_a^{cT} \ \hat{V}_b^{cT}] \in \mathbb{R}^{(n+2|\mathscr{E}|+2|\mathscr{N}|)}$ is an equilibrium of the interconnected system* (5.2)*,* (4.12) - (4.13) *and* (4.20)*, if the time derivative of the states in* (5.2)*, the line currents in* (4.12) *and the shunt capacitance voltages* (4.20) *are equal to zero.*

**Definition 5.2.4** *Let the system* (5.2) *and its equilibrium $(\hat{x},\hat{u}) \in X \times U$, where $X \subset \mathbb{R}^n$ and $U \subset \mathbb{R}^p$. The system* (5.2) *is locally strictly passive if there exists a continuously differentiable function $\mathscr{V}$ (called the storage function) such that*

$$(u-\hat{u})^T(y-\hat{y}) \geq \dot{\mathscr{V}} + \psi(x-\hat{x}),\ \forall (x,u) \in X \times U \tag{5.5}$$

*for some positive definite function $\psi(x-\hat{x})$. Additionally the above system is:*

- *locally input strictly passive if $(u-\hat{u})^T(y-\hat{y}) \geq \dot{\mathscr{V}} + \phi(u-\hat{u})$ for some positive definite $\phi$, $\forall u \neq \hat{u}$*

- *locally output strictly passive if* $(u-\hat{u})^T(y-\hat{y}) \geq \dot{\mathscr{V}} + \rho(y-\hat{y})$ *for some positive definite* $\rho$, $\forall y \neq \hat{y}$.

*In both the above cases, the inequalities should hold for all* $(x,u) \in X \times U$.

**Assumption 5.2.4** *For each* $i,\ j \in \mathscr{N}$, *each of the bus dynamical systems* (5.2) *satisfies any of the local passivity properties about* $[\hat{x}^T\ \hat{I}_a^{bT}\ \hat{I}_b^{bT}]$, *in the sense described in Definitions 5.2.3 - 5.2.4.*

As in [28] and [31], the above passivity properties hold without specifying the precise form of the bus dynamics. This assumption allows us to incorporate into the stability analysis of various power system components such as synchronous generators, inverter-based RES, loads, FACTS and HVDC lines. Additionally, more accurate, higher-order bus dynamical models along with their voltage and frequency regulation mechanisms can be also considered. Finally, to guarantee asymptotic convergence to the equilibria, the technical condition described in Assumption 5.2.3 will also be required to be satisfied by bus dynamics (5.2).

## 5.3 Main stability results

### 5.3.1 Static network representation

The passivity properties presented for both the network and the bus model are now exploited to show that the equilibria of the system (4.1) and (5.1) are asymptotically stable. This result which requires the satisfaction of Assumptions 5.2.1 - 5.2.3 is stated in the following theorem.

**Theorem 5.3.1** *Suppose there exists an equilibrium of the interconnected system (5.1), (4.1) for which the bus dynamics (5.1) satisfy Assumptions 5.2.1 - 5.2.3 for all* $i \in \mathscr{N}$. *Then this equilibrium is asymptotically stable, i.e. there exists an open neighbourhood S about this point such that for all initial conditions* $x(0) \in S$, *the solutions of the system converge to this point.*

**Proof of Theorem 5.3.1** *The dynamics (5.1) and (4.1) will be used together with Assumptions 5.2.1-5.2.3 to prove Theorem 5.3.1. In particular, we will show that the storage functions that follow from the passivity property can be used to construct a Lyapunov function for the network, with stability then deduced using Lasalle's theorem.*

*Since the passivity conditions for the bus dynamics are considered around the equilibrium point, we define the deviations from the corresponding equilibrium values* $\hat{I}_a, \hat{I}_b, \hat{x}, \hat{V}_a, \hat{V}_b$ *as*

$\tilde{I}_{a,i} = I_{a,i} - \hat{I}_{a,i},\ \tilde{I}_{b,i} = I_{b,i} - \hat{I}_{b,i},\ \tilde{x}_i = x_i - \hat{x}_i,\ \tilde{V}_{a,i} = V_{a,i} - \hat{V}_{a,i},\ \tilde{V}_{b,i} = V_{b,i} - \hat{V}_{b,i}$ *for the net current injection components, the states and the bus voltage components respectively.*

*We now consider the following candidate Lyapunov function for the closed-loop system (4.1) and (5.1):*

$$\mathscr{V}(x) = \sum_{i=1}^{|\mathscr{N}|} \mathscr{V}_i(x_i) \tag{5.6}$$

*where* $\mathscr{V}_i(x_i)$ *is the storage function of the bus dynamics with input* $u_i = [-\tilde{I}_{a,i}, -\tilde{I}_{b,i}]$ *and output* $y_i = [\tilde{V}_{a,i}, \tilde{V}_{b,i}]$*. Considering the passivity conditions described in Assumption 5.2.1, we calculate the derivative of the above Lyapunov function with respect to time. In particular, we get*

$$\begin{aligned} \dot{\mathscr{V}} &= \sum_{i=1}^{|\mathscr{N}|} \dot{\mathscr{V}}_i \leq \sum_{i=1}^{|\mathscr{N}|} \left( [-\tilde{I}_{a,i}\ -\tilde{I}_{b,i}] \begin{bmatrix} \tilde{V}_{a,i} \\ \tilde{V}_{b,i} \end{bmatrix} - \phi_i(-\tilde{I}_{a,i}, -\tilde{I}_{b,i}) \right) \\ &= -[\tilde{V}_a^T\ \tilde{V}_b^T] H_{2n} \begin{bmatrix} \tilde{V}_a \\ \tilde{V}_b \end{bmatrix} - \sum_{i=1}^{|\mathscr{N}|} \phi_i(-\tilde{I}_{a,i}, -\tilde{I}_{b,i}) \end{aligned} \tag{5.7}$$

*whenever* $(\tilde{V}_{a,i}, \tilde{V}_{b,i}) \in U_i$ *and* $\tilde{x}_i \in X_i$ *for all* $i \in \mathscr{N}$*. Since the matrix* $H_{2n}$ *and the scalar valued functions* $\phi_i$ *are positive semidefinite and positive definite respectively, the inequality (5.7) becomes* $\dot{\mathscr{V}} \leq 0$*.*

*We then make use of LaSalle's theorem to prove the asymptotic convergence of the system's trajectories to the equilibrium point. According to Assumption 5.2.3, the candidate Lyapunov function* $\mathscr{V}$ *has a strict local minimum at the equilibrium* $\hat{x}$*. Therefore, for a sufficiently small* $\varepsilon > 0$ *there exists a compact positively invariant set* $\Xi := \{x : \mathscr{V}(x) - \mathscr{V}(\hat{x}) \leq \varepsilon,\ \hat{x} \in \Xi,\ \Xi \text{ connected}\}$ *that lies in the neighborhoods stated in the assumptions. LaSalle's Invariance Principle can now be applied with the function* $\mathscr{V}$ *on the compact positively invariant set* $\Xi$*. This guarantees that all solutions of the interconnected system (5.1) and (4.1) with initial conditions* $x(0) \in \Xi$ *converge to the largest invariant set within* $\Upsilon := \Xi \cap \{x : \dot{\mathscr{V}} = 0\}$*. From the positive definiteness of function* $\phi$ *we have that* $\dot{\mathscr{V}} = 0$ *which implies that* $\tilde{I}_{a,i} = \tilde{I}_{b,i} = 0$*, i.e.* $I_{a,i} = \hat{I}_{a,i}$*,* $I_{b,i} = \hat{I}_{b,i}$*. Hence, from Assumption 5.2.2 we have that the only invariant set in* $\Upsilon$ *is the equilibrium point* $x(t) = \hat{x}$*. Therefore, for any initial condition* $x(0) \in \Xi$ *we have convergence to the equilibrium point, which completes the proof.* □

**Remark 5.3.1** *It should be noted that the stability conditions in Theorem 5.3.1 are decentralized as they are conditions on the local bus dynamics and do not require any information regarding the system and its structure. A distinctive feature of those is that the bus dynamics are formulated at the system reference frame, thus allowing to consider networks with losses as discussed in Chapter 4. In Chapter 6, it will be shown that these stability conditions are not conservative by applying those to real power networks with realistic data.*

### 5.3.2 Dynamic network representation

This section contains the main stability result when the proposed multi-input/multi-output stability analysis framework is adopted. This result which is independent of the network topology can provide decentralized guarantees for the asymptotic stability of any power system requiring only the local passivity conditions of Assumptions 5.2.3 - 5.2.4 to be satisfied by bus dynamics. Moreover, it is highlighted that these stability guarantees are derived without neglecting neither the dynamic nor the lossy nature of the lines.

**Theorem 5.3.2** *Suppose there exists an equilibrium of the interconnected system* (5.2)*,* (4.12) - (4.13) *and* (4.20) *for which the bus dynamics* (5.2) *satisfy Assumptions 5.2.3 - 5.2.4 and at least one of the local conditions presented in Assumption 5.2.4, for all* $i,\ j \in \mathcal{N}$*. Then, this equilibrium is asymptotically stable, i.e. there exists an open neighbourhood S about this point such that for all initial conditions* $[\hat{x}(0)^T\ \hat{I}_a(0)^T\ \hat{I}_b(0)^T\ \hat{V}_a^c(0)^T\ \hat{V}_b^c(0)^T] \in S$*, the solutions of the system converge to this point.*

**Proof of Theorem 5.3.2** *For the proof of Theorem 5.3.2 we employ the storage functions that follow from the passivity property of the branch, the capacitance and the bus dynamics to construct a candidate Lyapunov function for the interconnected system* (5.2)*,* (4.12) - (4.13) *and* (4.20)*. Stability will be then deduced using LaSalle's Invariance Principle [21].*

*We first consider the following candidate Lyapunov function for the interconnected system* (5.2)*,* (4.12)-(4.13) *and* (4.20)*:*

$$\mathscr{V}^S = \mathscr{V}^N + \mathscr{V}^C + \sum_{i=1}^{|\mathcal{N}|} \mathscr{V}_i. \tag{5.8}$$

*Considering that all necessary assumptions hold, we then calculate the derivative of the above Lyapunov function with respect to time. We get:*

$$\begin{aligned} \dot{\mathscr{V}}^S &= \dot{\mathscr{V}}^N + \dot{\mathscr{V}}^C + \sum_{i=1}^{|\mathcal{N}|} \dot{\mathscr{V}}_i \\ &= -(I_a - \hat{I}_a)^T R (I_a - \hat{I}_a) - (I_b - \hat{I}_b)^T R (I_b - \hat{I}_b) \\ &\quad - \sum_{i=1}^{|\mathcal{N}|} \left( \psi_i(x - \hat{x}) + \phi_i(u - \hat{u}) + \rho_i(y - \hat{y}) \right) \end{aligned} \tag{5.9}$$

*whenever* $(\hat{I}_{a,i}^b,\ \hat{I}_{b,i}^b) \in U_i$ *and* $\hat{x}_i \in X$*. Since the network's resistance matrix R and the functions* $\psi_i(x - \hat{x})$*,* $\phi_i(u - \hat{u})$ *and* $\rho_i(y - \hat{y})$ *are positive definite, the equation* (5.9) *becomes* $\dot{\mathscr{V}}^S \leq 0$*.*

*Subsequently, we use the LaSalle's theorem to prove the asymptotic convergence of the system's trajectories to the equilibrium point. According to Assumption 5.2.3, the candidate*

*Lyapunov function* $\mathscr{V}^S(x, I_a, I_b, V_a^c, V_b^c)$ *has a strict local minimum at the equilibrium of the interconnected system* $[\hat{x}^T\ \hat{I}_a^T\ \hat{I}_b^T\ \hat{V}_a^{cT}\ \hat{V}_b^{cT}]$. *Thus, for a sufficiently small* $\varepsilon > 0$ *there exists a compact positively invariant set* $\Xi := \{\mathscr{V}^S(x, I_a, I_b, V_a^c, V_b^c) - \mathscr{V}^S(\hat{x}, \hat{I}_a, \hat{I}_b, \hat{V}_a^c, \hat{V}_b^c) \leq \varepsilon,\ \hat{x} \in \Xi,\ \Xi\ connected\}$ *that lies in the neighborhoods stated in Assumption 5.2.4. LaSalle's Invariance Principle can now be applied with the function* $\mathscr{V}^S$ *on the compact positively invariant set* $\Xi$. *This guarantees that all solutions of the interconnected system* (5.2), (4.12) - (4.13) *and* (4.20) *with initial conditions* $[x(0)^T\ I_a(0)^T\ I_b(0)^T\ V_a^c(0)^T\ V_b^c(0)^T] \in \Xi$ *converge to the largest invariant set within* $\mathscr{D} := \Xi \cap \{x : \dot{\mathscr{V}}^S = 0\}$. *From Assumptions 5.2.3 - 5.2.4, we get that the only invariant set in* $\mathscr{D}$ *is the equilibrium point* $[\hat{x}^T\ \hat{I}_a^T\ \hat{I}_b^T\ \hat{V}_a^{cT}, \hat{V}_b^{cT}]$. *Therefore, for any initial condition* $[x(0)^T\ I_a(0)^T\ I_b(0)^T\ V_a^c(0)^T\ V_b^c(0)^T] \in \Xi$ *we have convergence to the equilibrium point, which completes the proof.* □

**Remark 5.3.2** *The above stability result is completely decentralized and identical to the one presented in Section 5.3.1. However, in this section, in addition to the dynamic nature of the network, more general passivity conditions were imposed on bus dynamics to guarantee the asymptotic convergence to the equilibrium. In particular, apart from an input-strict passivity condition, it was shown that asymptotic stability could also be deduced through either output-strict or strict passivity conditions on bus dynamics. Moreover, when the storage function of a power system component is positive definite, even a simple passivity condition can be sufficient to show that the interconnected system is local asymptotically stable. The previous statement will be verified in Section 6.3 through the design of an alternative voltage droop load controller.*

**Remark 5.3.3** *The passivity conditions in Theorem 5.3.2 are applied around a certain equilibrium of the system. This means that for inherently passive systems, these conditions are always satisfied. Nevertheless, for non-passive power system components (e.g. synchronous generators), these local conditions can only be satisfied when certain control mechanisms are enabled at the buses or when the power system operates within certain normal operating limits. For realistic examples illustrating the feasibility and the applicability of these local conditions on synchronous generators and grid-forming inverters, the reader can refer to [31, 35].*

## 5.4 Discussion

The multi-variable framework presented in the previous sections relies on the approach presented in [30, 31, 34] where the analysis was carried out in a *common system reference frame*, instead of each bus local $dq$ reference frame. In contrast to the majority of related

literature, the adoption of the proposed system reference frame approach allowed us to capture the natural passivity properties of the network which were then used for the derivation of completely decentralized stability results for the interconnected system. It is mentioned here that the passivity of the network was revealed without resorting to significant simplifications such as the consideration of lossless and static lines. These simplifications are usually necessary when the analysis is carried out using the local $dq$ coordinates due to the different bus frequencies and the voltage angles that are appearing in the network equations [35].

In addition to the lossy nature of network lines, the network's dynamic behavior was also taken into account. Such a network representation becomes crucial since the dynamic interaction of inverter-based DER with the rest of the system constitutes an important aspect in the analysis of the future power grids where RES share in power generation will dominate. Specifically, the dynamics of inverter-based DER are on similar time scales as the line dynamics while their controls are also significantly faster than traditional frequency and voltage control mechanisms [11]. As shown in [97], the dynamic coupling between inverter-based DER and the network is in many cases unstable although the capability of DER to employ fast-acting control mechanisms may lead to the expectation for more efficient frequency and voltage support.

Additionally, the flexibility provided regarding the accurate modelling of a variety of power system components constitutes another significant advantage of the proposed framework. In particular, the use of a broad class of dynamical systems to represent the bus dynamics allows us to adopt dynamical models of arbitrary complexity as well as a variety of control mechanisms. Note here that the adoption of higher-order dynamics can be easily carried out in a centralized stability analysis study in which all information regarding the power system is available. Such analysis, however, comes at the expense of computational efficiency as the employed methodologies for small-signal stability require considerable time to complete [18]. On the other hand, higher-order modelling becomes difficult when stability is deduced in a completely decentralized manner, using local conditions. In such cases, the elaborated analysis becomes more complex and often requires even resorting to simpler models or omitting the employed voltage and frequency control mechanisms. Even though these simplifications can facilitate stability analysis, they cannot ensure the accuracy of the derived results.

Finally, the proposed passivity-based framework can also drive the appropriate selection/tuning of the grid-connected components which are often non-passive. Specifically, the local passivity conditions presented in the previous paragraphs can assist in the design of more accurate distributed voltage and frequency control mechanisms or the improvement of existing controllers. At the same time, the use of such local conditions can significantly

reduce the complexity of the analysis since they are sufficient for ensuring the overall system stability and robustness without requiring the explicit knowledge of the network structure. Examples of the application of such passivity-based techniques can be found in [28, 31, 35] and Chapter 6.

# Chapter 6

# Applications

This chapter introduces several applications of the presented stability analysis approach that were initially introduced in [30, 31, 34, 35]. More specifically, Section 6.1 describes in detail how the inherent passive nature of the network in combination with the passivity indices arising across the power grid could be exploited to drive SVC employment. As will be shown, the proposed methodology for SVC placement, tuning and sizing can significantly enhance power system stability and robustness without resorting to significant simplifications or employing computationally intractable optimization techniques. Section 6.2 demonstrates the applicability and the feasibility of the presented passivity conditions on synchronous generators using realistic data. The proposed decentralized conditions are further exploited for the introduction of a modified excitation system that can passivate generator dynamics and thus, improve system response during generation-load imbalances. Section 6.3 deals with the design of an effective, demand-side voltage regulation scheme that can provide significant voltage support and assist in maintaining acceptable voltage levels across the grid. The proposed control mechanism can be used either in a centralized or decentralized fashion while its application at several buses of the network can improve the system's response even when the presented passivity conditions are not satisfied at all the buses. Finally, a brief discussion on an additional application of the proposed stability analysis approach on grid-forming inverters is also provided.

## 6.1 Passivity-based employment of SVCs for power system stability enhancement

### 6.1.1 Introduction

The undeniable need to overcome the numerous issues that arose across the power grid coerced system operators to seek for more accurate fast-acting control mechanisms for both the active and reactive power. FACTS devices have been identified in the recent past as a promising solution for mitigating such problems since they can improve system operation and increase their limits [25]. However, due to their relatively high cost, their placement across the network along with the appropriate sizing and tuning should be carefully selected [26].

Driven by the need to enhance power system stability and robustness and overcome the above issues, several works have been proposed for the optimal placement and tuning of FACTS devices. The majority of these works rely on optimization procedures, or sensitivity and stability indices [102–114]. Although they were shown to be very effective, their application remains difficult. Optimization techniques require solving nonlinear, mixed-integer, problems, which can prove computationally intractable. At the same time, approaches based on indices coming from the linearization of the system have inherent limitations concerning stability.

This section introduces a novel, passivity-based framework for Static Var Compensator (SVC) employment that can enhance the overall power system stability and robustness. In particular, the main contributions of this study, parts of which were published in [30], are:

- The identification of the most vulnerable -in terms of passivity- buses of the system for the SVC installation using the Gershgorin Circle Theorem.
- The derivation of a broad passivity-based tuning strategy which provides local stability guarantees and furthermore can lead to the overall enhancement of the power system stability.
- The determination of the appropriate size for the installed SVCs through the employment of the Kernel Density Estimation (KDE) tool for the analysis of the consumption data at the installation locations. This tool can significantly reduce the operational range of the installed SVCs and therefore, the cost of SVC installation.

Throughout the section, we also discuss the advantages of the proposed framework, while verifying its effectiveness through simulations on the IEEE 68-bus test system and a numerical

application of the proposed sizing methodology. As will be shown, significant improvement is achieved even when a small number of SVCs is installed across the grid.

### 6.1.2 Dynamic Models

#### SVC model

SVC installations comprise of one or more banks of fixed or switched shunt capacitors or reactors, of which at least one bank is switched by thyristors. These installations are usually connected to the system through a coupling transformer. In this section, SVCs are represented by a simple, linearized model which, although it facilitates the analysis, still captures the necessary dynamic characteristics. This model relies on the *Basic Model 1* presented in [115] and is described by

$$B_i^{svc}(s) = \frac{K_{R,i} \cdot (1 + sT_{1,i})}{(1 + sT_{R,i})(1 + sT_{2,i})}(V_i^{ref} - V_i) \tag{6.1}$$

where the variables $B_i^{svc}$, $V_i^{ref}$ and $V_i$ denote the SVC susceptance, the reference voltage, and the voltage magnitude at bus $i$, respectively. $K_{R,i}$ is the regulator gain constant while $T_{R,i}$, $T_{1,i}$ and $T_{2,i}$ are the regulator and the compensator lead and lag time constants.

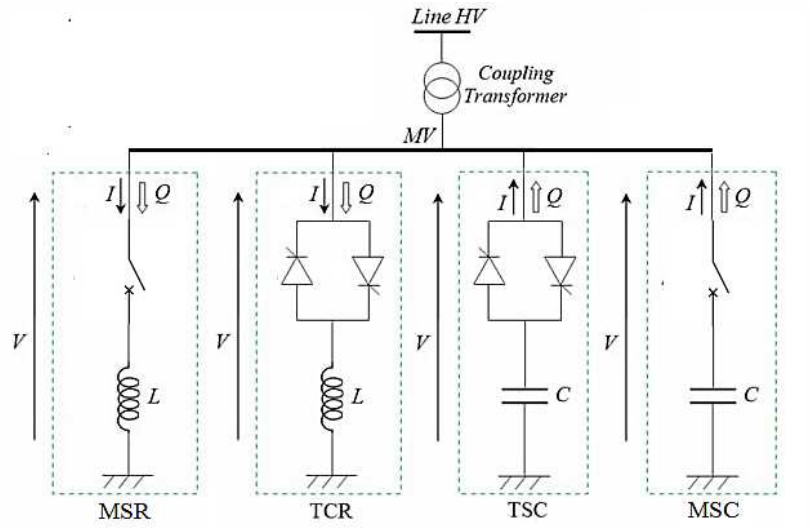


Fig. 6.1 Example of SVC structure

For the derivation of a proper SVC model that fits the adopted multi-input/multi-output network formulation, the transfer function (6.1) is first expressed in the time domain using the inverse Laplace transformation [38]. The derived second-order differential equation is

then written as a set of two first-order ODEs, that is the state-space form. Subsequently, by incorporating the mappings of the current output of the SVC, i.e.:

$$\bar{I}_i = jB_i^{svc}\bar{V}_i \;\rightarrow\; I_{a,i} = -B_i^{svc}V_{b,i} \;\text{ and }\; I_{b,i} = B_i^{svc}V_{a,i}$$

and the relations $V_i = \sqrt{V_{a,i}^2 + V_{b,i}^2}$ and $I_i = \sqrt{I_{a,i}^2 + I_{b,i}^2}$ into the previous set of ODEs, we create a new nonlinear state-space model with inputs the voltage components $V_{a,i}$ and $V_{b,i}$ and outputs the current components $I_{a,i}$ and $I_{b,i}$. By transforming the previous state-space model back to frequency domain, we finally get the following multi-variable system

$$\begin{bmatrix} I_{a,i} \\ I_{b,i} \end{bmatrix} = \underbrace{\begin{bmatrix} T_i^a(s) & T_i^b(s) + \hat{B}_i^{svc} \\ -T_i^b(s) - \hat{B}_i^{svc} & T_i^a(s) \end{bmatrix}}_{H_i^{svc}(s)} \begin{bmatrix} V_{a,i} \\ V_{b,i} \end{bmatrix}. \tag{6.2}$$

Note that the above system is derived through the linearization of the nonlinear SVC state-space model around its operating point and that in (6.2), $\hat{B}_i^{svc}$ is the susceptance of the SVC at this point. $H_i^{svc}(s)$ denotes the $2 \times 2$ proper transfer function matrix relating the voltage components $V_{a,i}$ and $V_{b,i}$ with the current components $I_{a,i}$ and $I_{b,i}$. The transfer functions $T_i^x(s)$ are given by

$$T_i^x(s) = \frac{K_I^x \cdot (1 + sT_1)}{(1 + sT_R)(1 + sT_2)}. \tag{6.3}$$

where $x \in \{a, b\}$. The gain constants $K_i^a$ and $K_i^b$ are derived through the linearization procedure and satisfy $K_i^a,\ K_i^b \geq 0$.

### Load model

Loads are represented by a constant impedance, dynamic model. Considering that for every load the following holds

$$\begin{aligned} \bar{I}_i =& I_{a,i} + jI_{b,i} = -Y_i^L\bar{V}_i = -(G_i^L + jB_i^L)(V_{a,i} + jV_{b,i}) \\ =& (-G_i^L V_{a,i} + B_i^L V_{b,i}) - j(B_i^L V_{a,i} + G_i^L V_{b,i}) \quad i \in \mathcal{N} \end{aligned}$$

the load model can be formulated as

$$\begin{bmatrix} I_{a,i} \\ I_{b,i} \end{bmatrix} = \underbrace{\frac{1}{1 + sT_l}\begin{bmatrix} -G_i^L & B_i^L \\ -B_i^L & -G_i^L \end{bmatrix}}_{H_i^L(s)} \begin{bmatrix} V_{a,i} \\ V_{b,i} \end{bmatrix} \tag{6.4}$$

where $H_i^L(s)$ is a $2\times 2$ transfer function matrix describing the dynamic behavior of loads. $G_i^L$ and $B_i^L$ denote the conductance and the susceptance of the load connected at bus $i$ while the term $\frac{1}{1+sT_l}$ is a delay term representing the dynamic response of the load during a change. In many cases, the aforementioned delay term is omitted and the model of (6.21) can be further simplified as follows:

$$\begin{bmatrix} I_{a,i} \\ I_{b,i} \end{bmatrix} = \underbrace{\begin{bmatrix} -G_i^L & B_i^L \\ -B_i^L & -G_i^L \end{bmatrix}}_{H_i^L} \begin{bmatrix} V_{a,i} \\ V_{b,i} \end{bmatrix}. \tag{6.5}$$

$H_i^L \in \mathbb{R}^{2\times 2}$ is now the matrix relating the voltage components with the net injected current components in the same manner as $H^N$ in the presented network model (4.1). It should also be noted that the negative sign in the models (6.4) and (6.5) appears due to the fact that $I_{a,i}$ and $I_{b,i}$ denote the components of the net absorbed current rather than the net injected current.

### 6.1.3 Passivity Indices in Power Grids

As discussed in [31] and Chapters 4 - 5, when stability analysis is carried out in a common reference frame using the network model (4.1), network lines retain their natural passivity properties. This finding is very important when stability is deduced in a decentralized manner since certain local passivity conditions on bus dynamics can improve the robustness or even guarantee the overall stability of a general power system.

It is now examined how the grid-connected loads affect the passivity of the network model (4.1) and thus, the overall stability of the system. We, therefore, define the following aggregate model derived by the parallel interconnection of the network and the aggregate load dynamics. We get

$$\begin{bmatrix} I_a \\ I_b \end{bmatrix} = H^{AGG} \begin{bmatrix} V_a \\ V_b \end{bmatrix} = \left(H^N + H^L\right) \begin{bmatrix} V_a \\ V_b \end{bmatrix} \tag{6.6}$$

where $H^{AGG}$ and $H^L$ denote the transfer function matrices of the aggregate network model and all the grid-connected loads respectively. The aggregate model (6.6) can be further simplified by omitting the loads delay term as described in the previous paragraphs. We therefore get:

$$\begin{bmatrix} I_a \\ I_b \end{bmatrix} = \begin{bmatrix} G^N - G^L & -B^N + B^L \\ B^N - B^L & G^N - G^L \end{bmatrix} \begin{bmatrix} V_a \\ V_b \end{bmatrix}. \tag{6.7}$$

Both the load models (6.4) and (6.5) show that the loads constitute a non-passive system since the matrices $H_i^L(s)$ and $H_i^L$ are not positive real and positive semidefinite, respectively

[20]. Thus, the incorporation of the loads into the analysis results in the violation of the network's passivity. Equivalently, we can state that the aggregate network model has a shortage of passivity or it lacks Input Feed-forward Passivity (IFP) [19].

**Remark 6.1.1** *It should be mentioned here that the use of constant impedance load models is a simplification made only for the identification of the most vulnerable buses of the grid. As will be discussed in the next section, the proposed SVC tuning methodology can be utilized using more accurate load dynamics.*

**Remark 6.1.2** *Although an overview of the passivity indices within power systems was provided, it was not discussed how the generators affect the overall passivity of the system. As explained in [31, 116], synchronous generators usually constitute non-passive dynamical systems which can often introduce several stability issues to the grid. However, in this study, it is considered that generators can be passivated with sufficiently high damping to guarantee the asymptotic stability of the system. Such applications where higher-order synchronous generator models are involved can be found in [27, 28, 31, 101].*

### 6.1.4 SVC Employment Framework Formulation

The current section presents the formulation of a novel passivity-based framework for the employment of SVCs. Particularly, the most suitable locations for SVC installation are first identified by assessing the vulnerability index of each bus across the network. A detailed methodology is then introduced for the tuning of installed SVCs. As explained, when SVCs are appropriately tuned can passivate the aggregate network model and subsequently enhance the power system stability. Finally, the consumption data at the locations of SVC installation are analyzed using KDE to determine the optimal size of installed SVCs. The proposed methodology for SVC employment is depicted in Figure 6.2. The stopping criterion of the proposed methodology can be a "budget" of SVCs, a stability margin, or a more sophisticated optimization procedure. More details on this will be provided in Section 6.1.5.

#### Passivity-based placement

For the identification of the network's vulnerable buses and thus the better locations for SVC installation, we use the Gershgorin Circle Theorem which was employed for the proof of Lemma 4.1.1. As can be observed, the passivity of the network model is directly related to the diagonal dominance of the conductance matrix of the network $G^N$. However, the incorporation of the grid-connected loads results in the violation of the network's passivity since the passivity of the aggregate network model (6.7) depends on the positive definiteness

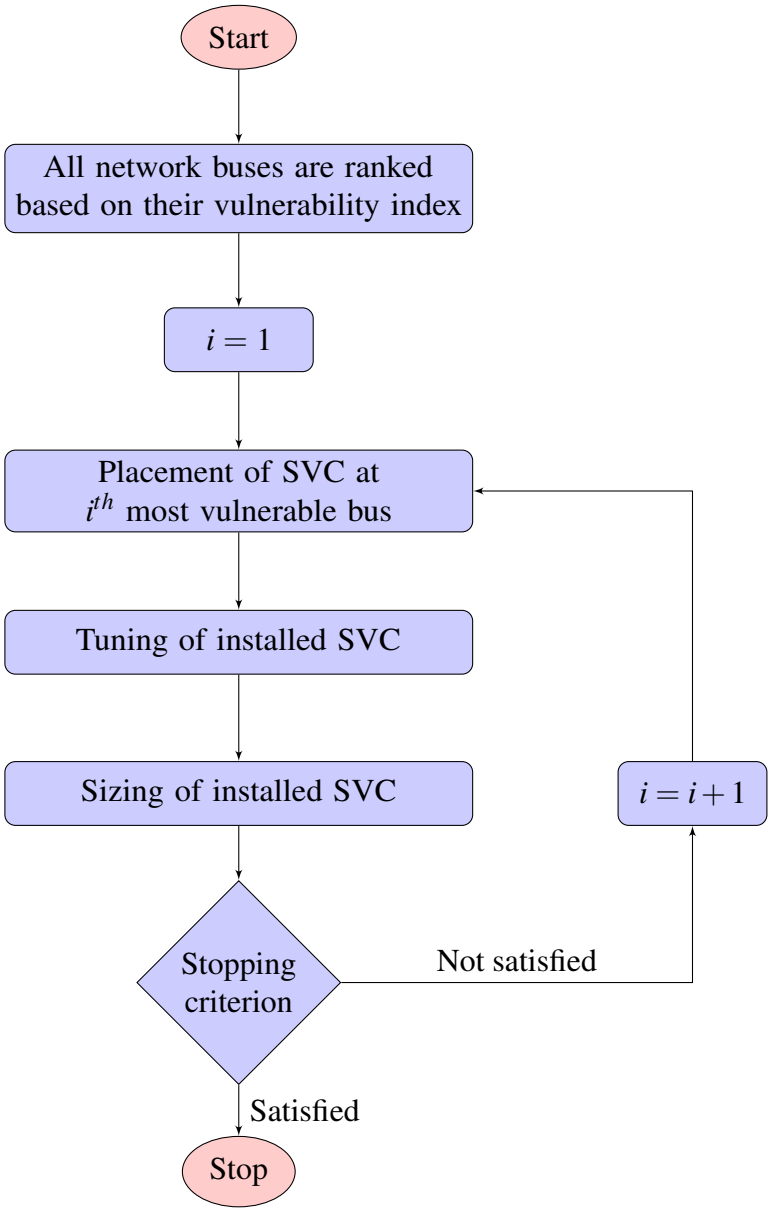


Fig. 6.2 The flowchart representation of the proposed approach for SVC employment.

of the aggregate conductance matrix $G^{AGG} = G^N - G^L$. As the load conductance matrix $-G^L$ constitutes a diagonal matrix with non-positive diagonal elements, the Gershgorin discs corresponding to the respective columns/rows of $G^{AGG}$ are displaced by $G_i^L$ towards the left half-plane. The graphical representation of the effect of the load incorporation into the analysis and thus, the violation of the passivity property satisfied by the power network are presented in Figure 6.3.

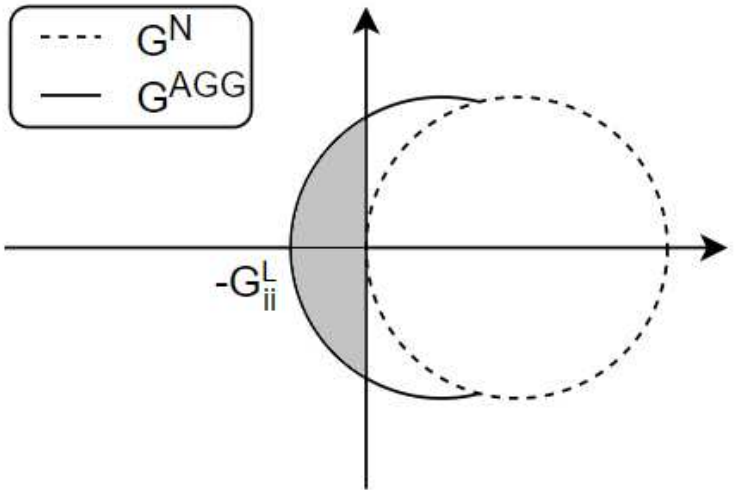


Fig. 6.3 Graphical representation of the Geshgorin disks corresponding to the $i^{th}$ column/row (bus $i$) of the matrices $G^N$ and $G^{AGG}$.

We now define the Gershgorin discs $D_i'(G_{ii}^{AGG}, R_i')$ of the aggregate conductance matrix where the diagonal element $G_{ii}^{AGG}$ denotes the center and $R_i' = \sum_{i \neq j} |G_{ij}^{AGG}|$ the radius of the disc corresponding to the column/row $i = 1, 2, \ldots, |\mathcal{N}|$. Each bus vulnerability index can be calculated as the percentage of the Gershgorin disk that lies in the left half-plane. The vulnerability index of bus $i$ is therefore given by

$$v_i = A_i' \,/\, A_i \times 100 \tag{6.8}$$

where $A_i'$ and $A_i$ denote the area of the disk lying at the left half plane and the total area of the Gershgorin disc $i$, respectively. A significant vulnerability indicates a high probability for the board to have an eigenvalue in the left half level. At the same time, this means that the power system is more likely to exhibit increased oscillating behavior without necessarily being unstable.

**Remark 6.1.3** *Note here that generator buses are excluded from the vulnerability index calculation and consequently from SVC installation since the damping of occurring low-*

*frequency oscillations is beyond the scope of this work. The suppression of this oscillatory behavior can be implemented through the coordinated tuning of SVCs and the generators' Power System Stabilizers (PSS) as in [117].*

### Passivity-based tuning

A novel passivity-based methodology for SVC tuning is being introduced in the following paragraphs. The presented approach relies on feed-forward passivation, i.e. the procedure to render a system that lacks passivity passive via feed-forward (parallel) interconnection [19]. In particular, the proposed tuning methodology is carried out in a completely decentralized manner considering that the SVCs that are installed at the optimal locations across the grid passivate the local dynamics and consequently improve the stability and the robustness of the system.

For the presentation of the proposed methodology, it is considered that a certain number of SVCs are installed at the most vulnerable locations of the power grid. Thus, the aggregate network model (6.6) now becomes

$$\begin{bmatrix} I_a \\ I_b \end{bmatrix} = \underbrace{\left(H^N + H^L + H^{SVC}\right)}_{H^{AGG'}} \begin{bmatrix} V_a \\ V_b \end{bmatrix} \tag{6.9}$$

where $H^{AGG'}$ and $H^{svc}$ are the transfer function matrices of the modified aggregate network and all grid-connected SVCs respectively. Figure 6.4 illustrates the modified aggregate network model which basically represents the parallel interconnection of the network and the SVC and the load dynamics. At the same time, the dynamics at the buses where SVCs are installed, can be represented by the following transfer function matrix which also resulted from the parallel interconnection of the load and the SVC that are connected to bus $i \in \mathscr{N}$:

$$\begin{bmatrix} I_{a,i} \\ I_{b,i} \end{bmatrix} = \underbrace{\left(H_i^L + H_i^{SVC}\right)}_{H_i^{BUS}} \begin{bmatrix} V_{a,i} \\ V_{b,i} \end{bmatrix}. \tag{6.10}$$

The tuning of the installed SVCs is now carried out based on the frequency domain conditions specified within Definition 2.6.3. From the dynamic models (6.2) and (6.21), it is observed that all the poles of $H_i^{BUS}$ are real and negative, thus, the first and the third condition in Definition 2.6.3 are satisfied. Using (6.2) and (6.4), we then derive $H_i^{BUS}(j\omega) +$

$H_i^{BUS,T}(-j\omega)$ which is given by

$$\begin{aligned} H_i^{BUS}(j\omega)+H_i^{BUS,T}(-j\omega) &= \frac{-2}{1+(\omega T_L)^2}\begin{bmatrix} G_i^L & jB_i^L \\ -jB_i^L & G_i^L \end{bmatrix} \\ &+ \frac{2}{(1+(\omega T_R)^2)(1+(\omega T_2)^2)}\begin{bmatrix} K_i^a\hat{K}_i & j\omega K_i^b\bar{K}_i \\ -j\omega K_i^b\bar{K}_i & K_i^a\hat{K}_i \end{bmatrix} \\ &= \begin{bmatrix} h_{i,a}^{BUS}(\omega) & h_{i,b}^{BUS}(\omega) \\ -h_{i,b}^{BUS}(\omega) & h_{i,a}^{BUS}(\omega) \end{bmatrix} \end{aligned} \tag{6.11}$$

where $\hat{K}_i = 1+\omega^2\left(T_{1_i}(T_{R,i}+T_{2,i})-T_{R,i}T_{2,i}\right)$ and $\bar{K}_i = T_{1,i}-T_{2,i}-T_{R,i}-\omega^2 T_{1,i}T_{2,i}T_{R,i}$. Considering that the local bus dynamics shall be passivated, the SVC parameters are appropriately selected in order to ensure that (6.11) is positive semidefinite, that is $H_i^{BUS}(j\omega)+H_i^{BUS,T}(-j\omega)\geq 0$. This is achieved if the parameters are selected so as $h_{i,a}^{BUS}(\omega)>0$ and $|h_{i,a}^{BUS}(\omega)|\geq|h_{i,b}^{BUS}(\omega)|$ for all $\omega\in\mathbb{R}^+$ [118].

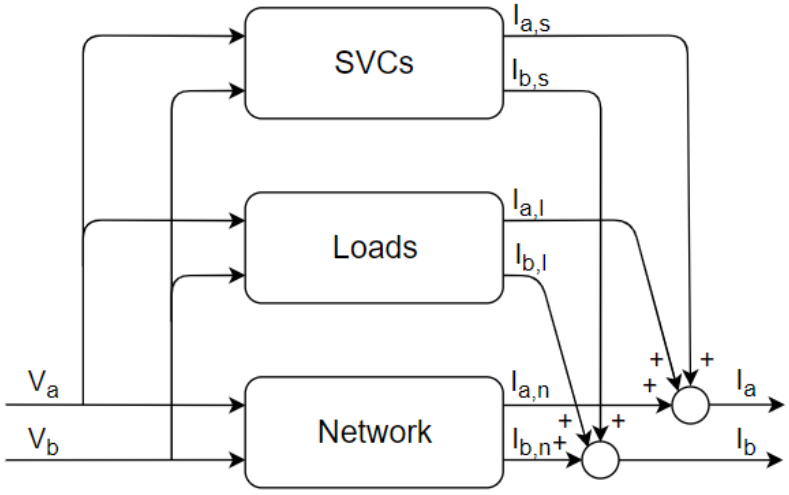


Fig. 6.4 The aggregate network model $H^{AGG'}$ as a parallel interconnection of the network, the SVC and the load dynamics.

Even though the appropriate SVC tuning depends on the explicit knowledge of load dynamics, some general criteria for the selection of SVC parameters are provided below to maximize their stabilization impact. The following criteria ensure that the SVC dynamics constitute a passive system which consequently leads to the enhancement of the power system stability and robustness:

- Set the regulator gain constant $K_{R,i} > G_i^L$. Such selection will ensure that the inequalities $K_i^a > G_i^L$ and $K_i^b > B_i^L$ are satisfied. These inequalities are necessary for the passivation of local bus dynamics especially at low frequencies.

- Select the values of time constants $T_{1,i}$, $T_{2,i}$ and $T_{R,i}$ such that $T_{2,i} \cdot T_{R,i}/(T_{2,i} + T_{R,i}) \leq T_{1,i} \leq 1 + T_{2,i} + T_{R,i}$. This ensures that SVC dynamics are passive (see Lemma 2 in [30]) and that even if bus dynamics are not completely passivated, the response of the system will be significantly improved.

- Select $T_{1,i}$ sufficiently large and $T_{2,i}$ sufficiently small[1], in order to provide to the power grid such damping to reduce the occurring power system oscillations ($0.8 - 10$Hz).

**Remark 6.1.4** *In cases where more advanced modeling of loads is considered the selection of SVC parameters could be more accurate, having, therefore, a larger impact on power grid stability and robustness. Particularly, in such cases, SVC tuning can be carried out graphically by ensuring that the loci of $H_i^{BUS}(j\omega) + H_i^{BUS,T}(-j\omega)$ lies entirely at the upper half of the complex plane.*

### Sizing

The operational range of an SVC is usually specified at the high voltage side of its coupling transformer. However, in order to precisely model the SVC, it is necessary to calculate its susceptance range at the medium voltage bus. Thus, considering that the reactance of the coupling transformer in per unit on $S_n$ base is $X_t$, the maximum (capacitive) and the minimum (reactive) susceptance of the SVC are given by:

$$B_{max} = \frac{1}{|\frac{S_n}{Q^{cap}}| + |X_t|} \tag{6.12}$$

$$B_{min} = \frac{1}{|\frac{S_n}{Q^{ind}}| - |X_t|}. \tag{6.13}$$

$Q^{cap}$ and $Q^{ind}$ denote the maximum capacitive and the maximum inductive reactive power on the high voltage side of the coupling transformer respectively, and they are derived based on local measurements of reactive power [115].

Alternatively, throughout this section, $Q^{cap}$ and $Q^{ind}$ are specified using KDE, a very useful statistical tool utilized to analyze the consumption data at the locations of SVC

[1] Under such selection of time constants, SVCs operate as phase lead compensators and consequently can improve the response of the system.

installation [119]. Particularly, it is considered that the local measurements of reactive power constitute a univariate, independent and identically distributed sample $(x_1, x_2, \dots x_n)$ where $n \in \mathbb{N}^+$. This is then divided into two smaller samples, each containing the positive (inductive) and the negative (capacitive) values of reactive power respectively, i.e. $(x_1^{ind}, x_2^{ind}, \dots x_{n_i}^{ind})$ and $(x_1^{cap}, x_2^{cap}, \dots x_{n_c}^{cap})$ where $n_i, n_c \in \mathbb{N}^+$ and $n_i + n_c = n$. The probability density functions of the aforementioned samples are then calculated using KDE by

$$f^{ind}(x) = \frac{1}{n_i h} \sum_{j=1}^{n_i} K\Big(\frac{x - x_j^{ind}}{h}\Big) \tag{6.14}$$

and

$$f^{cap}(x) = \frac{1}{n_c h} \sum_{j=1}^{n_c} K\Big(\frac{x - x_j^{cap}}{h}\Big) \tag{6.15}$$

respectively. In (6.14) and (6.15), $K$ denotes the selected kernel function while $h > 0$ is a smoothing parameter called the bandwidth. It should be mentioned here that although a wide range of kernel functions can be used, in this section, the historical data of the reactive power are analyzed using a normal kernel.

The cumulative density functions of the inductive and the capacitive reactive power are finally estimated as follows:

$$F^{ind}(x) = \int_{-\infty}^{x} f^{ind}(t)dt \tag{6.16}$$

$$F^{cap}(x) = \int_{-\infty}^{x} f^{cap}(t)dt. \tag{6.17}$$

Instead of selecting $Q^{ind} = max(x^{ind})$ and $Q^{cap} = max(x^{cap})$, the maximum inductive and the maximum capacitive reactive power can now be defined according to the operator's required robustness, that is the percentage of the consumption data that are required to lie within the operational range of the installed SVCs. This percentage usually varies between 90 and 100%. For clarity, the proposed sizing procedure is presented through a numerical application in Section 6.1.6.

### 6.1.5 Discussion

As described in the previous sections, the proposed passivity-based approach for SVC employment deals both with SVC placement, tuning and sizing. Despite its broadness, this approach does not require the employment of computationally expensive techniques for the identification of the better locations for SVC installation and their tuning. On the

contrary, it exploits features of passivity-based analysis to first sort all the buses according to their vulnerability index and then to guide SVC tuning. The proposed sizing methodology significantly decreases the cost of SVC using the statistical analysis of the reactive power profile at the buses selected for the installation.

This work also showed that SVCs are more effective when installed near or at large load centers and at buses where several lines are connected. This statement comes as a result of the methodology used to assess the vulnerability index of each bus, as its value relies on the radius of the respective Gershgorin disc, i.e. the sum of the conductances of the lines that are connected to this bus. This result is also corroborated by various voltage stability studies and existing SVC installations [120–122]. Additionally, the proposed framework can be further exploited to incorporate other FACTS devices (either shunt or series), such as TCSCs, UPFCs and STATCOMs. Apart from improving the robustness of the power system, these devices can further increase the transmission system transfer capability and reduce the transmission losses [25].

Finally, it should be mentioned here that the presented methodology for the identification of the better locations for SVC installation does not provide any information regarding the required number of SVCs. However, it can effectively prioritize their placement across the network when a 'budget' of SVCs is available or, a minimum stability margin shall always be satisfied. Alternatively, it can be applied to existing implementations for the placement of FACTS devices. Particularly, the vulnerability index can be either used to initiate the placement or incorporated into existing optimization problems to improve their convergence time and effectiveness. Such applications can be found in [107, 111, 113, 123, 124].

### 6.1.6 Framework Verification

#### Simulations

The presented framework is verified through several simulations on the IEEE New York / New England 68-bus interconnection system (Figure 6.5), using the Power System Toolbox (PST) [125, 126]. The aforementioned system consists of 16 generator and 24 load buses. The generators and the loads are represented by the sixth-order synchronous generator model and the ZIP model, respectively [93]. The generators are equipped with turbine governors, a simple excitation system and PSSs while loads include induction motors as well.

All simulations are carried out considering average loading at the load buses and the existence or not of PSSs on generators, for the following different cases: (i) no SVCs installed at the grid, (ii) four SVCs installed at the grid (5% of the system's buses), (iii) seven SVCs installed at the grid (10% of the system's buses), and (iv) ten SVCs installed at the grid

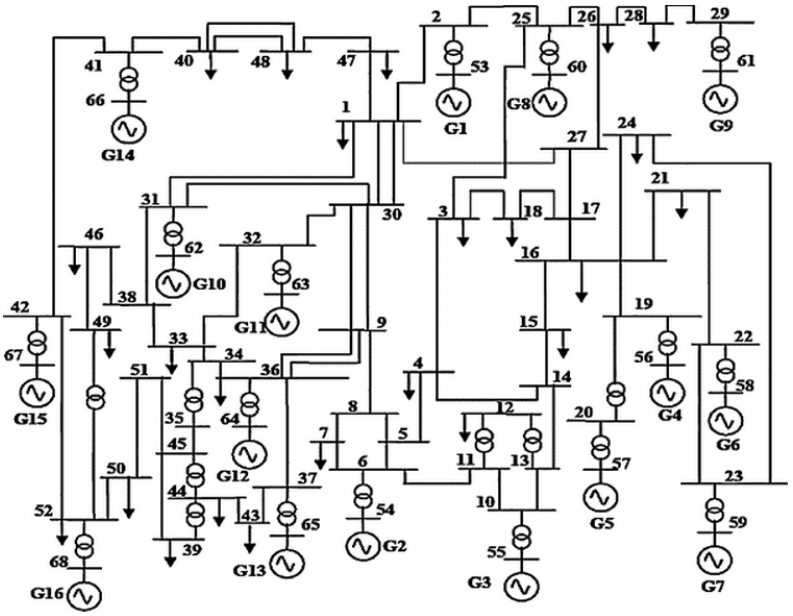


Fig. 6.5 Single line diagram of the IEEE 68-bus test system (New York / New England) [125].

(15% of the system's buses). SVCs are installed across the grid as shown in Table 6.1 based on the passivity-based framework presented in Section 6.1.4. To achieve the greatest stability improvement possible, the parameters of the installed SVCs were set as follows since consumption data are not available for this testbed: $K_{R,i} = 10 \cdot G_i^L$ pu, $T_R = 0.05$ s, $T_1 = 1.0$ s and $T_2 = 0.1$ s.

| Installed SVCs | Bus No. | min damping ratio (no PSSs) | min damping ratio (PSS) |
|---|---|---|---|
| 0 | - | -0.001964 | 0.04855 |
| 1 | 51 | -0.001971 | 0.04854 |
| 2 | 4 | -0.002071 | 0.04854 |
| 3 | 21 | -0.001288 | 0.0487 |
| 4 | 50 | -0.001288 | 0.0487 |
| 5 | 24 | -0.001197 | 0.04872 |
| 6 | 46 | -0.001197 | 0.04871 |
| 7 | 28 | 0.01998 | 0.0529 |
| 8 | 27 | 0.02025 | 0.05291 |
| 9 | 15 | 0.02042 | 0.05292 |
| 10 | 48 | 0.02042 | 0.05279 |

Table 6.1 The minimum damping ratio variation of the system compared to the population of the installed SVCs using the proposed passivity-based approach.

As can be seen from Figures 6.6 and 6.7, the application of SVCs using the proposed framework, damps the calculated modes when either PSSs are applied to the exciters of

generators or not. More specifically, for the case where no PSSs are applied, the application of SVCs on the most vulnerable buses stabilizes the system by moving all the eigenvalues to the left half-plane. Note that the test system was initially small-signal unstable. On the other hand, although the application of PSSs on the excitation systems of the generators improves further the small-signal stability of the test system, the SVC installation at the selected locations results in a more stable response. This improvement can be observed through the damping ratio[2] of both the local and the inter-area modes of the system which is significantly increased. Table 6.1 provides the variation of the minimum damping ratio of the system, according to the number of installed SVCs.

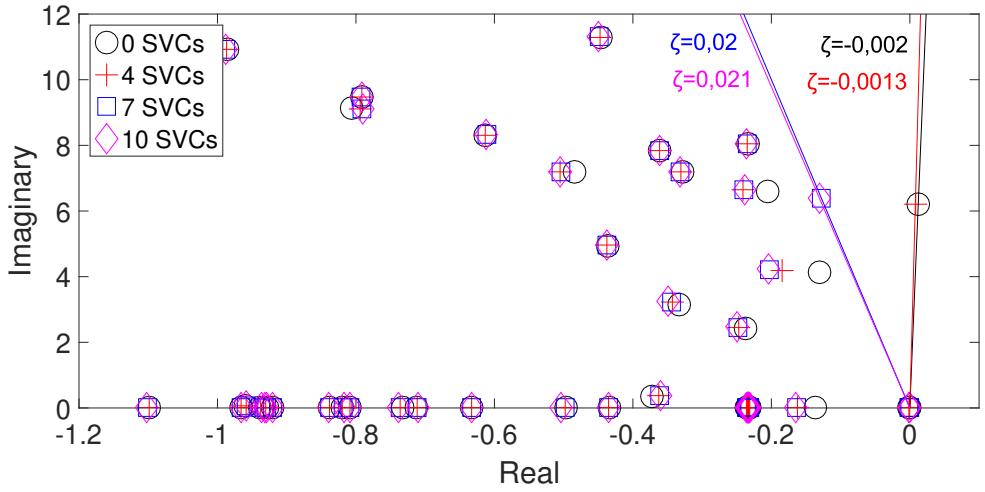


Fig. 6.6 Eigenanalysis of the IEEE 68-bus test system when no PSSs are applied to the generators.

For the dynamic simulations, a step load change of 100 MW is applied to the load buses 1, 7, 21 and 46 (a total load change of 400 MW). The enhancement of the system's stability is illustrated by the voltage and the frequency deviation at bus 24 (Figures 6.8 - 6.11) when PSSs are applied to generators or not. As observed, the proposed SVC employment approach results in a significantly improved response and the suppression of the occurring oscillations. It should be noted here that the SVCs were not designed to provide oscillation damping or target any specific oscillatory modes. On the contrary, the stability improvement arises through the passivation of the system. While not considered in this study, the application of a Power Oscillation Damping controller to the installed SVCs could facilitate the damping of inter-area oscillations and further enhance system stability.

[2]The damping ratio of an eigenvalue $\lambda = a + j\beta$ is defined as $\zeta = -\frac{a}{\sqrt{a^2+\beta^2}}$.

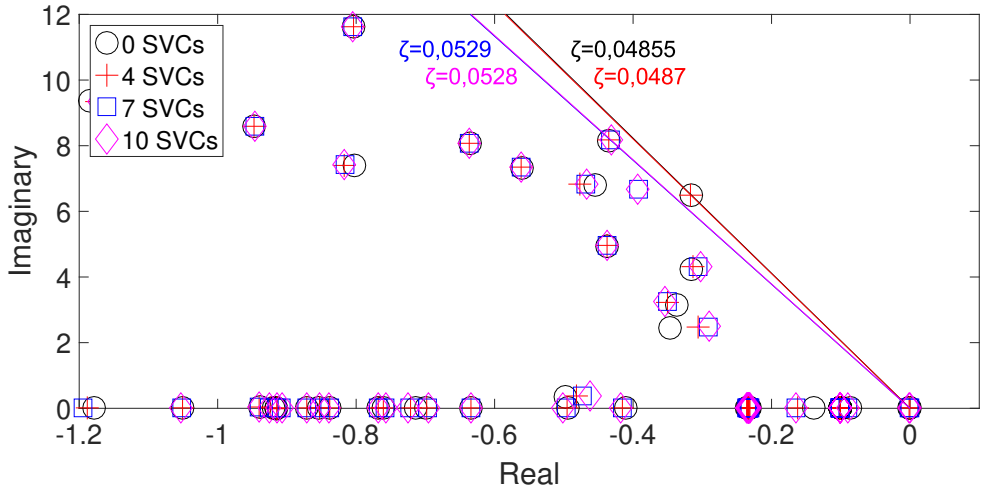


Fig. 6.7 Eigenanalysis of the IEEE 68-bus test system when PSSs are applied to the generators.

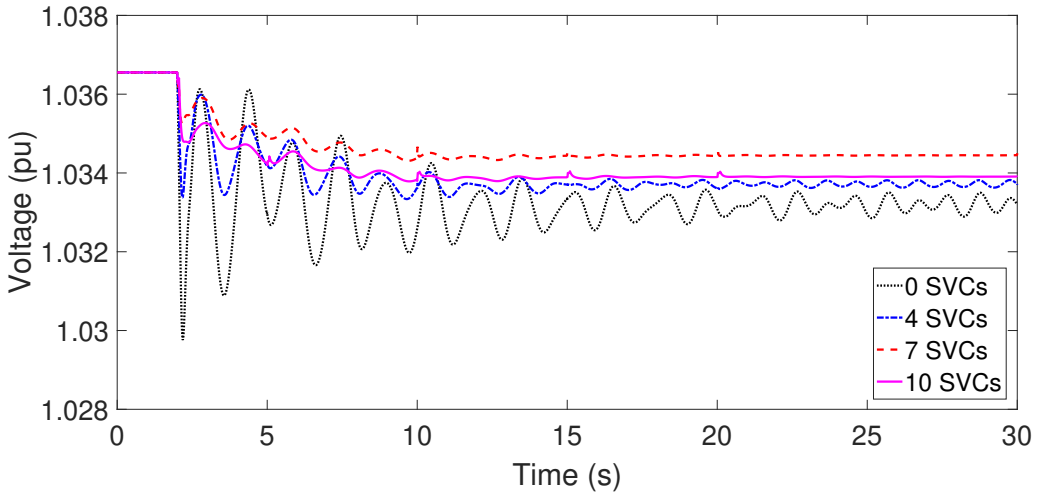


Fig. 6.8 Voltage deviation at bus 24 when the (a) 0, (b) 4, (c) 7 and (d) 10 most vulnerable buses of the network are equipped with appropriately tuned SVCs (no PSSs are applied to generators).

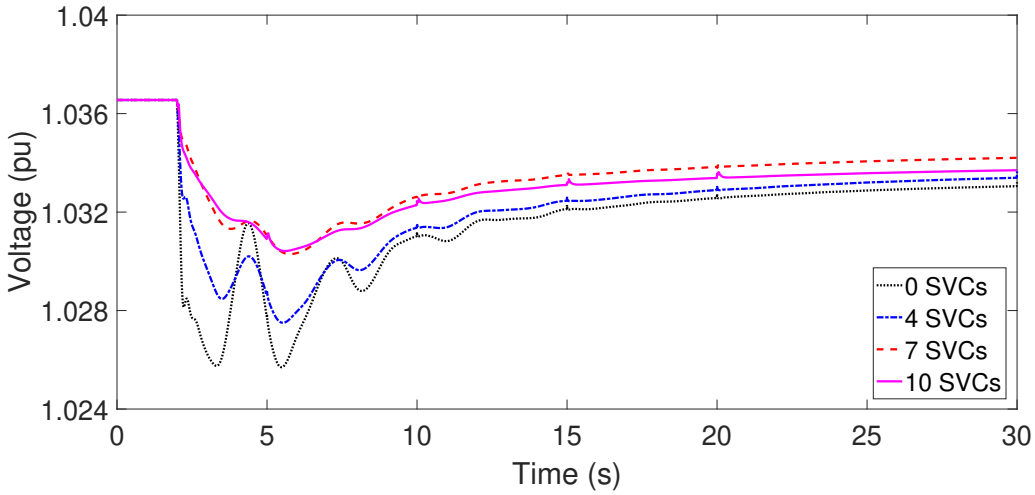


Fig. 6.9 Voltage deviation at bus 24 when the (a) 0, (b) 4, (c) 7 and (d) 10 most vulnerable buses of the network are equipped with appropriately tuned SVCs (PSSs are applied to generators).

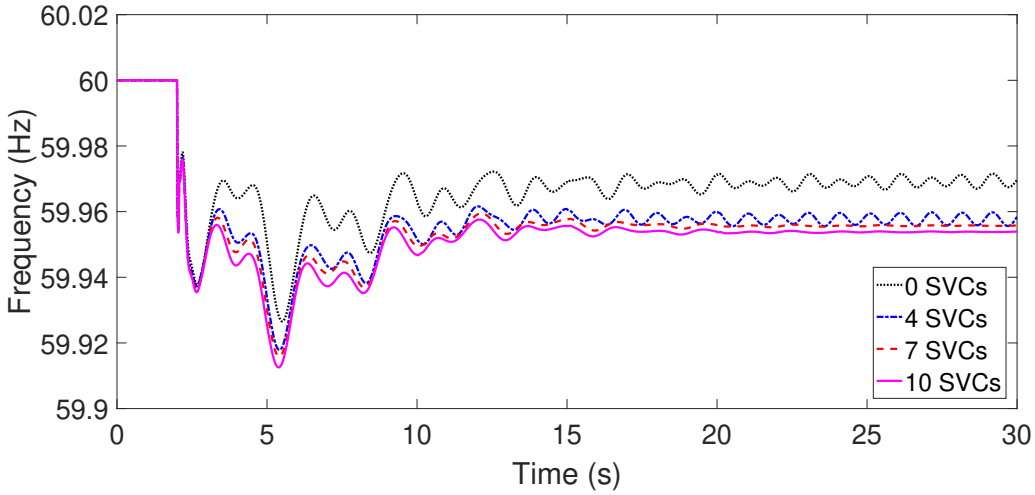


Fig. 6.10 Frequency deviation at bus 24 when the (a) 0, (b) 4, (c) 7 and (d) 10 most vulnerable buses of the network are equipped with appropriately tuned SVCs (no PSSs are applied to generators).

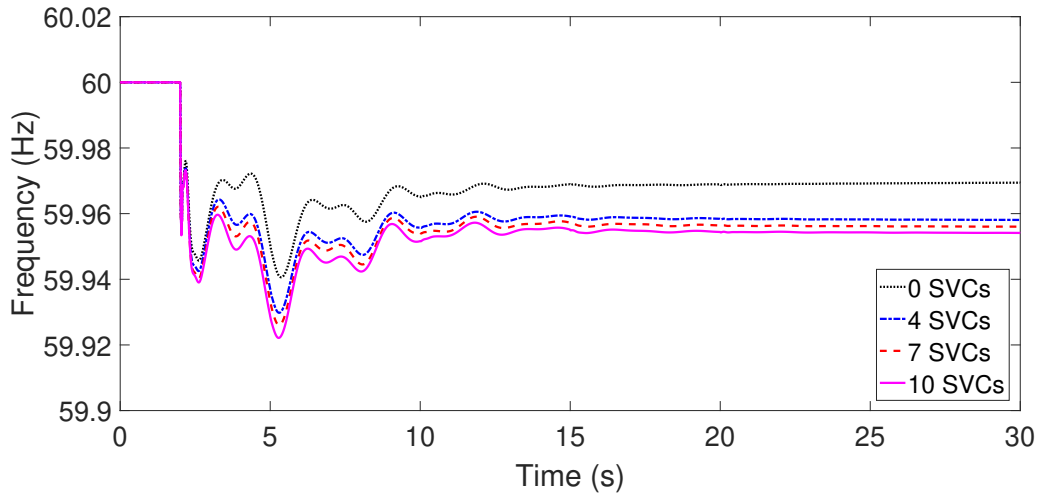


Fig. 6.11 Frequency deviation at bus 24 when the (a) 0, (b) 4, (c) 7 and (d) 10 most vulnerable buses of the network are equipped with appropriately tuned SVCs (PSSs are applied to generators).

Finally, the effectiveness of the proposed methodology is also verified through the profiles of bus voltages under both normal and heavy (40% above normal) loading conditions for each of the four cases mentioned above. The average percentage of steady-state voltage deviation[3] ($PVD$) for these operating conditions is provided in Table 6.2. As can be observed from the aforementioned table, the installation of SVCs across the network using the proposed framework can significantly improve the steady-state behaviour of the system as well.

| **Installed SVCs** | **Normal loading** | **Heavy loading** |
|---|---|---|
| 0 | 2.96% | 3.13% |
| 4 | 2.51% | 2.21% |
| 7 | 2.10% | 2.06% |
| 10 | 1.80% | 1.98% |

Table 6.2 The average percentage steady state voltage deviation of IEEE 68 bus test system under normal and heavy loading conditions.

### Numerical Application

The applicability of the proposed SVC sizing approach and its capability to reduce SVC installation cost is presented through the estimation of the appropriate size of an SVC installed at a certain bus. The proposed sizing methodology is carried out using two different sets of consumption data that are analyzed as described Section 6.1.4 (Figures 6.12 - 6.14). The

[3]The average percentage steady-state voltage deviation is calculated by $PVD = \frac{100}{|\mathcal{N}|}\sum_{i=1}^{|\mathcal{N}|}|1pu - V_i|$

maximum inductive and the maximum capacitive reactive power are selected as the upper and the lower limits wherein the 95% of the values of reactive power lies, that is

$$Q^{ind}_{KDE} = \{x : \ F^{ind}(x) \leq 0.95\} \quad \text{and} \quad Q^{cap}_{KDE} = \{x : \ F^{cap}(x) \leq 0.95\}.$$

As can be observed in Figure 6.12, using KDE to analyze the two different reactive power profiles at this bus provides useful information regarding the structure of the SVC installation. Specifically, the density of the reactive power profile can be used to select the number of fixed or mechanically switched capacitors/reactors. For example, for reactive power profile 1, a structure of two mechanically-switched reactors/capacitors and a thyristor-switched capacitor/reactor seems more proper due to the 'valley' of the reactive power around $0.5pu$. On the other hand, for reactive power profile 2, a mechanically-switched reactor/capacitor and a thyristor-switched capacitor/reactor would be more appropriate since the probability density of reactive power is uniform.

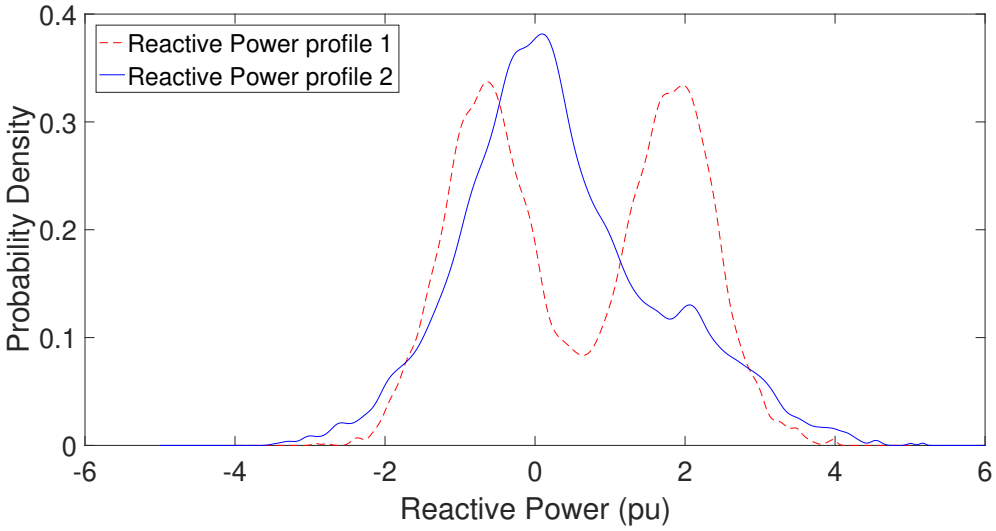


Fig. 6.12 The probability density functions of two different reactive power profiles (samples).

The use of KDE can also reduce the operational range of the SVC installation and consequently its cost. Specifically, as can be observed in Figures 6.13 and 6.14, requiring only the 95% of the values of the reactive power to lie within SVC's operational range (dotted line) results in a significant reduction of its capacity. The aforementioned reduction of the operational range for reactive power profiles 1 and 2 is provided in Table 6.3. Considering that $S_n = 100MVA$, the cost of each SVC installation can be estimated as in [113] using the

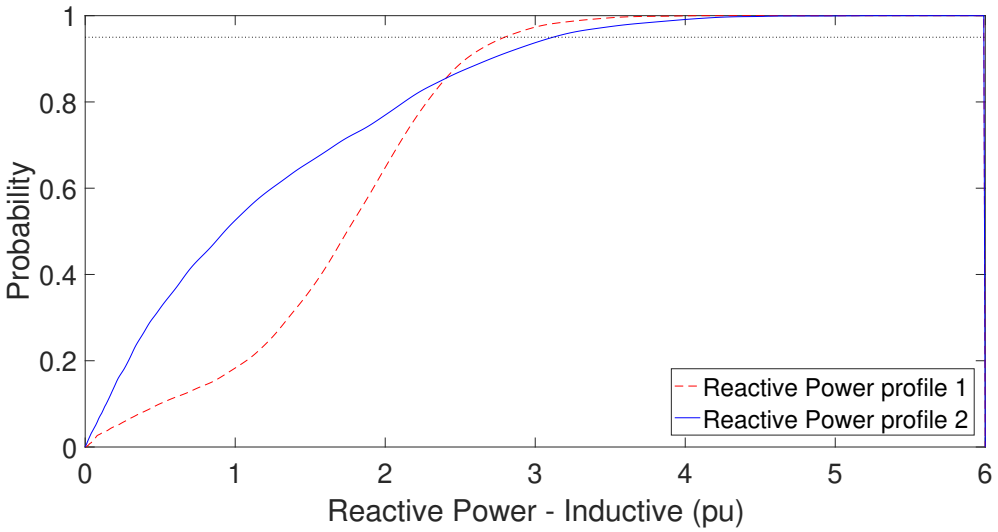


Fig. 6.13 The cumulative density functions of two different inductive reactive power profiles (samples).

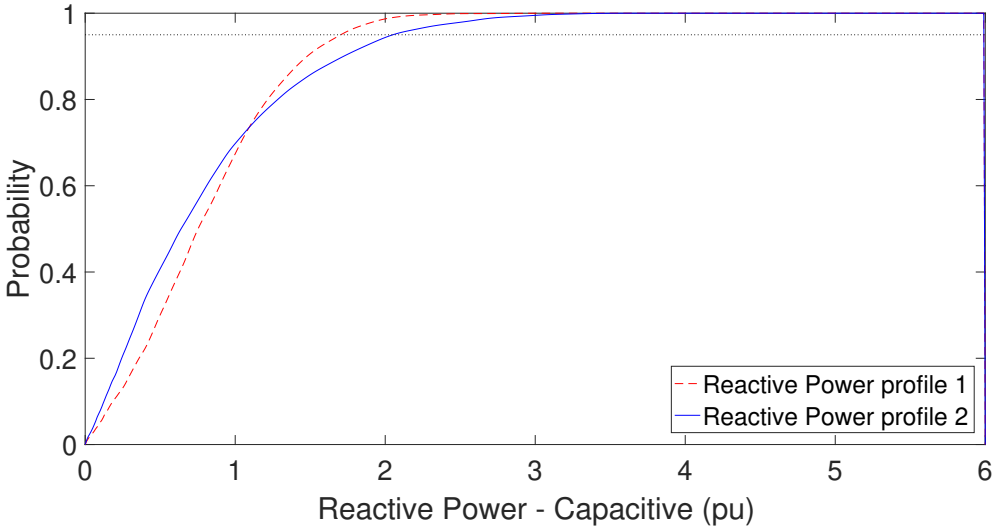


Fig. 6.14 The cumulative density functions of two different capacitive reactive power profiles (samples).

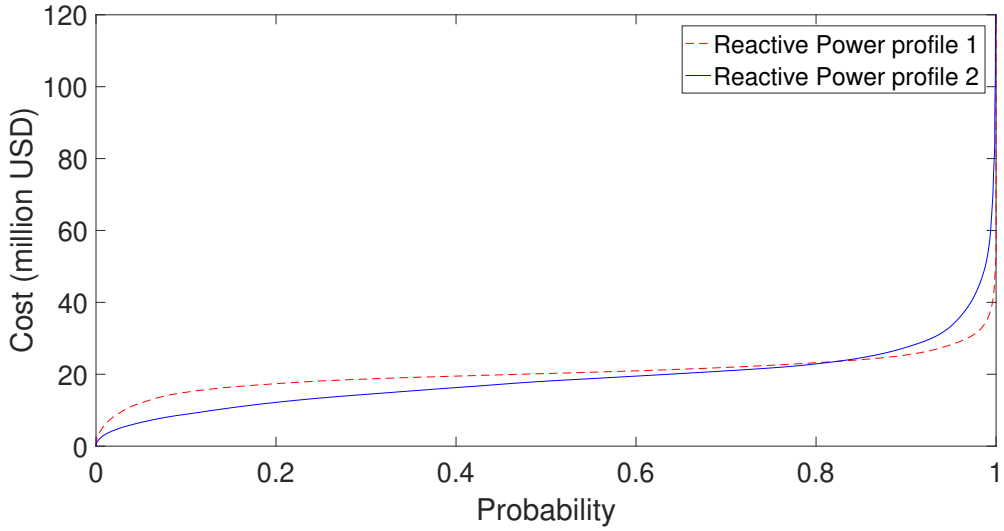


Fig. 6.15 The cost of the SVC installation versus the robustness of its selected reactive power range for the two different reactive power profiles (samples).

following cost model

$$Cost = 0.0003(Q^{ind} - Q^{cap})^2 - 0.3051(Q^{ind} - Q^{cap}) + 127.38 \quad [\$US/kVAr].$$

The total cost for the aforementioned numerical example is therefore: (a) 75.79 million US$ vs. 25.81 million US$ for sample 1 and (b) 36.50 million US$ vs. 22.88 million US$ for sample 2 when the traditional vs. the proposed approach is adopted. The exponential dependence between the cost of installation and the required robustness is finally illustrated in Figure 6.15.

| **Profile** | $Q^{ind}$ **(pu)** | $Q^{ind}_{KDE}$ **(pu)** | $Q^{cap}$ **(pu)** | $Q^{cap}_{KDE}$ **(pu)** |
|---|---|---|---|---|
| 1 | 5.17 | 3.13 | -3.47 | -2.05 |
| 2 | 3.99 | 2.80 | -2.53 | -1.70 |

Table 6.3 The selected values of maximum capacitive and the maximum inductive reactive power for profiles 1 and 2.

### 6.1.7 Conclusions

In the new era of low-inertia systems with high degrees of renewable penetration, it is becoming harder to ensure the stability and the resilience of electricity grids through conventional reinforcement methods. In this context, the current section presented a novel passivity-based framework for SVC employment to enhance the overall power system stability and robust-

ness. In particular, by exploiting findings in passivity-based control analysis and design, the proposed framework provided a detailed methodology for the identification of the most suitable locations for SVC installation and the proper SVC tuning. The derivation of this methodology was carried out without utilizing computationally intractable algorithms or solving complex optimization problems. Throughout this section, useful statistical analysis techniques were also employed to determine the appropriate size and structure of the installed SVCs and thus, to reduce their operational range and installation cost. The presented placement and tuning methodologies were verified through several simulations on the IEEE 68-bus test system, where a significantly improved system response was achieved, even when a small percentage of buses was equipped with SVCs. A numerical application was finally provided for the demonstration of the proposed sizing framework.

## 6.2 Verification of local passivity conditions on synchronous generators

### 6.2.1 Introduction

This section demonstrates the feasibility of the presented stability conditions on two testbed networks using realistic data. More specifically, the local passivity conditions introduced in Chapter 5, are applied to synchronous generators and as will be shown in the sequel, are in many cases satisfied despite being strict. These passivity conditions are further exploited to modify existing excitation systems and thus to improve power system response during disturbances. The presented results are finally verified through several simulations on the Two-Area Kundur test system and the IEEE 68-Bus test system.

### 6.2.2 Generator dynamics

The following paragraphs provide a brief description of the fourth-order generator model, which is widely considered to be sufficiently accurate to analyze electromechanical phenomena. Then, it is explained in detail how such a dynamic model can be incorporated into the presented stability analysis approach and assist in deriving useful information regarding the stability of the system. This model, which will also be used in the simulations presented at

the end of this section, is described by the following set of differential equations:

$$\begin{aligned} M_i\Delta\dot{\omega}_i &= P_i^m - P_i^e - D_i\Delta\omega_i \\ \dot{\delta}_i &= \Delta\omega_i \\ T'_{do,i}\dot{E}'_{q,i} &= E_{f,i} - E'_{q,i} + I_{d,i}(X_{d,i} - X'_{d,i}) \\ T'_{qo,i}\dot{E}'_{d,i} &= -E'_{d,i} - I_{q,i}(X_{q,i} - X'_{q,i}) \end{aligned} \tag{6.18}$$

where the electrical power $P_i^e = E'_{q,i}I_{q,i} + E'_{d,i}I_{d,i} + (X'_{d,i} - X'_{q,i})\, I_{d,i}\, I_{q,i}$. The synchronous generator represented by (6.18), is modeled in its local dq-reference frame. It is represented by the transient emfs $E'_{d,i}$ and $E'_{q,i}$ behind the transient reactances $X'_{d,i}$ and $X'_{q,i}$ as defined by the following equation:

$$\begin{bmatrix} V_{q,i} \\ V_{d,i} \end{bmatrix} = \begin{bmatrix} E'_{q,i} \\ E'_{d,i} \end{bmatrix} - \begin{bmatrix} R_i & -X'_{d,i} \\ X'_{q,i} & R_i \end{bmatrix} \begin{bmatrix} I_{q,i} \\ I_{d,i} \end{bmatrix}. \tag{6.19}$$

As observed, the above synchronous generator model forms a 2-input/2-output system with inputs the currents $-I_{d,i}$ and $I_{q,i}$, and outputs the voltages $V_{d,i}$ and $V_{q,i}$. In order to allow the coupling with the network model (4.1), the generator dynamics have to be transformed into the system reference frame. This transformation is carried out through the incorporation of the mappings (3.29) - (3.32) into the synchronous generator dynamics (6.19). We therefore get:

$$\begin{bmatrix} V_{a,i} \\ V_{b,i} \end{bmatrix} = T_i^{-1} \begin{bmatrix} E'_{q,i} \\ E'_{d,i} \end{bmatrix} - T_i^{-1} \begin{bmatrix} R_i & -X'_{d,i} \\ X'_{q,i} & R_i \end{bmatrix} T_i \begin{bmatrix} I_{a,i} \\ I_{b,i} \end{bmatrix} \tag{6.20}$$

Table 6.4 Description of the main variables and parameters appearing in the synchronous generator models

| **Variables** | | **Parameters** | |
|---|---|---|---|
| $\Delta\omega$ | Frequency deviation | $M$ | Moment of inertia |
| $\delta$ | Stator's phase angle | $D$ | Damping coefficient |
| $E'_d$ | d-axis transient EMF | $X_d$ | d-axis synchronous reactance |
| $E'_q$ | q-axis transient EMF | $X'_d$ | d-axis transient reactance |
| $I_d$ | d-axis current | $T'_d$ | d-axis open-circuit time constant |
| $I_q$ | q-axis current | $X_q$ | q-axis synchronous reactance |
| $V_d$ | d-axis bus voltage | $X'_q$ | q-axis transient reactance |
| $V_q$ | q-axis bus voltage | $T'_q$ | q-axis open-circuit time constant |
| $P^m$ | Mechanical power | $R_i$ | stator windings resistance |
| $P^e$ | Electrical power | | |

As can now be observed, the above generator model matches the class of bus models (5.1). The dynamic model of the generator corresponds to the vector function $f_i$ while equations

(6.20) match to the vector functions $g_i$. The presented formulation still holds for the second and the third-order synchronous generator models, where the transient emfs $E'_{d,i}$ and $E'_{q,i}$, respectively, are assumed to remain constant. Higher-order models, such as the fifth or the sixth order models can also be incorporated in this framework in an analogous way. In these models, the synchronous generators are represented by their sub-transient emfs $E''_{d,i}$ and $E''_{q,i}$ behind the sub-transient reactances $X''_{d,i}$ and $X''_{q,i}$. More detailed information about generator modeling can be found in [48, 93, 94].

As discussed earlier, the generator dynamics can be expanded further to introduce the dynamics of frequency or/and voltage control mechanisms, thus allowing the derivation of more accurate stability results. Such frequency and voltage control mechanisms include several types of turbine governors, exciters and power system stabilizers. A graphical representation of the adaption of a synchronous generator model to the proposed framework along with the incorporation of frequency and voltage control is provided in Figure 6.16. It is highlighted here that the passivity conditions which ensure the asymptotic stability of the equilibria, refer to the bus dynamics and not specifically to the voltage and the frequency control systems that are applied. This feature allows us to include more advanced regulation mechanisms which in most cases are not passive (e.g. turbine governors, excitation systems). This is an important advantage since such dynamics are often omitted in approaches commonly presented in the related literature, due to the additional complexity they introduce.

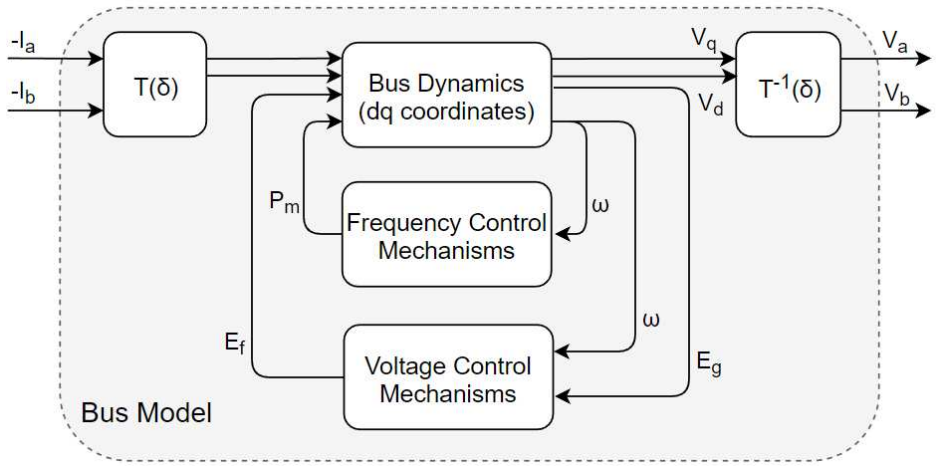


Fig. 6.16 A graphical representation of a generator model expressed in system reference frame.

### 6.2.3 Framework verification

The proposed framework and the derived stability results are now verified through applications on the Two Areas Kundur Test System [48] and the IEEE New York / New England 68-bus interconnection system [125]. These applications focus on generator buses and are carried out using the Power System Toolbox (PST) [126]. Within the simulations, the generators are modelled by the fourth-order dynamics (6.18) on which both frequency and voltage control mechanisms are applied. Specifically, frequency and voltage control are carried out by turbine governors and exciters respectively, while PSSs are applied to the generator's excitation system to effectively damp the occurring oscillations. The adopted models of the turbine governors and the exciters are described in the Laplace domain by

$$P_i^m = \frac{(1+sT_{3,i})(1+sT_{4,i})}{(1+sT_{s,i})(1+sT_{c,i})(1+sT_{5,i})}(P_{ref,i}^m - K_i^{TG}\Delta\omega_i)$$

and

$$E_{f,i} = \frac{K_i^A}{(1+sT_{A,i})}\left(V_i^{ref} + V_i^{PSS} - \frac{1}{(1+sT_{R,i})}|E_{g,i}|\right)$$

respectively. For the PSSs we use the conventional PSS model which is also given in Laplace domain by

$$V_i^{PSS} = K_i^{PSS}\frac{sT_{w,i}(1+sT_{1,i})(1+sT_{3,i})}{(1+sT_{w,i})(1+sT_{2,i})(1+sT_{4,i})}\Delta\omega_i.$$

In the above transfer functions, the variables defined with the letter T and the letter K denote the time constants and the gains of the respective control mechanism. Additionally, $P_{ref,i}^m$ is the mechanical power reference input of the turbine governor, $V_i^{ref}$ is the voltage reference input of the exciter and $V_i^{PSS}$ is the supplementary input injected by the PSS to the exciter. Finally, $|E_{g,i}|$ represents the magnitude of the generator's terminal voltage and is given by $|E_{g,i}| = \sqrt{E_{q,i}^2 + E_{q,i}^2}$ [126].

The dynamics of each generator bus individually are linearized about an equilibrium to facilitate the verification of the passivity property on the generator buses of the test systems. The equilibria are identified by solving a Power Flow problem for each test system respectively[4]. To verify the passivity of the bus models we use Linear Matrix Inequalities (LMIs) whose application on passivity verification is extensively described in [100, Section 2]. An alternative way to verify the passivity of bus dynamics with transfer matrix $G_i(s)$, is by checking the positive definiteness of the matrix $G_i(\mathrm{j}\omega) + G_i^{\mathrm{T}}(-\mathrm{j}\omega)$ as indicated in [127].

[4]It should be noted that the phase difference $\delta_i$ between each local (d,q) and the system reference frame is obtained from each generator's q-axis transient emf $E'_{q,i}$, rather than the q-axis bus voltage $V_{q,i}$.

In particular, the positive definiteness is ensured when the eigenvalues of the matrix are positive[5].

We first deal with the Four Machine Two-Areas Kundur Test System which is widely used for stability studies. The passivity of the four generator buses is verified using LMIs, for the following four different cases: (i) no turbine governor / no exciter / no PSS, (ii) turbine governor / no exciter / no PSS, (iii) turbine governor / exciter / no PSS and (iv) turbine governor / exciter / PSS. All generator buses are not passive when neither of the available control mechanisms is employed. When turbine governors are added to generators, bus dynamics are slightly damped but they still remain non-passive. The exciters further passivate the generator buses making buses 1 and 2 passive. Buses 11 and 12 still remain non-passive. Finally, the application of PSSs to the generators completely passivates the dynamics.

The proposed approach is also applied on the generator buses of the IEEE 68 bus test system. According to the derived results, the generator buses are also non-passive for the cases (i) and (ii). In both cases, the power system collapses after a sudden change of load across the network. On the other hand, when the excitation system is applied to the generators, the generator buses are considerably damped and, although the system presents an oscillatory behaviour, it remains stable when a generation-load mismatch occurs. To be more specific, the application of the excitation system on the grid-connected generators makes generator buses 53, 59, 61 and 64 passive while the rest remain non-passive. Finally, the incorporation of the PSSs at the generator exciters passivates further the generator buses and results in a more stable and robust operation. All generator buses are now passive[6] except from buses 58, 62, 63 and 65. However, we can achieve to passivate these generator buses by slightly increasing the transient reactances $X'_d$ and $X'_q$ of the respective generators (approximately 15%). These results are illustrated in Figures 6.17 and 6.18 which present the frequency and the voltage deviation at bus 27 respectively, when a sudden change of 1pu is applied at the load buses 1, 9 and 18. This change corresponds to a total change of 300 MW (the IEEE 68 bus test system consists of a total load of 18.33 GW). Since the system collapses when the excitation system is not applied to the generators, the respective figures for the cases (i) and (ii) are omitted. We should also mention that, although not all the generator buses are passive, the power system is stable. As extensively discussed in previous chapters, passivity is a sufficient condition for stability which implies that the power system can be stable even if not all buses are passive. It should be noted that its essence is that it is a decentralized condition, and any decentralized stability condition is in general only sufficient as to derive a

[5]Note that the eigenvalues of $G_i(\mathrm{j}\omega) + G_i^{\mathrm{T}}(-\mathrm{j}\omega)$ are always real as the matrix is Hermitian.

[6]It should be noted that the passivity property was verified for all choices of reference bus for the angles $\delta_i$. The choice of reference did not affect the passivity property since the relative values of the angles are close to 0.

necessary and sufficient stability condition, the explicit knowledge of the dynamics of the whole power grid is required. From these results, it becomes clear that under a proper design of the control mechanisms which are applied to the generators, we can achieve to completely passivate the generator buses of the network, and thus to ensure the asymptotic stability of the power system.

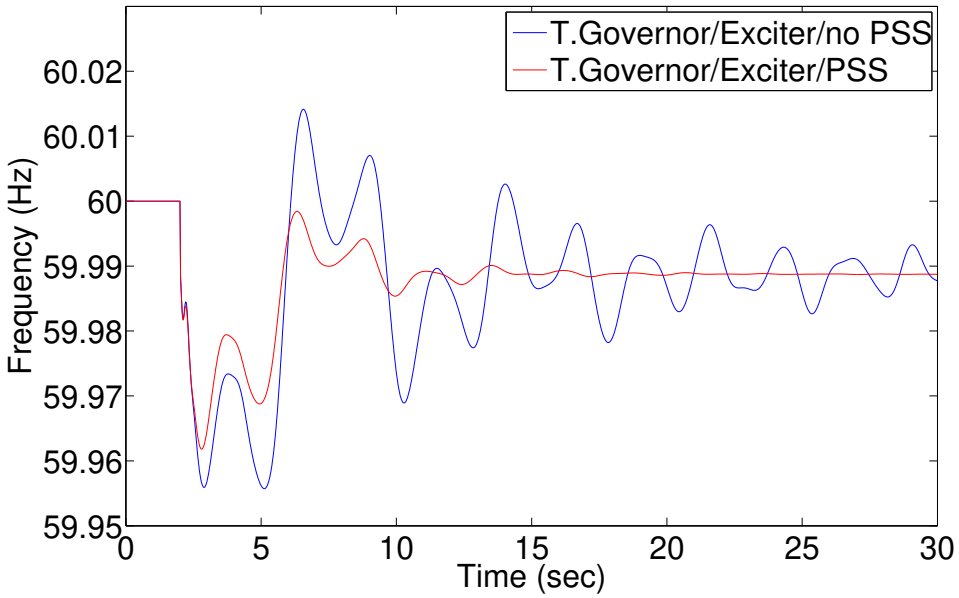


Fig. 6.17 Frequency deviation at bus 27 after a sudden change of 1pu at the load buses 1, 9 and 18.

### 6.2.4 Modification of generator's excitation system

In order to demonstrate how existing control mechanisms can be designed to satisfy the passivity property, we consider a generator bus with turbine/governor where the dynamics are non-passive without excitation control, and also a simple first-order exciter leading to marginally non-passive dynamics. It is then discussed how modifying the exciter by adding an additional phase lead compensator can passivate the dynamics. In particular, the model of the modified exciter is described in the Laplace domain as

$$E_{f,i} = \frac{K_a}{1+sT_a}\frac{1+sT_c}{1+sT_b}E_{g,i}.$$

The idea is to choose the time constants of the aforementioned lead/lag compensator so that appropriate phase lead is added in the problematic frequency range where the passivity

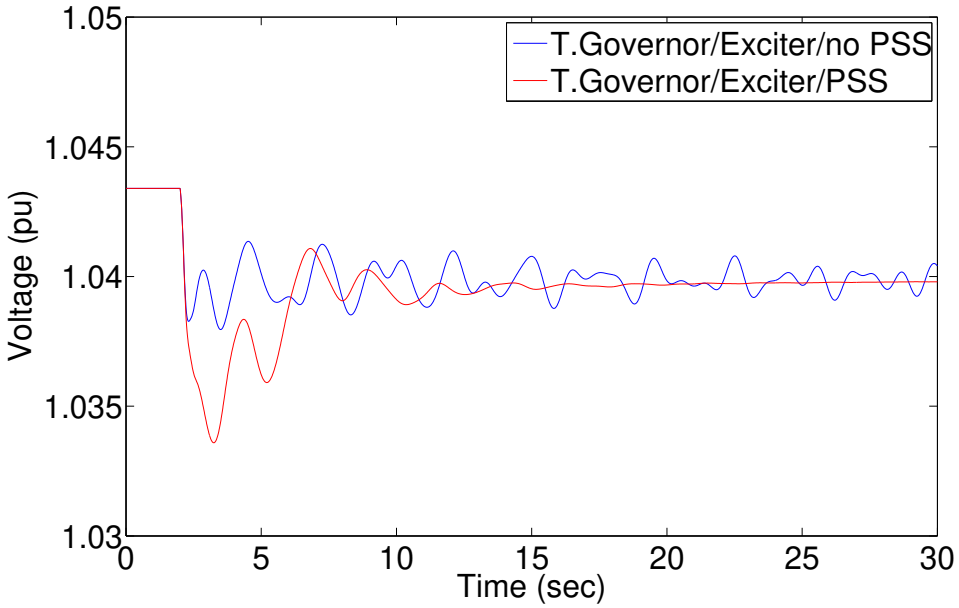


Fig. 6.18 Voltage deviation at bus 27 after a sudden change of 1pu at the load buses 1, 9 and 18.

property is violated, thus leading to bus dynamics that are now passive. This process is demonstrated in Figure 6.19 where the eigenvalues of the matrix $G(j\omega)+G^{\mathrm{T}}(-j\omega)$ are illustrated at different frequencies, where $G(s)$ is the transfer function of the linearized dynamics (5.1) at generator bus 53. The figure shows the eigenvalues[7] in the regime where the passivity property is violated. In particular, as seen from the figure the passivity property is violated in the frequency range $\omega \in [0.1, 1000]$ rads/sec (since the eigenvalues are negative) when no exciter or the simple first-order exciter are used. The figure also shows that the addition of an appropriately tuned lead/lag compensator passivates the dynamics. It should be noted that the essence of this design process is that it is decentralized, based on only the local bus dynamics, without requiring at each bus to be aware of the dynamics of the entire network as in classical small-signal analysis.

The performance of the system, when the passivity based-design described above is applied at all buses within the network, is illustrated in Figures 6.20 and 6.21. The aforementioned figures present the frequency and the voltage deviation, respectively, at bus 27, when a sudden change of 3pu is applied at the load buses 1, 9, 18, 20, 37 and 42. As can be seen, the introduction of an appropriately tuned lead/lag compensator to the excitation system of the generator results in a significantly less oscillatory behavior of the system. Note

[7] Note that $G(s)$ is a $2\times 2$ matrix and for convenience in the presentation only one of the two eigenvalues is shown where the passivity condition is violated.

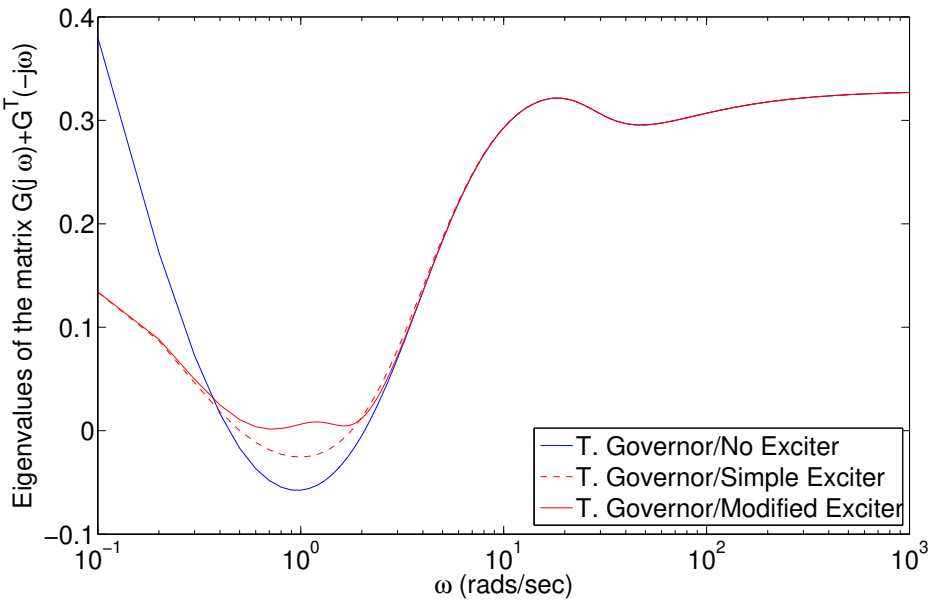


Fig. 6.19 Eigenvalues of $G(j\omega)+G^{\mathrm{T}}(-j\omega)$, where $G(s)$ is the transfer function of the linearized dynamics (5.1) at generator bus 53. The figure shows the eigenvalues in the problematic range where the passivity property is violated.

here that for the dynamic simulation, we considered a total load change of 1800 MW which corresponds to 10% of the grid-connected load.

The stability enhancement achieved through the modification of the initial simple exciter is also illustrated through the eigenanalysis of the test system. As can be seen from Figure 6.22, the application of a lead/lag compensator to synchronous generator excitation system passivates the bus dynamics and significantly damps the calculated modes. More specifically, when the simple exciter violating the passivity property is employed to the generators, the system is small-signal unstable since there exists an eigenvalue with a positive real part. On the other hand, the application of the modified exciter on the generators stabilizes the system moving all the eigenvalues to the left half-plane. Moreover, the proposed lead/lag compensator to the excitation system of the generators yields a good damping ratio[8] for the modes of the system.

### 6.2.5 Conslusions

This section verified the feasibility and the applicability of the presented local passivity conditions on two testbed power systems. As was shown, these conditions were, in many

[8]The damping ratio of an eigenvalue $\lambda = a + j\beta$ is defined as $z = -\frac{a}{\sqrt{a^2+\beta^2}}$.

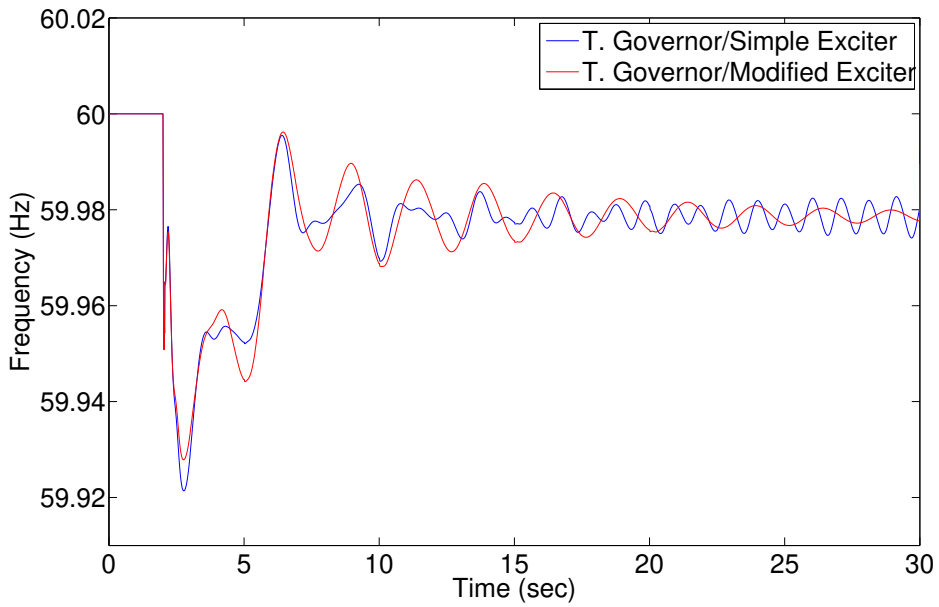


Fig. 6.20 Frequency deviation at bus 27 after a sudden change of 3pu at the load buses 1, 9, 18, 20, 37 and 42.

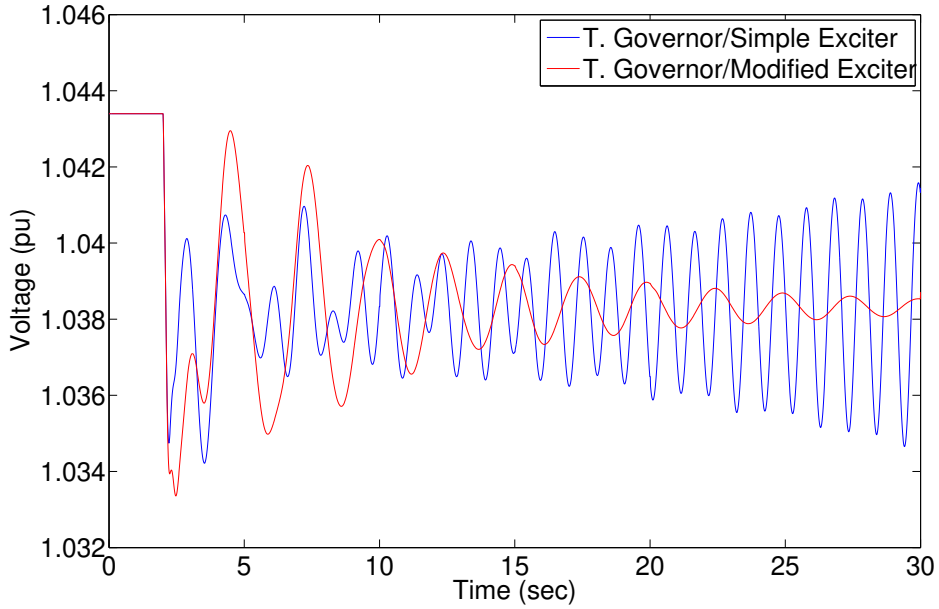


Fig. 6.21 Voltage deviation at bus 27 after a sudden change of 3pu at the load buses 1, 9, 18, 20, 37 and 42.

cases, satisfied despite being strict and conservative. Their satisfaction was directly related to the existence or not of certain control mechanisms such as the turbine governors, the

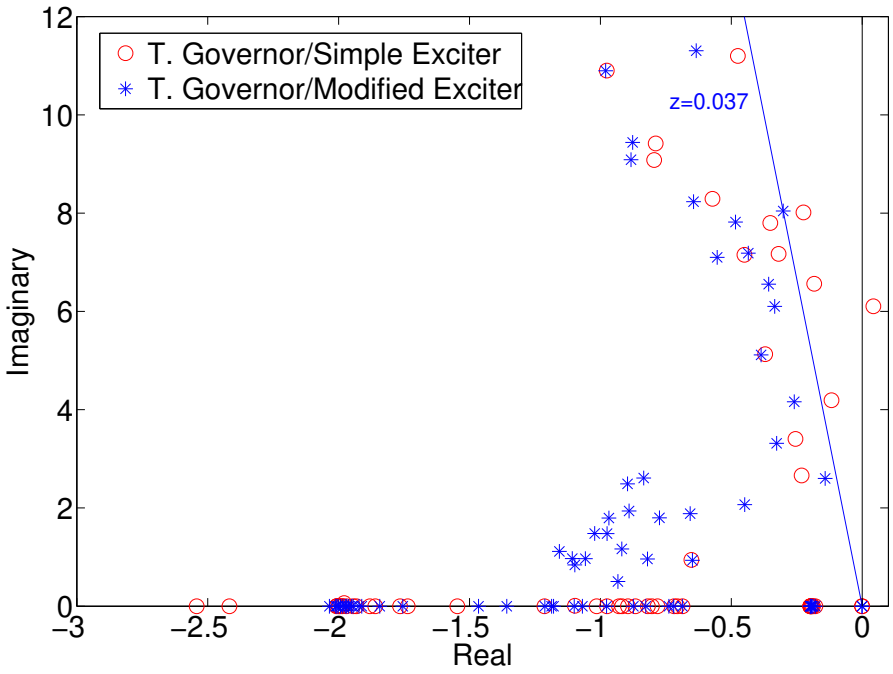


Fig. 6.22 Eigenvalues of the linearized network dynamics of the IEEE 68 bus test system.

excitation systems and the PSSs. Moreover, these local conditions can be utilized to adjust or modify existing control mechanisms and thus, to improve their performance. This procedure was demonstrated through the modification of synchronous generators' excitation system. The modified exciter rendered bus dynamics passive and thus enhanced power system stability and robustness during generation-load imbalances.

## 6.3 Passivity-based design of a load-side voltage control mechanism

### 6.3.1 Introduction

As indicated in Chapter 1, during the last years, existing power networks have been through critical and rapid changes as a result of the continuously increasing penetration of Distributed Energy Resources (DER) and the unbundling of electricity markets. In particular, a large share of DER has been recently connected in distribution grids while consumers are now more active in power system operation through their participation in power generation and the system's ancillary services [2]. Although these changes can aid to make existing power systems "greener" and more efficient, they have introduced serious difficulties to

Transmission and Distribution System Operators (TSOs & DSOs) since the transmission and distribution networks are forced to operate close to their limits. The large amount of DER across the grid in combination with their intermittent nature and the variability of loading in current competitive electricity market environments resulted in serious congestion problems, the reduction of the system's operational efficiencies as well as significant electrical losses. Moreover, these changes introduced serious power quality issues since maintaining acceptable voltage levels across the distribution feeders under all loading conditions, constitutes a very difficult task for DSOs [128].

Various equipment, such as Load Tap Changer (LTC) transformers, line AVRs, and fixed or switched capacitors are currently utilized to facilitate operators in regulating the voltage in a decentralized manner using appropriate voltage setpoints or centralized, through setpoints sent by a Supervisory Control and Data Acquisition Distribution Management System (SCADA/DMS) [128, 129]. Additionally, a variety of Volt/Var control mechanisms for LTC transformers, AVRs and DER have been proposed in recent literature to improve the system's voltage response further and thus, to overcome the problems caused by the rapid increase of DER [130–135]. More recently, flexible loads were identified as an alternative, very promising solution for providing ancillary services to the system through their participation in electricity markets [136]. Both centralized and decentralized controllers have been proposed to adjust the demand to contribute in either frequency and/or voltage regulation [22, 23, 135, 137].

Driven by the interest to incorporate loads in power system operation, this section presents an effective, demand-side, voltage-droop regulation scheme that can provide significant voltage support and assist in maintaining acceptable voltage levels across the grid. More specifically, by considering certain passivity conditions on bus (load) dynamics, we propose a voltage control mechanism that can regulate the bus voltage through the utilization of the available controllable loads across the system either in a centralized or a decentralized manner. Its formulation is carried out taking into account both the lossy and the dynamic nature of the network, thus providing guarantees for increased performance and robustness. Finally, the effectiveness of the proposed load-side voltage-droop control mechanism is verified through several dynamic simulations on the IEEE 68 Bus Test System and the IEEE 37 Node Test Feeder.

### 6.3.2 Controller design

The proposed, demand-side voltage droop controller was initially introduced in [33, 34] to provide the necessary voltage support to distribution grids. Its design relies on the fact that

all loads can be represented by a constant impedance model as follows:

$$\begin{bmatrix} V_{a,i}^b \\ V_{b,i}^b \end{bmatrix} = \begin{bmatrix} R_i^L & -X_i^L \\ X_i^L & R_i^L \end{bmatrix} \begin{bmatrix} -I_{a,i}^l \\ -I_{b,i}^l \end{bmatrix} \tag{6.21}$$

where $R_i^L$ and $X_i^L$ denote the resistance and the impedance of the load connected at bus $i$, respectively. Note that the negative sign in (6.21) appears since $I_{a,i}^l$ and $I_{b,i}^l$ denote here the components of the net absorbed current rather than the net injected current. It is also considered that a part of these loads is controllable and thus can participate in system operation. We thus introduce a negative feedback control mechanism that can regulate voltage through the control of the current absorbed by these loads. The proposed mechanism can be illustrated in Fig. 6.23 and is described by the following set of differential equations:

$$\begin{bmatrix} \dot{I}_{a,i}^{cl} \\ \dot{I}_{b,i}^{cl} \end{bmatrix} = A_i^c \begin{bmatrix} I_{a,i}^{cl} \\ I_{b,i}^{cl} \end{bmatrix} + B_i^c \begin{bmatrix} V_{a,i}^b - V_{a,i}^{ref} \\ V_{b,i}^b - V_{b,i}^{ref} \end{bmatrix}. \tag{6.22}$$

$I_{a,i}^{cl}$ and $I_{b,i}^{cl}$, and $V_{a,i}^{ref}$ and $V_{b,i}^{ref}$ denote the phasor components of the mechanism's output current and the reference voltage at bus $i$ respectively. The matrices $A_i^c$, $B_i^c \in \mathbb{R}^{2\times 2}$ in (6.22) are given as follows:

$$A_i^c = \frac{1}{T_{c,i}} \begin{bmatrix} -1 & 0 \\ 0 & -1 \end{bmatrix} \quad \text{and} \quad B_i^c = \frac{1}{T_{c,i}} \begin{bmatrix} k_{a,i}^c & k_{b,i}^c \\ -k_{b,i}^c & k_{a,i}^c \end{bmatrix}$$

where $k_{a,i}^c, k_{b,i}^c \geq 0$ are the gain constants and $T_{c,i}$ is the time constant of the controller.

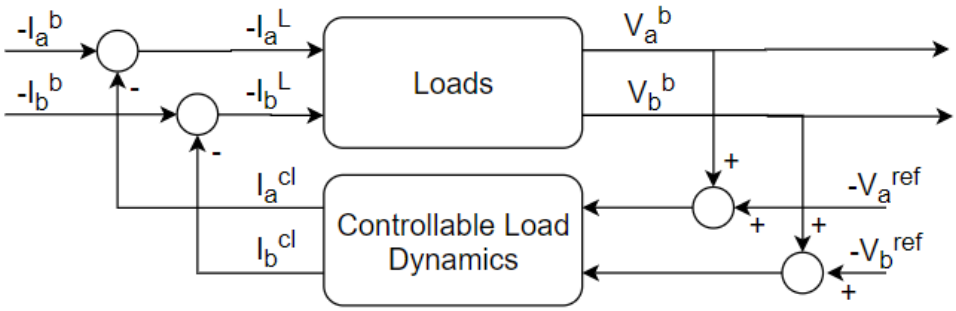


Fig. 6.23 The load-side voltage controller connected in a negative feedback arrangement to bus/load dynamics.

**Remark 6.3.1** *The reference inputs $V_{a,i}^{ref}$ and $V_{b,i}^{ref}$ are derived through the Park-Clarke transformation of a voltage reference setpoint $V_i^{ref}$ using the same angle difference $\delta_i$.*

### 6.3.3 Passivity of load dynamics

To guarantee the asymptotic stability of the interconnected system presented in Fig. 5.1, the controllable load dynamics (6.21) and (6.22) and the rest of the power system components must satisfy one of the local passivity conditions presented in Definition 5.2.4. We, therefore, provide the following proposition wherein we show that the controllable load dynamics are passive and thus can assist in power system operation during disturbances.

**Proposition 6.3.1** *The controllable load dynamics* (6.21) *and* (6.22) *constitute a* 2*-input* $\times$ 2*-output passive system.*

**Proof of Proposition 6.3.1** *For the proof of the Proposition 6.3.1 we consider the following storage function for the load dynamics* (6.21) *and* (6.22)*:*

$$\mathscr{V}_i^L = \frac{T_{c,i}}{2({k_{a,i}^c}^2 + {k_{b,i}^c}^2)} [I_{a,i}^{cl}\ I_{b,i}^{cl}] \begin{bmatrix} k_{a,i}^c & -k_{b,i}^c \\ k_{b,i}^c & k_{a,i}^c \end{bmatrix} \begin{bmatrix} I_{a,i}^{cl} \\ I_{b,i}^{cl} \end{bmatrix}. \tag{6.23}$$

*The positive semidefiniteness of the above storage function follows here easily from the skew-symmetry of the matrix $B_i^c$ and the fact that both the gain constants $k_{a,i}^c$ and $k_{b,i}^c$ are positive. The controllable load dynamics are therefore passive if the following inequality holds:*

$$u_i^T y_i = [-I_{a,i}^b\ -I_{b,i}^b] \begin{bmatrix} V_{a,i}^b \\ V_{b,i}^b \end{bmatrix} \geq \dot{\mathscr{V}}_i^L \tag{6.24}$$

*for all $i \in \mathscr{N}$. Considering that $\Delta V_{a,i} = V_{a,i}^b - V_{a,i}^{ref}$ and $\Delta V_{b,i} = V_{b,i}^b - V_{b,i}^{ref}$, we then calculate the derivative of the storage function* (6.23) *which is given by:*

$$\begin{aligned} \dot{\mathscr{V}}_i^L =& \frac{-1}{({k_{a,i}^c}^2 + {k_{b,i}^c}^2)} [I_{a,i}^c\ I_{b,i}^c] \begin{bmatrix} k_{a,i}^c & -k_{b,i}^c \\ k_{b,i}^c & k_{a,i}^c \end{bmatrix} \begin{bmatrix} I_{a,i}^c \\ I_{b,i}^c \end{bmatrix} \\ & + [I_{a,i}^c\ I_{b,i}^c] \begin{bmatrix} \Delta V_{a,i} \\ \Delta V_{b,i} \end{bmatrix} \\ =& \frac{-{k_{a,i}^c}^2}{({k_{a,i}^c}^2 + {k_{b,i}^c}^2)} ({I_{a,i}^{cl}}^2 + {I_{b,i}^{cl}}^2) \\ & - R_i^L ({I_{a,i}^l}^2 + {I_{b,i}^l}^2) + [-I_{a,i}^b\ -I_{b,i}^b] \begin{bmatrix} V_{a,i}^b \\ V_{b,i}^b \end{bmatrix}. \end{aligned} \tag{6.25}$$

*Since $R_i^L,\ k_{a,i}^c,\ k_{b,i}^c \geq 0$, the equation* (6.25) *satisfies $\dot{\mathscr{V}}_i^L \leq u_i^T y_i$ and this completes the proof* $\square$.

**Remark 6.3.2** *A significant advantage of this voltage droop controller lies in the fact that it can be employed in either centralized or decentralized fashion. More specifically, the voltage setpoints can be defined locally at the loads (e.g. thermal loads controlled by power electronics) or can be received from a SCADA/DMS during voltage dips or rises.*

**Remark 6.3.3** *As will be shown in the sequel, although it is not required for all power system components to satisfy any of the previous passivity conditions, the employment of the presented voltage droop controller on several loads can significantly improve the response of the system during disturbances. This finding relies on the fact that additional damping is provided to the grid through the utilization of the proposed control scheme.*

### 6.3.4 Simulations

The effectiveness of the load-side voltage droop controller presented in the previous paragraphs is verified through several dynamic simulations on the IEEE 68 Bus Test System and the IEEE 37 Node Test Feeder [125]. These test systems are illustrated in Figs. 6.5 and 6.24, respectively. All dynamic simulations are implemented using the Power System Toolbox (PST), assuming that the grid-connected loads are balanced and modeled using the classic ZIP model. For the simulations on the IEEE 37 Node Test Feeder, it is also considered that the feeder is connected to an infinite bus representing the rest of the power system.

Firstly, for the simulations on the IEEE 68 Bus Test System, it is considered that a sudden load change of 100MW occurs at buses 1, 7, 21, 28 and 46 while loads at buses 3, 4, 16, 24, 26, 33, 40, 47, 49 and 50 are equipped with the proposed voltage control mechanism. The gain and the time constants of the load-side voltage controller are set at all buses as follows: $K_a = 5pu$, $K_b = 1pu$ and $T_c = 0.1sec$.

The effect of the proposed controller is illustrated in Figs. 6.25 - 6.26 by the voltage and the frequency deviation at bus 32, when PSSs are applied to generators or not. As can be observed from both figures, the proposed real-time load controller can significantly improve the response of the system in both cases as it reduces the bus voltage deviation. It should also be mentioned that this improvement on both the voltage and the frequency was achieved without requiring all power system components (synchronous generators) to satisfy certain passivity conditions. Instead, the employment of such voltage droop controller at the loads provided additional damping to the system and thus increased its reliability and robustness during disturbances.

On the other hand, for the dynamic simulations IEEE 37 Node Test Feeder, it is considered that a sudden load change of 500kW occurs at the nodes 724, 728, 735 and 740 (total 2MW), while loads connected at the nodes 713, 722, 725, 729, 731, 737, 741 and 742 employ

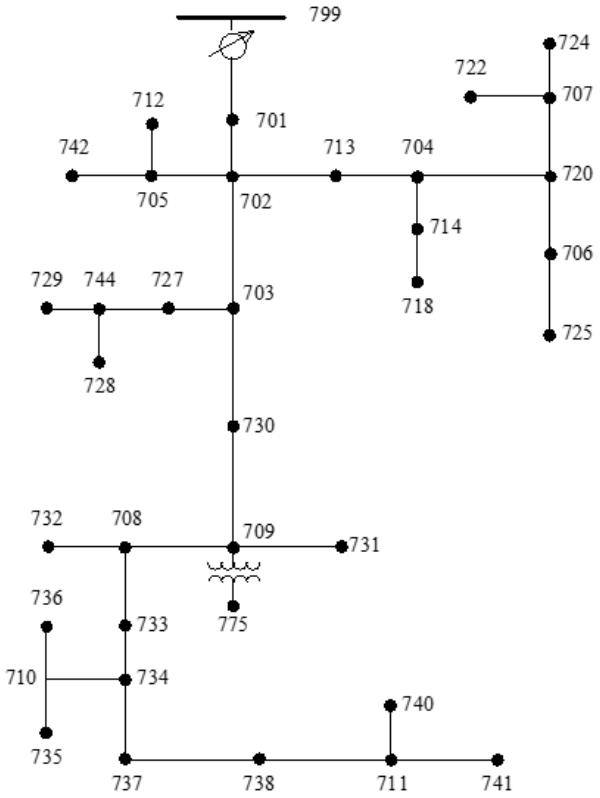


Fig. 6.24 Single line diagram of IEEE 37 Node Test Feeder [125].

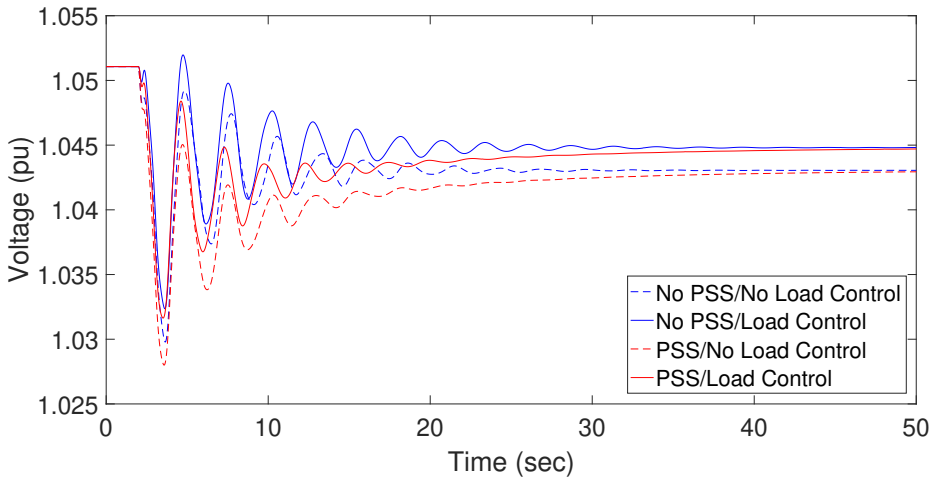


Fig. 6.25 Voltage deviation at bus 32 after a sudden load change at buses 1, 7, 21, 28 and 46.

the proposed voltage control mechanism. The gain constants $K^c_{a,i}$ and $K^c_{b,i}$ were selected proportionally to the load connected at each node while $T_{c,i}$ was set 0.1sec for all controllable

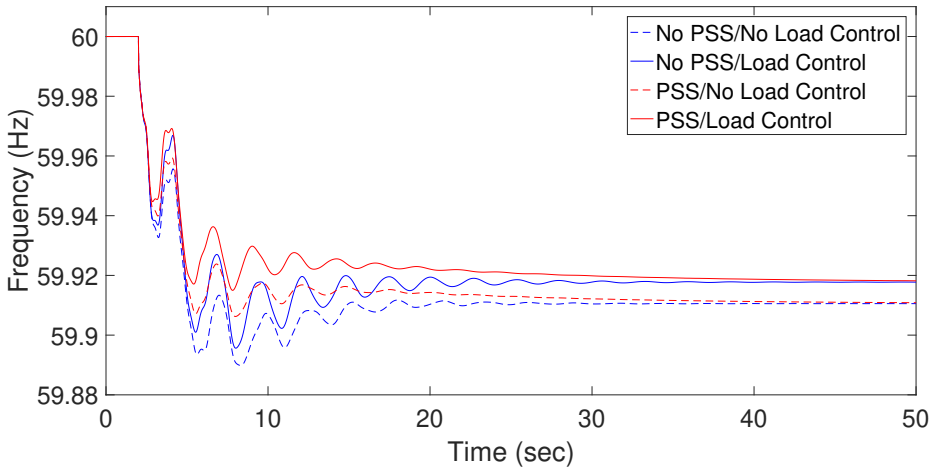


Fig. 6.26 Frequency deviation at bus 32 after a sudden load change at buses 1, 7, 21, 28 and 46.

loads. The effectiveness of the proposed control strategy is represented in Figures 6.27 and 6.28 where we illustrate the voltage and the frequency deviation at the worst impacted node of the system, that is the node 775, for the following two different cases: (a) No control at the loads, (b) Voltage control at the loads.

From Figure 6.27, one can observe that the proposed voltage controlllers significantly reduce the bus voltage deviation across the feeder when a sudden generation-load imbalance occurs. Furthermore, as shown in Figure 6.28, the control mechanism improves the system's frequency response as well since during their operation, controllable loads, apart from their absorbed reactive power, decrease their absorbed active power as well to contribute in voltage regulation.

### 6.3.5 Conclusions

The current section dealt with the presentation of an effective, demand-side voltage regulation scheme that can provide significant voltage support and assist in maintaining acceptable voltage levels across the grid. In particular, by considering certain passivity conditions on bus (load) dynamics, we proposed a voltage control mechanism that can regulate the bus voltage through the utilization of the available controllable loads across the system either in a centralized or a decentralized manner. Its formulation was carried out taking into account both the lossy and the dynamic nature of the network, thus providing guarantees for increased performance and robustness. Finally, the effectiveness of the proposed control mechanism

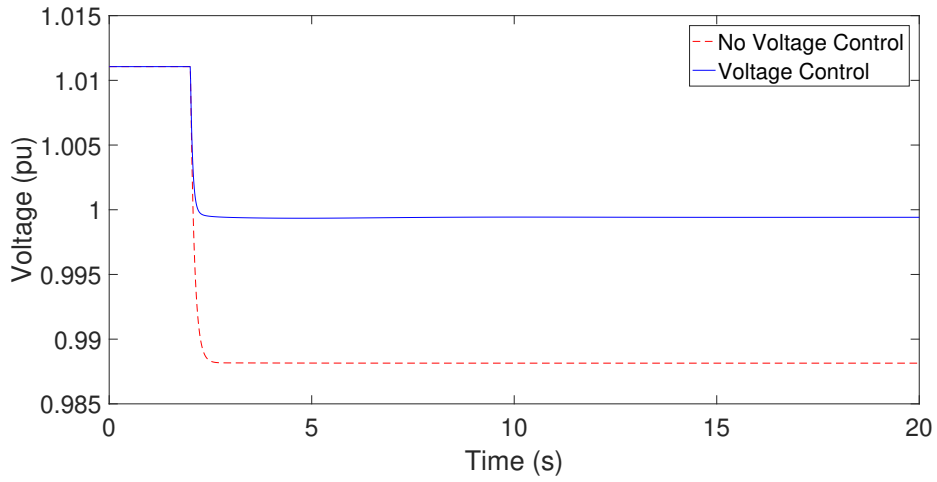


Fig. 6.27 Voltage deviation at the node 775 after a sudden load change of 500kW at the nodes 724, 728, 735 and 740.

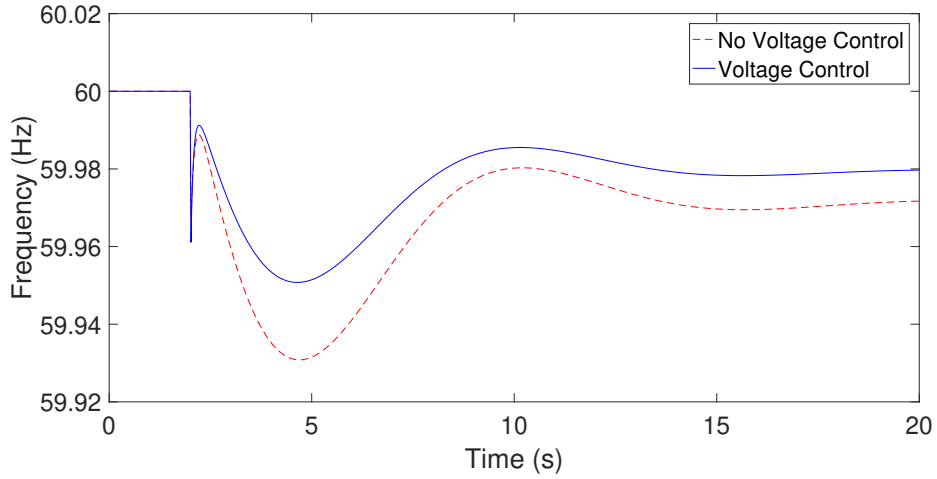


Fig. 6.28 Frequency deviation at the node 775 after a sudden load change of 500kW at the nodes 724, 728, 735 and 740.

was verified through several dynamic simulations on the IEEE 68 Bus Test System and the IEEE 37 Node Test Feeder.

## 6.4 Verification of local passivity conditions on grid-forming inverters

Finally, the current section briefly discusses an additional application of the stability analysis and control design approach presented throughout this thesis. This application which was

introduced in [35], extended the analysis of power system components in a common frame of reference to grid-forming voltage source converters using an alternative dynamic network representation than the one given by the differential equations (4.12)-(4.13) and (4.20). It should also be noted that this application is identical to the application presented in Section 6.2 for synchronous generators since it utilizes the presented decentralized conditions to provide stability guarantees for power networks with grid-forming converters and thus, improve the stability and dynamic response of the system.

In particular, in [35], we used the following dynamical model to represent the power network:

$$\begin{aligned} C\dot{V}_{ab}^{b} &= I_{ab}^{n} + \begin{bmatrix} 0 & \omega_s C \\ -\omega_s C & 0 \end{bmatrix} V_{ab}^{b} + \begin{bmatrix} E & 0 \\ 0 & E \end{bmatrix} I_{ab} \\ L\dot{I}_{ab} &= \begin{bmatrix} -R & \omega_s L \\ -\omega_s L & -R \end{bmatrix} I_{ab} - \begin{bmatrix} E^T & 0 \\ 0 & E^T \end{bmatrix} V_{ab}^{b} \end{aligned} \tag{6.26}$$

with inputs $u = {I_{ab}^{n}}^T = [I_a^{nT}\ I_b^{nT}]$ the vectors of the net injected current components, states $x = I_{ab}^T = [I_a^T\ I_b^T]$ the vectors of the line current components and outputs $y = {V_{ab}^{b}}^T = [{V_a^b}^T\ {V_b^b}^T]$ the vectors of the bus voltage components. The matrices $R$, $L$ and $C \in \mathbb{R}^{|\mathcal{N}|\times|\mathcal{N}|}$ are the diagonal matrices of the line resistances, line inductances and equivalent capacitances, respectively, and $\omega_s$ is the constant synchronous frequency. On the other hand, grid-forming inverter dynamics are LCL-filtered and include the dynamical models of the following parts/mechanisms:

1. the frequency droop
2. the angle droop, and
3. the matching control.

The above dynamics which are usually expressed in the local $dq$ reference frame, are extensively described in [97, 138–143]. Similarly to synchronous generator dynamics, grid-forming inverter dynamics were also transformed into the system reference frame using Park-Clarke transformation (3.29) - (3.32) to fit the proposed multi-variable stability analysis approach.

The novelty of this work lies in the fact that we showed the applicability of passivity-based design in a common reference frame to grid-forming converters through the assessment of the passivity properties of various existing control schemes. It should be highlighted here that, even though passivity conditions for grid-connected inverters have been analyzed

extensively [144], grid-forming converters are in general more difficult to stabilize in a large scale network due to their mutual interaction.

Moreover, we showed that the passivity of grid-forming converters could be enhanced using these local conditions through a simple modification of the angle droop controller. This improvement has been implemented by combining the concept of virtual resistance with angle droop to form a controller which authors called modified angle droop [145]. Several simulations were also carried out to compare various control schemes and verify the improved performance when the passivity property is satisfied.

# Chapter 7

# Conclusions

This chapter concludes this thesis by summarizing its main contributions and providing suggestions and ideas for further future research.

## 7.1 Conclusive summary

As described in the previous chapters, the current PhD thesis focused on the decentralized stability analysis of existing power grids and the design of new, more effective control mechanisms. For the derivation of the presented results, several tools from non-linear analysis, Lyapunov theory and passivity analysis were employed.

The main contributions of this PhD are the following:

1. The development of a multi-variable, system reference frame approach that can provide reliable stability guarantees as the analysis is carried out using more detailed dynamic models: The proposed approach relied on the transformation of both the network and bus dynamics into a common system reference frame instead of local $dq$ coordinates. Based on this transformation, the network equations were formulated as an input-output system which was shown to be passive even when the network's lossy and dynamic nature is considered. As extensively discussed, the adoption of such a network model and the revelation of the network's natural passivity properties can significantly enhance the accuracy and the reliability of the derived stability results.

2. The introduction of local, passivity constraints for bus dynamics: The imposition of these passivity conditions on bus dynamics in combination with the passivity property of the employed network model ensured the asymptotic stability of the interconnected system in a completely decentralized manner. Such decentralized stability guarantees

could play a significant role in the future development of existing power systems that are dominated by numerous DG units and sparsely-located energy storage facilities.

3. The derivation of a novel methodology to design effective, fast-acting, distributed control mechanisms: The proposed decentralized control design which relies on the above local passivity conditions, could provide significant plug-n-play capabilities and adaptivity to the continuously evolving power grids. Such a design methodology could also reduce the complexity of the analysis since it does not require the implicit knowledge of the system.

The above contributions were further exploited throughout this thesis, for the derivation of additional theoretical and technical results. These results include some derivative contributions and practical applications of the proposed stability analysis and control design approach, and are summarized below as follows:

1. The use of a broad class of systems to represent bus dynamics: Using such a general class of dynamics facilitated the incorporation of more accurate, higher-order dynamical models for a variety of power system components and control mechanisms within the proposed framework. The adoption of this modeling approach could be crucial for the derivation of more reliable, system-wide stability results.

2. The verification of the proposed approach through applications on several testbeds using realistic data of synchronous generators and grid-forming RES: Through these applications, it was shown, that the presented passivity conditions are not conservative despite being strict. At the same time, they can be utilized for the modification of the employed control mechanisms and therefore, the improvement of power system's dynamic response during disturbances.

3. The introduction of a novel passivity-based framework for SVC employment to enhance the overall power system stability and robustness: The proposed framework provided detailed information regarding (a) the identification of the most vulnerable -in terms of passivity- buses of the system for the SVC installation, (b) the derivation of a broad passivity-based tuning strategy which can provide local stability guarantees and lead to the overall enhancement of the power system stability and (c) the determination of the appropriate size for the installed SVCs.

4. The design of an effective load-side voltage controller: The presented voltage control mechanism was proven capable of providing significant voltage support and assisting in maintaining acceptable voltage levels across the grid.

The above contributions are presented in detail throughout Chapters 4 - 6. These three main contribution chapters are being summarized below to provide an appropriate interpretation of the presented analysis and results.

The main technical content of this PhD thesis was presented in Chapter 4. In particular, the power network equations were formulated as a multi-input/multi-output system expressed into a common system reference frame instead of each bus local $dq$ coordinates. Through this reference frame transformation, it was showed that any power network with arbitrary topology constitutes a passive system even when its lossy and dynamic nature are taken into account. The two different network representations derived through the presented analysis, that is the static (equations (4.1)) and the dynamic (equations (4.12)-(4.13) and (4.20) for branch and capacitance dynamics respectively) network model, can be effectively utilized for the deduction of significant, system-wide, stability results in a completely decentralized manner. The feasibility, accuracy and effectiveness of these network models were verified through several numerical applications and dynamic simulations on the Kundur Four-Machine Two-Areas and a simple Four-Area test system, respectively. As it has been shown, the use of a lossless network model could lead to less accurate results while the adoption of a dynamic network representation could be crucial for the stability analysis and control design of future, low-inertia power grids.

Chapter 5 dealt with the incorporation of bus dynamics into the proposed multi-variable framework. As extensively discussed, power system components were modeled by the broad classes of dynamical systems (5.1) and (5.2), considering that each of the power system components forms either a 2-input/2-output or 4-input/4-output system to fit with the proposed network formulation. In contrast to the recent literature, these dynamic models were expressed into the system reference frame by incorporating the mappings $T$ and $T^{-1}$ (equations (3.29)-(3.32)) into the bus dynamics. The use of such a broad, system reference frame representation for bus dynamics allowed the introduction of appropriate local passivity conditions that when satisfied by bus dynamics can ensure the asymptotic stability of the interconnected system (see Theorems 5.3.1 and 5.3.2). Finally, this framework was shown to be capable of facilitating the incorporation of a variety of power system components such as synchronous generators, loads, FACTS devices and inverter-based RES along with their frequency and voltage control regimes.

Finally, several applications of the proposed multi-variable approach for power system stability analysis and control were presented in Chapter 6. More specifically, Section 6.1, focused on the introduction of a novel passivity-based SVC employment methodology that can significantly enhance power system stability and robustness. The presented methodology relied upon the identification of the most vulnerable - in terms of passivity - buses of

the system and thus the optimal locations for SVC installation. Section 6.2 demonstrated the applicability and the feasibility of the presented passivity conditions on synchronous generators using realistic data. The proposed decentralized conditions were further exploited for the design of a modified excitation system that can passivate generator dynamics and thus, improve system response during generation-load imbalances. Throughout Section 6.3, the proposed approach was used to design an effective, demand-side voltage regulation scheme that can provide significant voltage support and assist in maintaining acceptable voltage levels across the grid. This control mechanism can be used either in a centralized or decentralized fashion and its application at several buses of the network can improve the system's response even when the presented passivity conditions are not satisfied at all the buses. Finally, a brief discussion on an additional application of the proposed stability analysis approach on grid-forming inverters was also provided.

## 7.2 Future work

The stability analysis and control design approach presented in this thesis motivates further research to address various questions that naturally arise from its study. Below, I would like to discuss several relevant ideas and suggestions to extend this work and thus to contribute to the further development of existing power grids.

The proposed multi-variable approach, in combination with the presented passivity conditions, could be utilized for the design of new control mechanisms that can effectively participate in power system operation. More specifically, as the number of distributed power system components (e.g. inverter-based RES, inverter-based storage systems, electric vehicles) increases, the introduction of appropriately designed controllers can provide significant support to existing frequency and voltage regulation regimes. The design of such distributed controllers requires the multi-variable formulation of the adopted dynamical models and can be implemented without the explicit knowledge of the network structure.

It would also be interesting to study further the relaxation of the local passivity conditions presented in Chapter 5 for bus dynamics. As it was extensively discussed in Sections 6.2 and 6.4, these conditions are marginally violated by several generation units such as synchronous generators and grid-forming inverters. Although this violation does not necessarily imply instability, it constitutes a significant obstacle for guaranteeing the asymptotic stability of an interconnected system. The satisfaction of these conditions requires the employment of appropriately modified control mechanisms. One similar study dealing with the introduction of less conservative conditions beyond the traditional passivity approaches was also presented in [101].

An interesting work would also be the extension of the proposed SVC employment methodology to include other FACTS devices. In particular, the introduction of several types of FACTS devices in combination with the derivation of an appropriate passivity-based approach to identify the optimal FACTS population will further enhance the stability and the robustness of the system. Such an extension will also provide additional capabilities for more effective control of active and reactive power flows across the grid.

It would also be of high interest to extend the recent literature by elaborating a quantitative comparison study of all decentralized stability analysis approaches. Such an analysis would be very useful for the future development of power system stability and control since it will provide significant insights for the existing low-inertia power networks and facilitate the introduction of new, more effective control mechanisms. Nevertheless, the quantitative comparison of various approaches would require the definition of various performance indices able to compare stability analysis methods with different levels of modeling approximation, applicability and complexity. This procedure would be extremely challenging since a common test system and methodology need to be developed with the different approximations, all the methods implemented, and their results compared.

Finally, a significant improvement of the proposed stability analysis approach would be the extension of its timescale through the incorporation of more detailed dynamical models. As the dynamic phenomena occurring across the existing power grids are becoming much faster, the capability of considering even more accurate power system dynamics would be of great interest. These dynamic phenomena could be analyzed in more detail providing at the same time, the necessary means to overcome such contingencies and thus to enhance power system robustness.

# REFERENCES


[1] Adoption of the Paris Agreement, *Framework Convention on Climate Change*. United Nations, 2015.

[2] H. Sun, N. Hatziargyriou, L. Carpanini, H. V. Poor, and M. A. S. Fornié, *Smarter Energy: From Smart Metering to the Smart Grid*. IET, 2016.

[3] H. Lund, "Renewable energy strategies for sustainable development," *Energy*, vol. 32, no. 6, pp. 912–919, 2007.

[4] H. Lund, *Renewable energy systems: a smart energy systems approach to the choice and modeling of 100% renewable solutions*. Academic Press, 2014.

[5] J. A. P. Lopes, F. J. Soares, and P. M. R. Almeida, "Integration of electric vehicles in the electric power system," *Proceedings of the IEEE*, vol. 99, no. 1, pp. 168–183, 2010.

[6] J. M. Griffin and S. L. Puller, *Electricity deregulation: choices and challenges*, vol. 4. University of Chicago Press, 2009.

[7] P. L. Joskow, "Lessons learned from electricity market liberalization," *The Energy Journal*, vol. 29, no. 2, 2008.

[8] The European Commission, *European Smart Grids Technology Platform*. The European Commission, 2006.

[9] A. Ipakchi and F. Albuyeh, "Grid of the future," *IEEE Power and Energy magazine*, vol. 7, no. 2, pp. 52–62, 2009.

[10] A. Ulbig, T. S. Borsche, and G. Andersson, "Impact of low rotational inertia on power system stability and operation," *IFAC Proceedings Volumes*, vol. 47, no. 3, pp. 7290–7297, 2014.

[11] F. Milano, F. Dörfler, G. Hug, D. J. Hill, and G. Verbič, "Foundations and challenges of low-inertia systems," in *2018 Power Systems Computation Conference (PSCC)*, pp. 1–25, IEEE, 2018.

[12] S. Yasmeena and G. T. Das, "A review of technical issues for grid connected renewable energy sources," *International Journal of Energy and Power Engineering*, vol. 4, no. 5-1, pp. 22–32, 2015.

[13] A. Ulbig and G. Andersson, "On operational flexibility in power systems," in *2012 IEEE Power and Energy Society General Meeting*, pp. 1–8, IEEE, 2012.

[14] I. Dudurych, M. Burke, L. Fisher, M. Eager, and K. Kelly, "Operational security challenges and tools for a synchronous power system with high penetration of non-conventional sources," *CIGRE Science & Engineering*, vol. 7, 2017.

[15] N. Acharya and N. Mithulananthan, "Locating series FACTS devices for congestion management in deregulated electricity markets," *Electric Power Systems Research*, vol. 77, no. 3-4, pp. 352–360, 2007.

[16] P. L. Joskow, "California's electricity crisis," *Oxford Review of Economic Policy*, vol. 17, no. 3, pp. 365–388, 2001.

[17] J. Taylor and P. VanDoren, "California's electricity crisis," in *Electricity Pricing in Transition*, pp. 245–265, Springer, 2002.

[18] P. Aristidou and G. Hug, "Accelerating the computation of critical eigenvalues with parallel computing techniques," in *2016 Power Systems Computation Conference (PSCC)*, pp. 1–8, IEEE, 2016.

[19] J. Bao, P. L. Lee, and B. E. Ydstie, *Process control: the passive systems approach*. PhD thesis, Springer-Verlag, 2007.

[20] N. Kottenstette, M. J. McCourt, M. Xia, V. Gupta, and P. J. Antsaklis, "On relationships among passivity, positive realness, and dissipativity in linear systems," *Automatica*, vol. 50, no. 4, pp. 1003–1016, 2014.

[21] H. K. Khalil, *Nonlinear Systems*. Prentice Hall, 3rd ed., 2002.

[22] O. Ma, N. Alkadi, P. Cappers, P. Denholm, J. Dudley, S. Goli, M. Hummon, S. Kiliccote, J. MacDonald, N. Matson, *et al.*, "Demand response for ancillary services," *IEEE Transactions on Smart Grid*, vol. 4, no. 4, pp. 1988–1995, 2013.

[23] D. S. Callaway and I. A. Hiskens, "Achieving controllability of electric loads," *Proceedings of the IEEE*, vol. 99, no. 1, pp. 184–199, 2010.

[24] R. Teodorescu, M. Liserre, and P. Rodriguez, *Grid converters for photovoltaic and wind power systems*, vol. 29. J. Wiley & Sons, 2011.

[25] N. G. Hingorani and L. Gyugyi, *Understanding facts*. IEEE press, 2000.

[26] Y.-H. Song and A. Johns, *Flexible ac transmission systems (FACTS)*. No. 30, IET, 1999.

[27] E. Devane, A. Kasis, C. Spanias, M. Antoniou, and I. Lestas, "Distributed frequency control and demand-side management," in *Smarter Energy: From Smart Metering to the Smart Grid* (H. Sun, N. Hatziargyriou, L. Carpanini, H. V. Poor, and M. A. S. Fornié, eds.), ch. 9, pp. 157–192, IET, 2016.

[28] A. Kasis, E. Devane, C. Spanias, and I. Lestas, "Primary frequency regulation with load-side participation Part I: stability and optimality," *IEEE Transactions on Power Systems*, 2016.

[29] C. Spanias, P. Nikolaidis, and I. Lestas, "Techno-economic analysis of the potential conversion of the outdated moni power plant to a large scale research facility," in *5th International Conference on Renewable Energy Sources & Energy Efficiency*, pp. 208–220, 2016.

[30] C. Spanias, P. Aristidou, M. Michaelides, and I. Lestas, "Power system stability enhancement through the optimal, passivity-based, placement of SVCs," in *2018 Power Systems Computation Conference (PSCC)*, IEEE, 2018.

[31] C. Spanias and I. Lestas, "A system reference frame approach for stability analysis and control of power grids," *IEEE Transactions on Power Systems*, vol. 34, no. 2, pp. 1105–1115, 2018.

[32] C. Spanias, P. Aristidou, and M. Michaelides, "A dynamical multi-input/multi-output network formulation for stability analysis in AC microgrids," in *Innovative Smart Grid Technologies (ISGT) Europe*, pp. 1–5, 2019.

[33] C. Spanias, P. Aristidou, and M. Michaelides, "Demand-side Volt/Var/Watt regulation for effectivevoltage control in distribution grids," in *Innovative Smart Grid Technologies (ISGT) Europe*, pp. 1–5, 2019.

[34] C. Spanias, P. Aristidou, and M. Michaelides, "A passivity-based framework for stability analysis and control including power network dynamics," *IEEE Systems Journal*, 2020.

[35] J. Watson, Y. Ojo, C. Spanias, and I. Lestas, "Stability of power networks with grid-forming converters," in *2019 IEEE Powertech Conference*, pp. 1–6, IEEE, 2019.

[36] M. Argyrou, C. Spanias, C. Marouchos, S. Kalogirou, and P. Christodoulides, "Energy management and modeling of a grid-connected BIPV system with battery energy storage," in *54th International Universities Power Engineering Conference (UPEC)*, pp. 1–6, IEEE, 2019.

[37] S. Sastry, *Nonlinear systems: analysis, stability, and control*, vol. 10. Springer Science & Business Media, 2013.

[38] R. C. Dorf and R. H. Bishop, *Modern control systems*. Pearson, 2011.

[39] A. Vannelli and M. Vidyasagar, "Maximal lyapunov functions and domains of attraction for autonomous nonlinear systems," *Automatica*, vol. 21, no. 1, pp. 69–80, 1985.

[40] A. Trofino, "Robust stability and domain of attraction of uncertain nonlinear systems," in *Proceedings of the 2000 American Control Conference. ACC (IEEE Cat. No. 00CH36334)*, vol. 5, pp. 3707–3711, IEEE, 2000.

[41] B. Tibken, "Estimation of the domain of attraction for polynomial systems via lmis," in *Proceedings of the 39th IEEE Conference on Decision and Control (Cat. No. 00CH37187)*, vol. 4, pp. 3860–3864, IEEE, 2000.

[42] L. L. Grigsby, *Power system stability and control*. CRC press, 2016.

[43] "First report of power system stability," *Transactions of the American Institute of Electrical Engineers*, vol. 56, no. 2, pp. 261–282, 1937.

[44] C. P. Steinmetz, "Power control and stability of electric generating stations," *Transactions of the American Institute of Electrical Engineers*, vol. XXXIX, no. 2, pp. 1215–1287, 1920.

[45] P. Pourbeik, P. S. Kundur, and C. W. Taylor, "The anatomy of a power grid blackout-root causes and dynamics of recent major blackouts," *IEEE Power and Energy Magazine*, vol. 4, no. 5, pp. 22–29, 2006.

[46] A. Atputharajah and T. K. Saha, "Power system blackouts-literature review," in *2009 International Conference on Industrial and Information Systems (ICIIS)*, pp. 460–465, IEEE, 2009.

[47] P. Kundur, J. Paserba, V. Ajjarapu, G. Andersson, A. Bose, C. Canizares, N. Hatziargyriou, D. Hill, A. Stankovic, C. Taylor, *et al.*, "Definition and classification of power system stability IEEE/CIGRE joint task force on stability terms and definitions," *IEEE Transactions on Power Systems*, vol. 19, no. 3, pp. 1387–1401, 2004.

[48] P. Kundur, N. J. Balu, and M. G. Lauby, *Power system stability and control*, vol. 7. McGraw-Hill, 1994.

[49] P. Mattavelli, A. M. Stankovic, and G. C. Verghese, "Ssr analysis with dynamic phasor model of thyristor-controlled series capacitor," *IEEE Transactions on Power Systems*, vol. 14, no. 1, pp. 200–208, 1999.

[50] N. Hatziargyriou, J. Milanović, C. Rahmann, V. Ajjarapu, C. Cañizares, I. Erlich, D. Hill, I. Hiskens, I. Kamwa, B. Pal, *et al.*, "Stability definitions and characterization of dynamic behavior in systems with high penetration of power electronic interfaced technologies," 2020.

[51] J. Paserba *et al.*, "Analysis and control of power system oscillation," *CIGRE special publication*, vol. 38, no. 07, 1996.

[52] M. Mynuddin, K. Roknuzzaman, P. Biswas, and M. Tanjimuddin, "Stability study of power system," *Journal of Energy and Power Engineering*, vol. 4, no. 2, pp. 43–50, 2015.

[53] A.-A. Fouad and V. Vittal, *Power system transient stability analysis using the transient energy function method*. Pearson Education, 1991.

[54] A. Fouad and V. Vittal, "The transient energy function method," *International Journal of Electrical Power & Energy Systems*, vol. 10, no. 4, pp. 233–246, 1988.

[55] M. Pai, *Energy function analysis for power system stability*. Springer Science & Business Media, 2012.

[56] M. Pai, *Power system stability: analysis by the direct method of Lyapunov*, vol. 3. North-Holland, 1981.

[57] S. Gomes, N. Martins, and C. Portela, "Computing small-signal stability boundaries for large-scale power systems," *IEEE Transactions on Power Systems*, vol. 18, no. 2, pp. 747–752, 2003.

[58] I. Sandberg, "On the-boundedness of solutions of nonlinear functional equations," *Bell System Technical Journal*, vol. 43, no. 4, pp. 1581–1599, 1964.

[59] G. Zames, "On the input-output stability of nonlinear time-varying feedback systems," *IEEE Transactions on Automatic Control*, vol. 11, pp. 228–238, 1966.

[60] A. Van der Schaft, *L2-gain and passivity techniques in nonlinear control*. Springer, 2000.

[61] Y. Guo, D. J. Hill, and Y. Wang, "Nonlinear decentralized control of large-scale power systems," *Automatica*, vol. 36, no. 9, pp. 1275–1289, 2000.

[62] Y. Guo, Z.-P. Jiang, and D. J. Hill, "Decentralized robust disturbance attenuation for large-scale nonlinear systems," *IFAC Proceedings Volumes*, vol. 31, no. 17, pp. 847–852, 1998.

[63] J. Liu, B. H. Krogh, and B. E. Ydstie, "Decentralized robust frequency control for power systems subject to wind power variability," in *IEEE Power and Energy Society General Meeting*, pp. 1–8, IEEE, 2011.

[64] C. Zhao, U. Topcu, N. Li, and S. Low, "Design and stability of load-side primary frequency control in power systems," *IEEE Transactions on Automatic Control*, vol. 59, no. 5, pp. 1177–1189, 2014.

[65] E. Mallada, C. Zhao, and S. Low, "Optimal load-side control for frequency regulation in smart grids," in *52nd Annual Allerton Conference on Communication, Control and Computing (Allerton)*, pp. 731–738, IEEE, 2014.

[66] J. Machowski, S. Robak, J. Bialek, J. Bumby, and N. Abi-Samra, "Decentralized stability-enhancing control of synchronous generator," *IEEE Transactions on Power Systems*, vol. 15, no. 4, pp. 1336–1344, 2000.

[67] S. Bolognani and S. Zampieri, "A distributed control strategy for reactive power compensation in smart microgrids," *IEEE Transactions on Automatic Control*, vol. 58, no. 11, pp. 2818–2833, 2013.

[68] Y. Wang, D. J. Hill, and G. Guo, "Robust decentralized control for multimachine power systems," *IEEE Transactions on Circuits and Systems I: Fundamental Theory and Applications*, vol. 45, no. 3, pp. 271–279, 1998.

[69] C. Zhao, U. Topcu, and S. H. Low, "Frequency-based load control in power systems," in *2012 American Control Conference (ACC)*, pp. 4423–4430, IEEE, 2012.

[70] C. Zhao, U. Topcu, and S. H. Low, "Optimal load control via frequency measurement and neighborhood area communication," *IEEE Transactions on Power Systems*, vol. 28, no. 4, pp. 3576–3587, 2013.

[71] S. Benahdouga, D. Boukhetala, and F. Boudjema, "Decentralized high order sliding mode control of multimachine power systems," *International Journal of Electrical Power & Energy Systems*, vol. 43, no. 1, pp. 1081–1086, 2012.

[72] D. D. Siljak, D. M. Stipanovic, and A. I. Zecevic, "Robust decentralized turbine/governor control using linear matrix inequalities," *IEEE Transactions on Power Systems*, vol. 17, no. 3, pp. 715–722, 2002.

[73] M. T. Alrifai, M. F. Hassan, and M. Zribi, "Decentralized load frequency controller for a multi-area interconnected power system," *International Journal of Electrical Power & Energy Systems*, vol. 33, no. 2, pp. 198–209, 2011.

[74] E. Devane, A. Kasis, C. Spanias, M. Antoniou, and I. Lestas, "Distributed frequency control and demand-side management," *Smarter Energy: From Smart Metering to the Smart Grid*, vol. 2, p. 245, 2016.

[75] H. Miyagi and A. Bergen, "Stability studies of multimachine power systems with the effects of automatic voltage regulators," *IEEE Transactions on Automatic Control*, vol. 31, no. 3, pp. 210–215, 1986.

[76] A. J. Van der Schaft and B. M. Maschke, "Port-Hamiltonian systems on graphs," *SIAM Journal on Control and Optimization*, vol. 51, no. 2, pp. 906–937, 2013.

[77] B. Maschke, R. Ortega, and A. J. Van Der Schaft, "Energy-based lyapunov functions for forced hamiltonian systems with dissipation," *IEEE Transactions on Automatic Control*, vol. 45, no. 8, pp. 1498–1502, 2000.

[78] Y. Wang, D. Cheng, C. Li, and Y. Ge, "Dissipative hamiltonian realization and energy-based l 2-disturbance attenuation control of multimachine power systems," *IEEE Transactions on Automatic Control*, vol. 48, no. 8, pp. 1428–1433, 2003.

[79] S. Fiaz, D. Zonetti, R. Ortega, J. Scherpen, and A. Van der Schaft, "A port-hamiltonian approach to power network modeling and analysis," *European Journal of Control*, vol. 19, no. 6, pp. 477–485, 2013.

[80] T. Stegink, C. De Persis, and A. Van der Schaft, "A unifying energy-based approach to stability of power grids with market dynamics," *IEEE Transactions on Automatic Control*, vol. 62, no. 6, pp. 2612–2622, 2017.

[81] J. Schiffer, E. Fridman, R. Ortega, and J. Raisch, "Stability of a class of delayed port-hamiltonian systems with application to microgrids with distributed rotational and electronic generation," *Automatica*, vol. 74, pp. 71–79, 2016.

[82] J. Schiffer, R. Ortega, A. Astolfi, J. Raisch, and T. Sezi, "Conditions for stability of droop-controlled inverter-based microgrids," *Automatica*, vol. 50, no. 10, pp. 2457–2469, 2014.

[83] S. Y. Caliskan and P. Tabuada, "Compositional transient stability analysis of multi-machine power networks," *IEEE Transactions on Control of Network Systems*, vol. 1, no. 1, pp. 4–14, 2014.

[84] T. Stegink, C. De Persis, and A. van der Schaft, "Optimal power dispatch in networks of high-dimensional models of synchronous machines," in *55th Conference on Decision and Control (CDC)*, pp. 4110–4115, IEEE, 2016.

[85] M. Andreasson, R. Wiget, D. V. Dimarogonas, K. H. Johansson, and G. Andersson, "Distributed primary frequency control through multi-terminal hvdc transmission systems," in *American Control Conference (ACC)*, pp. 5029–5034, IEEE, 2015.

[86] S. Trip, M. Bürger, and C. De Persis, "An internal model approach to (optimal) frequency regulation in power grids with time-varying voltages," *Automatica*, vol. 64, pp. 240–253, 2016.

[87] S. Trip and C. De Persis, "Distributed optimal load frequency control with non-passive dynamics," *IEEE Transactions on Control of Network Systems*, vol. 5, no. 3, pp. 1232–1244, 2017.

[88] J. Schiffer, D. Zonetti, R. Ortega, A. M. Stanković, T. Sezi, and J. Raisch, "A survey on modeling of microgrids: From fundamental physics to phasors and voltage sources," *Automatica*, vol. 74, pp. 135–150, 2016.

[89] J. Rocabert, A. Luna, F. Blaabjerg, and P. Rodriguez, "Control of power converters in ac microgrids," *IEEE transactions on power electronics*, vol. 27, no. 11, pp. 4734–4749, 2012.

[90] J. Schiffer, E. Fridman, and R. Ortega, "Stability of a class of delayed port-hamiltonian systems with application to droop-controlled microgrids," in *54th Conference on Decision and Control (CDC)*, IEEE, 2015.

[91] A. R. Bergen and V. Vittal, *Power systems analysis*. Prentice Hall, 2000.

[92] J. D. Glover, M. S. Sarma, and T. Overbye, *Power System Analysis & Design, SI Version*. Cengage Learning, 2012.

[93] J. Machowski, J. Bialek, and J. Bumby, *Power system dynamics: stability and control*. J. Wiley & Sons, 2011.

[94] P. W. Sauer and M. Pai, "Power system dynamics and stability," *Urbana*, vol. 51, 1997.

[95] ENTSO-E, "Commission regulation (eu) 2016/631 of 14 april 2016 establishing a network code on requirements for grid connection of generators," *OJ*, vol. L 112, pp. 1–68, 2016-04-27.

[96] R. A. Horn and C. R. Johnson, *Matrix analysis*. Cambridge university press, 2012.

[97] N. Pogaku, M. Prodanovic, and T. C. Green, "Modeling, analysis and testing of autonomous operation of an inverter-based microgrid," *IEEE Transactions on power electronics*, vol. 22, no. 2, pp. 613–625, 2007.

[98] S. Boyd, L. El Ghaoui, E. Feron, and V. Balakrishnan, *Linear matrix inequalities in system and control theory*, vol. 15. Siam, 1994.

[99] A. Kasis, E. Devane, and I. Lestas, "On the stability and optimality of primary frequency regulation with load-side participation," in *54th Conference on Decision and Control (CDC)*, pp. 2621–2626, IEEE, 2015.

[100] M. J. McCourt and P. J. Antsaklis, "Demonstrating passivity and dissipativity using computational methods," *ISIS*, p. 008, 2013.

[101] E. Devane, A. Kasis, M. Antoniou, and I. Lestas, "Primary frequency regulation with load-side participation Part II: beyond passivity approaches," *IEEE Transactions on Power Systems*, vol. 32, no. 5, pp. 3519–3528, 2017.

[102] X. Li, P. Li, C. Q. Le, *et al.*, "A novel approach for determining optimal number and placement of static var compensator device to enhance the dynamic performance in power systems," *Electrical Engineering*, vol. 100, no. 3, pp. 1517–1533, 2018.

[103] V. Le, X. Li, Y. Li, Y. Cao, and C. Le, "Optimal placement of tcsc using controllability gramian to damp power system oscillations," *International Transactions on Electrical Energy Systems*, vol. 26, no. 7, pp. 1493–1510, 2016.

[104] L. Van Dai, X. Li, P. Li, and L. C. Quyen, "An optimal location of static var compensator based on gramian critical energy for damping oscillations in power systems," *IEEJ Transactions on Electrical and Electronic Engineering*, vol. 11, no. 5, pp. 577–585, 2016.

[105] R. MÍnguez, F. Milano, R. ZÁrate-MiÑano, and A. J. Conejo, "Optimal network placement of SVC devices," *IEEE Transactions on Power Systems*, vol. 22, pp. 1851–1860, Nov 2007.

[106] E. Ghahremani and I. Kamwa, "Optimal placement of multiple-type FACTS devices to maximize power system loadability using a generic graphical user interface," *IEEE Transactions on Power Systems*, vol. 28, pp. 764–778, May 2013.

[107] M. M. Farsangi, H. Nezamabadi-pour, Y.-H. Song, and K. Y. Lee, "Placement of SVCs and selection of stabilizing signals in power systems," *IEEE Transactions on Power Systems*, vol. 22, no. 3, pp. 1061–1071, 2007.

[108] S. Gerbex, R. Cherkaoui, and A. J. Germond, "Optimal location of multi-type FACTS devices in a power system by means of genetic algorithms," *IEEE Transactions on Power Systems*, vol. 16, no. 3, pp. 537–544, 2001.

[109] S. Gerbex, R. Cherkaoui, and A. Germond, "Optimal location of FACTS devices to enhance power system security," in *Power Tech Conference Proceedings, 2003 IEEE Bologna*, vol. 3, pp. 7–pp, IEEE, 2003.

[110] S. Sakthivel, D. Mary, R. Vetrivel, and V. S. Kannan, "Optimal location of SVC for voltage stability enhancement under contingency condition through pso algorithm," *International Journal of Computer Applications (0975–8887)*, vol. 20, no. 1, 2011.

[111] E. Ghahremani and I. Kamwa, "Optimal placement of multiple-type FACTS devices to maximize power system loadability using a generic graphical user interface," *IEEE Transactions on Power Systems*, vol. 28, no. 2, pp. 764–778, 2013.

[112] R. Benabid, M. Boudour, and M. Abido, "Optimal location and setting of svc and tcsc devices using non-dominated sorting particle swarm optimization," *Electric Power Systems Research*, vol. 79, no. 12, pp. 1668–1677, 2009.

[113] M. Saravanan, S. M. R. Slochanal, P. Venkatesh, and J. P. S. Abraham, "Application of particle swarm optimization technique for optimal location of FACTS devices considering cost of installation and system loadability," *Electric Power Systems Research*, vol. 77, no. 3-4, pp. 276–283, 2007.

[114] M. Haque, "Best location of svc to improve first swing stability limit of a power system," *Electric Power Systems Research*, vol. 77, no. 10, pp. 1402–1409, 2007.

[115] C. Taylor, G. Scott, and A. Hammad, "Static var compensator models for power flow and dynamic performance simulation," *IEEE Transactions on Power Systems*, vol. 9:1, Feb 1994.

[116] J. Quintero, V. Vittal, G. T. Heydt, and H. Zhang, "The impact of increased penetration of converter control-based generators on power system modes of oscillation," *IEEE Transactions on Power Systems*, vol. 29, no. 5, pp. 2248–2256, 2014.

[117] M. Abido and Y. Abdel-Magid, "Coordinated design of a pss and an svc-based controller to enhance power system stability," *International Journal of Electrical Power & Energy Systems*, vol. 25, no. 9, pp. 695–704, 2003.

[118] R. Bhatia, *Positive definite matrices*. Princeton university press, 2009.

[119] B. W. Silverman, *Density estimation for statistics and data analysis*. Routledge, 2018.

[120] C. Chang and J. Huang, "Optimal svc placement for voltage stability reinforcement," *Electric Power Systems Research*, vol. 42, no. 3, pp. 165–172, 1997.

[121] M. Moghavvemi and M. Faruque, "Effects of facts devices on static voltage stability," in *2000 TENCON Proceedings. Intelligent Systems and Technologies for the New Millennium (Cat. No. 00CH37119)*, vol. 2, pp. 357–362, IEEE, 2000.

[122] ABB, "Static Var Compensator: An insurance for improved grid system stability and reliability." https://library.abb.com/en/results, 2015. Online; accessed 29 January 2019.

[123] R. Mínguez, F. Milano, R. Zárate-Miñano, and A. J. Conejo, "Optimal network placement of SVC devices," *IEEE Transactions on Power Systems*, vol. 22, no. 4, pp. 1851–1860, 2007.

[124] R. Sirjani, A. Mohamed, and H. Shareef, "Optimal placement and sizing of Static Var Compensators in power systems using improved harmony search algorithm," *Przeglad Elektrotechniczny*, vol. 87, no. 7, pp. 214–218, 2011.

[125] G. Rogers, *Power system oscillations*. Springer Science & Business Media, 2012.

[126] J. Chow, G. Rogers, and K. Cheung, "Power system toolbox," *Cherry Tree Scientific Software,[Online] Available: http://www. ecse. rpi. edu/pst/PST. html*, vol. 48, p. 53, 2000.

[127] N. Kottenstette and P. J. Antsaklis, "Relationships between positive real, passive dissipative, & positive systems," in *American Control Conference (ACC)*, pp. 409–416, IEEE, 2010.

[128] H. V. Padullaparti, Q. Nguyen, and S. Santoso, "Advances in volt-var control approaches in utility distribution systems," in *2016 IEEE Power and Energy Society General Meeting (PESGM)*, pp. 1–5, IEEE, 2016.

[129] M. J. Krok and S. Genc, "A coordinated optimization approach to volt/var control for large power distribution networks," in *Proc. of the 2011 American Control Conference*, pp. 1145–1150, IEEE, 2011.

[130] K. Baker, A. Bernstein, E. Dall'Anese, and C. Zhao, "Network-cognizant voltage droop control for distribution grids," *IEEE Transactions on Power Systems*, vol. 33, no. 2, pp. 2098–2108, 2018.

[131] S. Rahimi, M. Marinelli, and F. Silvestro, "Evaluation of requirements for volt/var control and optimization function in distribution management systems," in *2012 IEEE International Energy Conference and Exhibition (ENERGYCON)*, pp. 331–336, IEEE, 2012.

[132] P. Jahangiri and D. C. Aliprantis, "Distributed volt/var control by pv inverters," *IEEE Transactions on power systems*, vol. 28, no. 3, pp. 3429–3439, 2013.

[133] V. Borozan, M. E. Baran, and D. Novosel, "Integrated volt/var control in distribution systems," in *2001 IEEE Power Engineering Society Winter Meeting. Conference Proceedings (Cat. No. 01CH37194)*, vol. 3, pp. 1485–1490, IEEE, 2001.

[134] V. Calderaro, G. Conio, V. Galdi, G. Massa, and A. Piccolo, "Optimal decentralized voltage control for distribution systems with inverter-based distributed generators," *IEEE Transactions on Power Systems*, vol. 29, no. 1, pp. 230–241, 2014.

[135] J. Smith, W. Sunderman, R. Dugan, and B. Seal, "Smart inverter volt/var control functions for high penetration of pv on distribution systems," in *2011 IEEE/PES Power Systems Conference and Exposition*, pp. 1–6, IEEE, 2011.

[136] M. H. Albadi and E. F. El-Saadany, "Demand response in electricity markets: An overview," in *2007 IEEE Power Engineering Society General Meeting*, pp. 1–5, IEEE, 2007.

[137] K. Anderson and A. Narayan, "Simulating integrated volt/var control and distributed demand response using gridspice," in *2011 IEEE First International Workshop on Smart Grid Modeling and Simulation (SGMS)*, pp. 84–89, IEEE, 2011.

[138] J. Driesen and K. Visscher, "Virtual synchronous generators," in *2008 IEEE Power and Energy Society General Meeting-Conversion and Delivery of Electrical Energy in the 21st Century*, pp. 1–3, IEEE, 2008.

[139] H. Bevrani, T. Ise, and Y. Miura, "Virtual synchronous generators: A survey and new perspectives," *International Journal of Electrical Power & Energy Systems*, vol. 54, pp. 244–254, 2014.

[140] C. Arghir, T. Jouini, and F. Dörfler, "Grid-forming control for power converters based on matching of synchronous machines," *Automatica*, vol. 95, pp. 273–282, 2018.

[141] R. Majumder, A. Ghosh, G. Ledwich, and F. Zare, "Angle droop versus frequency droop in a voltage source converter based autonomous microgrid," in *2009 IEEE Power & Energy Society General Meeting*, pp. 1–8, IEEE, 2009.

[142] M. C. Chandorkar, D. M. Divan, and R. Adapa, "Control of parallel connected inverters in standalone ac supply systems," *IEEE Transactions on Industry Applications*, vol. 29, no. 1, pp. 136–143, 1993.

[143] M. Cespedes and J. Sun, "Impedance modeling and analysis of grid-connected voltage-source converters," *IEEE Transactions on Power Electronics*, vol. 29, no. 3, pp. 1254–1261, 2013.

[144] L. Harnefors, X. Wang, A. G. Yepes, and F. Blaabjerg, "Passivity-based stability assessment of grid-connected vscs—an overview," *IEEE Journal of emerging and selected topics in Power Electronics*, vol. 4, no. 1, pp. 116–125, 2015.

[145] X. Wang, Y. W. Li, F. Blaabjerg, and P. C. Loh, "Virtual-impedance-based control for voltage-source and current-source converters," *IEEE Transactions on Power Electronics*, vol. 30, no. 12, pp. 7019–7037, 2014.